

För Reference

NOT TO BE TAKEN FROM THIS ROOM

Ex LIBRIS
UNIVERSITATIS
ALBERTAEENSIS



THE UNIVERSITY OF ALBERTA

THE YARROW CREEK - SPIONKOP CREEK COPPER DEPOSIT,
SOUTHWESTERN ALBERTA

by



RONALD JAMES GOBLE, B.Sc.

A THESIS

SUBMITTED TO THE FACULTY OF GRADUATE STUDIES
IN PARTIAL FULFILMENT OF THE REQUIREMENTS FOR THE DEGREE
OF MASTER OF SCIENCE

DEPARTMENT OF GEOLOGY

EDMONTON, ALBERTA

FALL, 1970

UNIVERSITY OF ALBERTA
FACULTY OF GRADUATE STUDIES

The undersigned certify that they have read, and recommend to the Faculty of Graduate Studies for acceptance, a thesis entitled "The Yarrow Creek - Spionkop Creek Copper Deposit, Southwestern Alberta" submitted by Ronald James Goble in partial fulfilment of the requirements for the degree of Master of Science.

ABSTRACT

Petrographic and sulphur isotopic studies have been carried out on selected samples collected from the Yarrow Creek - Spionkop Creek copper deposit of southwestern Alberta.

Petrographic studies reveal that deposition of an initial generation of the copper sulphides in the sediments occurred during diagenesis. This corresponds to a period of intrusion of diabasic sills and dykes in the area. The sulphides deposited at this time included pyrite, bornite, (chalcocite), chalcopyrite, sphalerite, and a pale blue covellite. The copper sulphides were in part replaced by a later generation of dark blue covellite and by a subsequent generation of malachite and azurite. Similarities between the sedimentary and intrusive specimen suites suggest that the copper was derived from the sediments and mobilized by solutions at the time of intrusion of the diabases.

The sulphur within the solutions from which the sulphides were deposited appears to have been relatively highly enriched in S^{34} ($\delta S^{34} = +25\%$). Simple deposition of the sulphides from such a 'heavy' solution as it moved out from the diabase intrusives does not satisfy the geochemical model set up, however, and it is believed that mixing of solutions from the intrusives with 'heavy' sulphur-bearing solutions in the sediments must have occurred. This suggests that the principle source of the sulphur (and copper) may have been the sediments. Some variation from the expected δS^{34} values

is due to local variations in the fugacity of oxygen.

ACKNOWLEDGEMENTS

The writer is particularly indebted to Dr. R.D. Morton, who supervised the researching of this thesis, for advice, assistance, and encouragement on the project. The guidance and assistance of Dr. H. Ohmoto with the sulphur isotope studies was of particular help to the writer and is gratefully acknowledged. Dr. P. Fritz assisted in outlining the research project and in the isotopic studies. The advice of Dr. H. Baadsgaard in the laboratory has been invaluable.

Assistance with the preparation of sulphide samples and with the use of the mass spectrometer in the Department of Physics was kindly provided by Dr. H.R. Krouse and Mr. R.J. Shaw. Mr. C.B. Sullivan prepared the thin sections used in the study.

Financial assistance has been provided by a Graduate Teaching Assistantship and a National Research Council Bursary (1969-70).

Finally the writer would in particular like to express his thanks to his father, Frank Goble, for assistance and encouragement with this thesis project.

TABLE OF CONTENTS

	<u>PAGE</u>
<u>CHAPTER I. INTRODUCTION</u>	1
Foreword	1
Geographical setting	2
Geological setting	2
Previous work	3
<u>CHAPTER II. GENERAL GEOLOGY</u>	8
Regional geological and tectonic setting	8
Stratigraphy	9
Summary and conclusions	20
Structure	20
Summary and conclusions	22
Igneous activity	23
<u>CHAPTER III. METALLIFEROUS DEPOSITS</u>	27
Introduction	27
The Yarrow Creek - Spionkop Creek deposit	28
Related mineralization	29
Summary and conclusions	30
<u>CHAPTER IV. ORE MICROSCOPY</u>	31
Sedimentary suite	31
Mineralogy	31
Textural relationships	33
Parageneses	37
Intrusive suite	39
Mineralogy	39
Textural relationships	48

Parageneses	50
Summary	51
<u>CHAPTER V. SULPHIDE GEOCHEMISTRY</u>	57
Introduction	57
Analytical methods	62
Temperature of mineralizing solutions	64
Pressure of mineralizing solutions	66
Mineral stability relationships	66
Solution geochemistry	70
Evaluation of results	90
Summary and conclusions	92
<u>CHAPTER VI. COMPARISONS WITH OTHER AREAS</u>	95
Introduction	95
Comparisons with other deposits in the	
Belt - Purcell series	96
Comparisons with deposits outside North America	101
(i) Russian deposits	102
(ii) Kupferschiefer - Rotliegende deposits	103
(iii) Zambian - Congolese Copperbelt	104
Mode of deposition	101
SUMMARY AND CONCLUSIONS	107
BIBLIOGRAPHY OF CITED REFERENCES	109
APPENDIX A. DESCRIPTION AND LOCATION OF SPECIMENS	A-1
APPENDIX B. COMPUTATIONS	A-8
Mineral stabilities	A-8
Solution geochemistry	A-13

Sulphur isotopesA-13

LIST OF FIGURES

	<u>PAGE</u>
Figure 1: Photograph of Yarrow Creek - Spionkop Creek	4
Figure 2: Photograph of Blind Canyon	4
Figure 3: Photograph of folding, Yarrow Creek	5
Figure 4: Photograph of formations, Yarrow Creek ...	5
Figure 5: Location map of Yarrow Creek - Spionkop Creek deposit	6
Figure 6: Regional geologic map of Lewis series	7
Figure 7: Stratigraphic succession	11
Figure 8: Correlation chart of Belt-Purcell-Lewis series	12
Figure 9: Geologic map of Yarrow Creek - Spionkop Creek deposit	13
Figure 10: Photograph of mottling of argillites, Yarrow Creek	16
Figure 11: Photograph of mud balls, Yarrow Creek	16
Figure 12: Photograph of current marks, Yarrow Creek	17
Figure 13: Photograph of ripple marks, Yarrow Creek .	17
Figure 14: Photograph of cross-stratification, Yarrow Creek	18
Figure 15: Photograph of sole markings, Yarrow Creek	18
Figure 16: Photograph of salt crystal casts, Yarrow Creek	25

Figure 17:	Photograph of plagioclase phenocrysts, Yarrow Creek	25
Figure 18:	Photomicrograph of oolitic hematite, Yarrow Creek	40
Figure 19:	Photomicrograph of oolitic chalcedony and hematite, Yarrow Creek	40
Figure 20:	Photomicrograph of chalcedony ooliths, Spionkop Creek	41
Figure 21:	Photomicrograph of chalcedony oolith, Spionkop Creek	41
Figure 22:	Photomicrograph of pseudo-oolitic pyrite, Yarrow Creek	42
Figure 23:	Photomicrograph of pseudo-oolitic pyrite, Yarrow Creek	42
Figure 24:	Photomicrograph of detrital spinel, Yarrow Creek	43
Figure 25:	Photomicrograph of detrital spinel, Yarrow Creek	43
Figure 26:	Photomicrograph of copper sulphides, Spionkop Creek	44
Figure 27:	Photomicrograph of copper sulphides, Spionkop Creek	44
Figure 28:	Photomicrograph of copper sulphides, Yarrow Creek	45
Figure 29:	Photomicrograph of copper sulphides, Spionkop Creek	45
Figure 30:	Photomicrograph of chalcopyrite, Yarrow	

	Creek	46
Figure 31:	Photomicrograph of copper and iron sulphides, Yarrow Creek	46
Figure 32:	Photomicrograph of copper sulphides, Yarrow Creek	52
Figure 33:	Photomicrograph of chalcocite and magnetite, Spionkop Creek	52
Figure 34:	Photomicrograph of copper and zinc sulphides, Yarrow Creek	53
Figure 35:	Photomicrograph of skeletal magnetite, Yarrow Creek	53
Figure 36:	Paragenetic sequence of sedimentary suite, Yarrow Creek - Spionkop Creek deposit	54
Figure 37:	Paragenetic sequence of intrusive suite, Yarrow Creek - Spionkop Creek deposit	55
Figure 38:	Plot of sulphur isotopic composition of sulphur-bearing species against temperature	61
Figure 39:	Mineral stability diagram - 600°C	67
Figure 40:	Mineral stability diagram - 400°C	67
Figure 41:	Mineral stability diagram - 200°C	68
Figure 42:	Mineral stability diagram - 100°C	68
Figure 43:	Mineral stability diagram - 25°C	69
Figure 44:	Plot of equilibrium constant variation with temperature for the sulphur-bearing species and water	72
Figure 45:	Plot of Henry's Law Constant variation	

	with temperature for H_2S , CO_2	75
Figure 46:	Plot of variations of activity coefficients of sulphur-bearing species with temperature	76
Figure 47:	Plot of sulphur isotopic composition of samples against height above base of Grinnell formation	85
Figure 48:	Sample position within Yarrow Creek - Spionkop Creek deposit plotted against geology	86
Figure 49:	Map of postulated Precambrian rift valley in relationship to the Purcell-Belt series	99
Figure 50:	Map of belts of mineralization in western United States	100

LIST OF TABLES

	<u>PAGE</u>
Table 1: Fluid inclusion and isotope temperatures ..	65
Table 2: Constants used for solution geochemistry calculations	77
Table 3: Solution geochemistry at 100°C	79
Table 4: Solution geochemistry at 200°C	80
Table 5: Solution geochemistry at 400°C	81
Table 6: Solution geochemistry at 600°C	82
Table 7: Sample isotopic composition and description	84
Table 8: Comparison of Yarrow Creek - Spionkop Creek deposit with Russian deposits	102
Table 9: Comparison of Yarrow Creek - Spionkop Creek deposit with Kupferschiefer - Rotliegende deposits	103
Table 10: Comparison of Yarrow Creek - Spionkop Creek deposit with Zambian - Congolese Copperbelt deposits	104
Table 11: Thermodynamic data used for mineral stability calculations	A-10
Table 12: Solution geochemistry at 100°C	A-14
Table 13: Solution geochemistry at 200°C	A-15
Table 14: Solution geochemistry at 400°C	A-15
Table 15: Solution geochemistry at 600°C	A-16

CHAPTER I - INTRODUCTION

Foreword

Mining interest in the Yarrow Creek - Spionkop Creek area of southwestern Alberta was initiated by the staking of an outcrop of cupriferous quartzite in the area during the first decade of the Twentieth Century. These claims were never recorded and interest lapsed until the fall of 1963, when this and other similar outcrops were again staked. During 1963, 1964, and 1965 limited exploration was undertaken in the area by the author's family and other interested parties and led to the staking of some 150 mining claims in the area. Present holdings in the vicinity are equivalent to more than 2500 regular-sized mining claims.

An exploration program carried out by Kennco Explorations (Western) Limited on the Canadian outcrops of the Grinnell formation and its equivalents first revealed to the author the possibility of a syngenetic sedimentary origin for the extensive copper mineralization within the Grinnell formation. Work was begun by the author in the fall of 1968 on a research program, under the direction of Dr. R.D. Morton, designed to determine the origin of these copper deposits. Sampling for isotopic and microscopic studies was carried out in the fall of 1968 and in the spring and fall of 1969. Laboratory studies were carried out during the 1969-1970 University session.

This thesis presents the results of sulphur isotope and petrographic studies of selected samples collected from the

upper Appekunny formation, the Grinnell formation, and the lower Siyeh formation within the Yarrow Creek - Spionkop Creek area. Comparisons are made with similar-type deposits found throughout the world and a proposal is made for the origin of the Yarrow Creek - Spionkop Creek deposit.

Geographical setting

The Yarrow Creek - Spionkop Creek deposit is situated within the Clarke Range of the Rocky Mountains near the Canada-United States border. The area lies approximately fifteen miles north of the southwest corner of Alberta between latitudes $49^{\circ}12'N$ and $49^{\circ}14'N$, and between longitudes $113^{\circ}59'W$ and $114^{\circ}01'W$. Topographically the area is moderately rugged with a maximum relief of 2500 feet. Slopes are low to near vertical with sparse vegetation on the upper slopes.

Access to the Grinnell formation is facilitated by the less resistant nature of this formation compared to the overlying Siyeh formation, this giving rise to numerous scree slopes with occasional cliff faces composed of the more resistant quartzites. Mapping and sample collecting is somewhat hampered by this same feature, however, since tracing of sedimentary beds is sometimes difficult.

Geological setting

The Yarrow Creek - Spionkop Creek deposit is located within the Appekunny and Grinnell formations of the Precam-

brian Lewis series. OBRADOVICH and PETERMAN (1967) dated the Newland Limestone, equivalent to the overlying Siyeh formation, and the Chamberlain Shale, equivalent to the underlying Aldridge formation, at 1315 ± 35 million years (Rb-Sr). This places the time of deposition of the Appekunny and Grinnell formations at approximately 1300 million years ago. The two formations have since been thrust, as part of the Lewis thrust sheet, over Paleozoic and Mesozoic strata within the Clarke Range. To the west the Lewis thrust sheet is cut by the Flathead fault, which CLARK (1954) concludes to be a normal fault, downthrown to the west. The Lewis series is intruded by a set of diabasic sills and dykes which HUNT (1958) concludes to be related to the extrusion of the Purcell andesitic lava around 1100 million years ago.

Previous work

Reconnaissance geological studies of the area were carried out by DAWSON (1886), DALY (1912), HUME (1932), and CLAPP (1932). FENTON and FENTON (1937) studied the Lewis series in Waterton Lakes and Glacier National Parks and defined the Appekunny and Grinnell formations. DOUGLAS (1953) mapped the Waterton Lakes National Park area and PRICE (1962) mapped the Flathead map area. HUNT (1958, 1961) studied the intrusive diabasic sills and the Purcell extrusives within the area. STEVENSON (1968) prepared a detailed geological map of the Yarrow Creek - Spionkop Creek district.



Fig.1. Yarrow Creek - Spionkop Creek viewed from east.
Yarrow Creek to left, Spionkop Creek to right of photo.

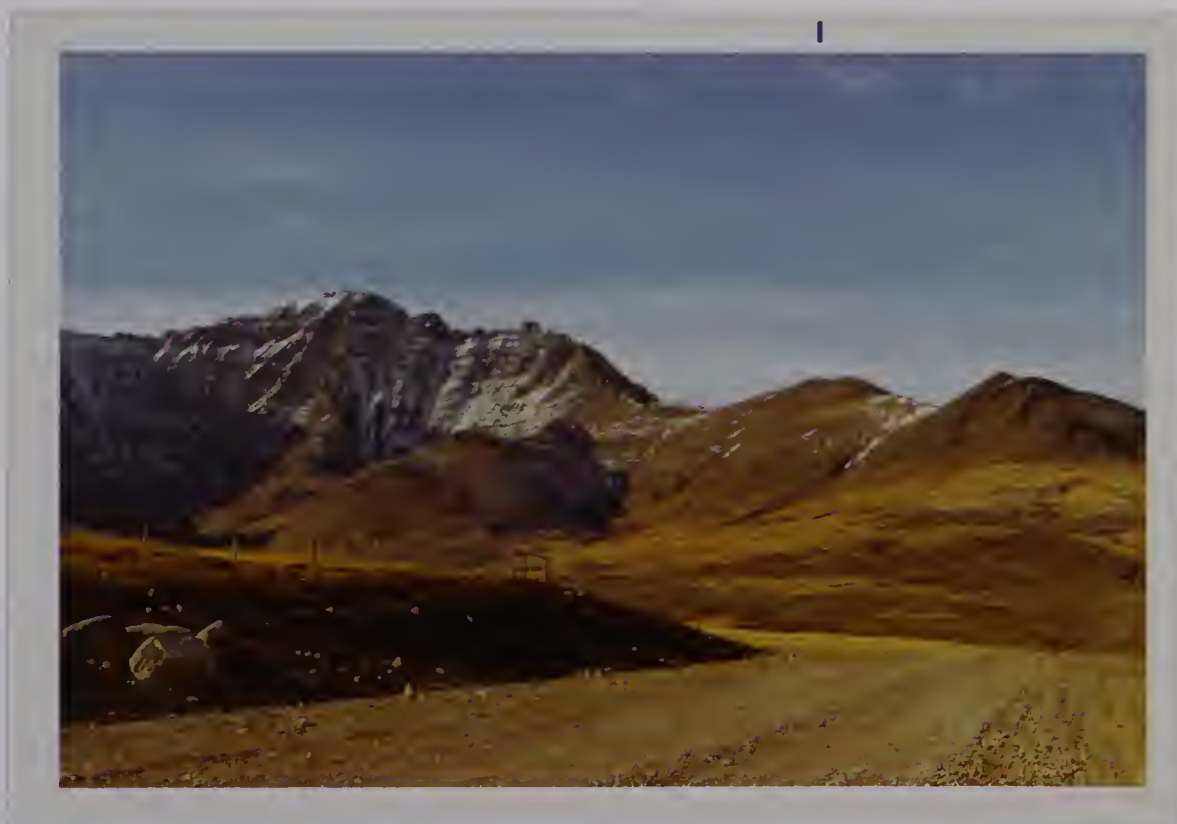


Fig.2. Blind Canyon viewed from east. Precambrian
Siyeh, Grinnell, and Appekunny formations (background)
overlying Paleozoic and Mesozoic formations (foreground).



Fig.3. Folding in Appekunny quartzites and argillites, Yarrow Creek.

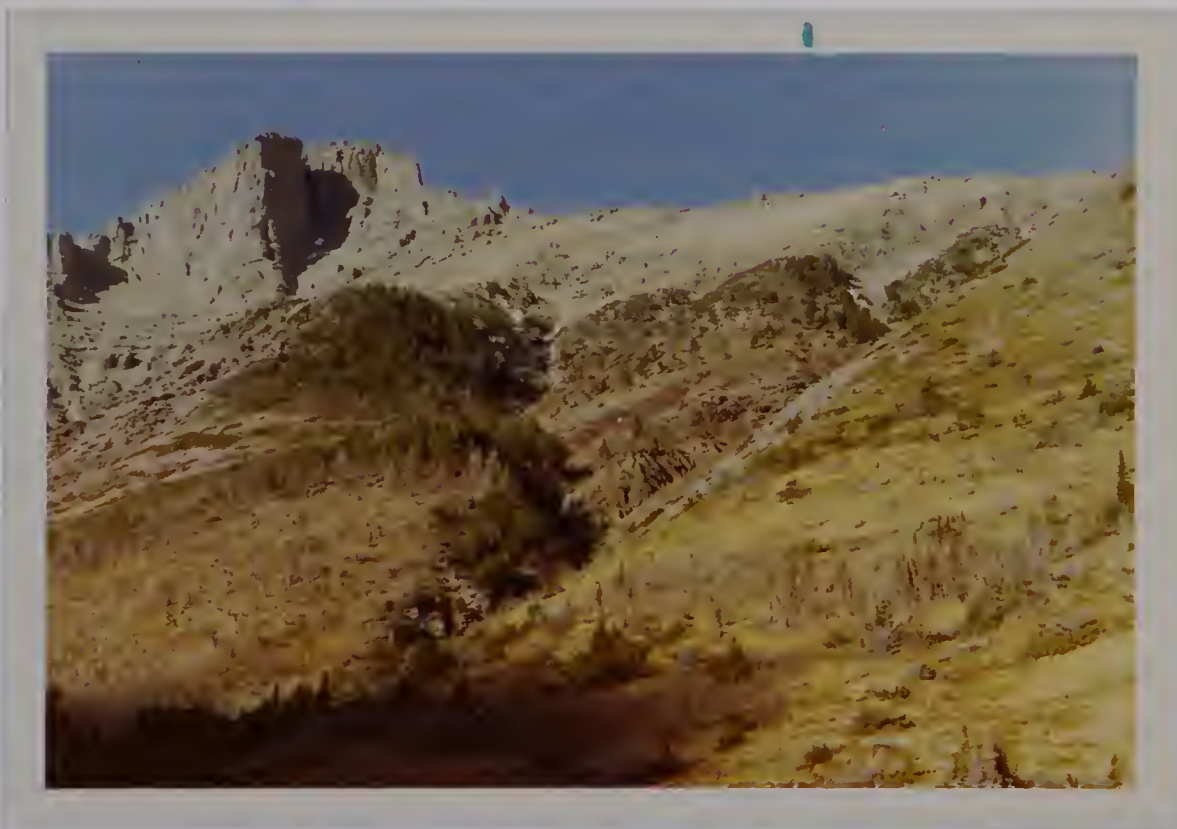
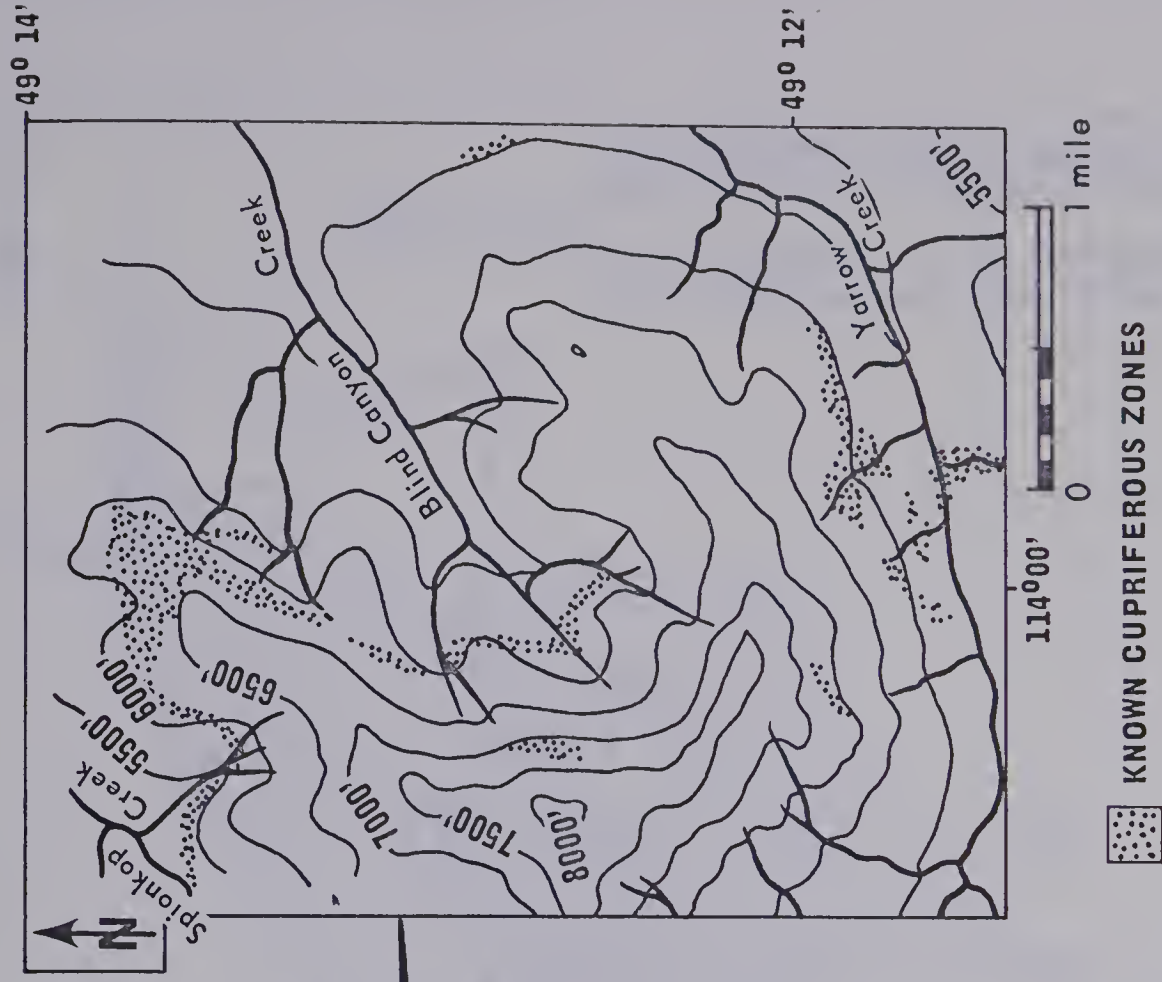
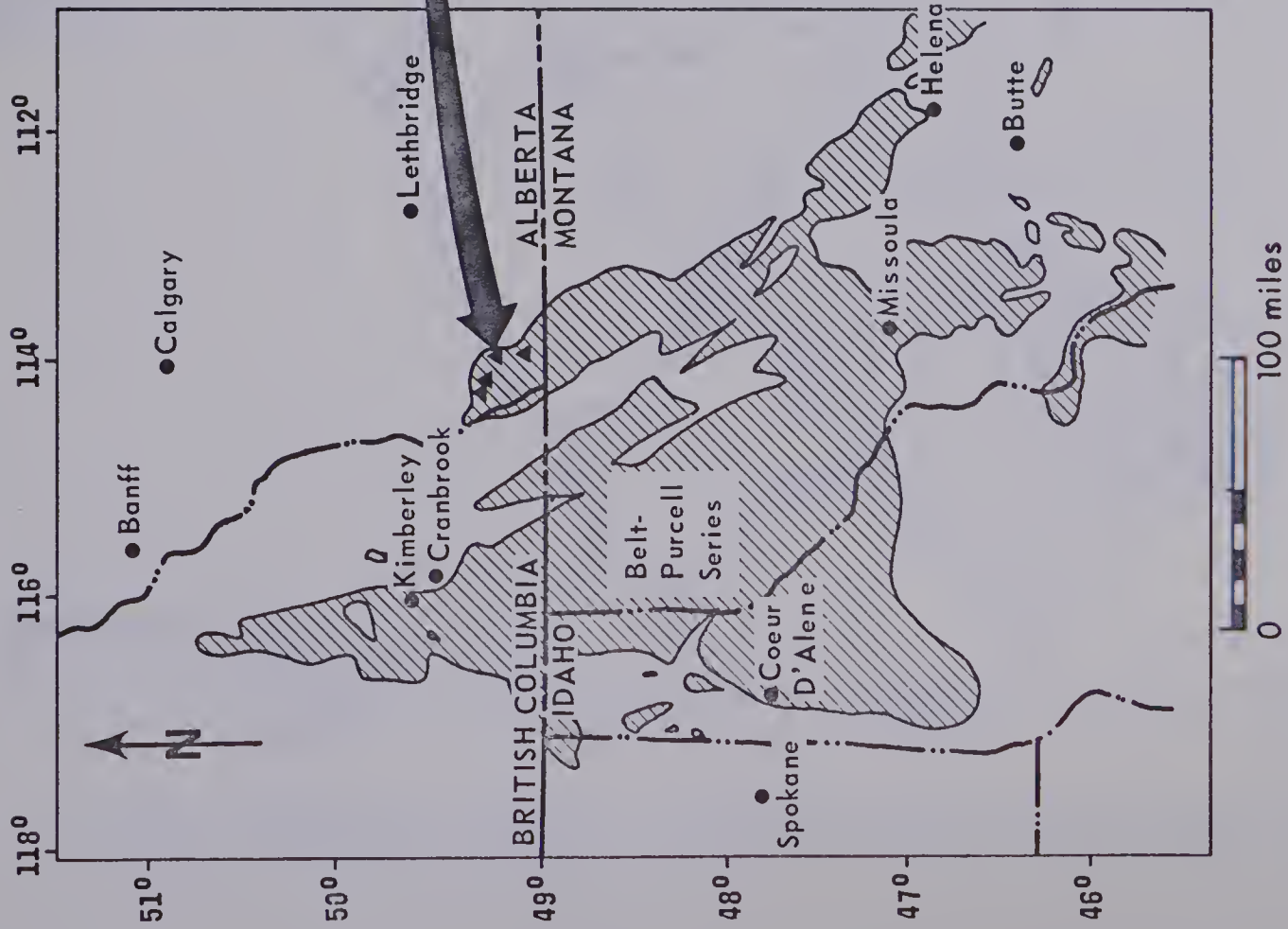


Fig.4. Siyeh formation (cliffs) overlying Grinnell formation (red talus slopes), and Appekunny formation (greenish talus slopes in foreground), Yarrow Creek.



▲ KNOWN CU OCCURRENCES IN BELT-PURCELL SERIES

Fig.5. Location map of Yarrow Creek - Spionkop Creek deposit.

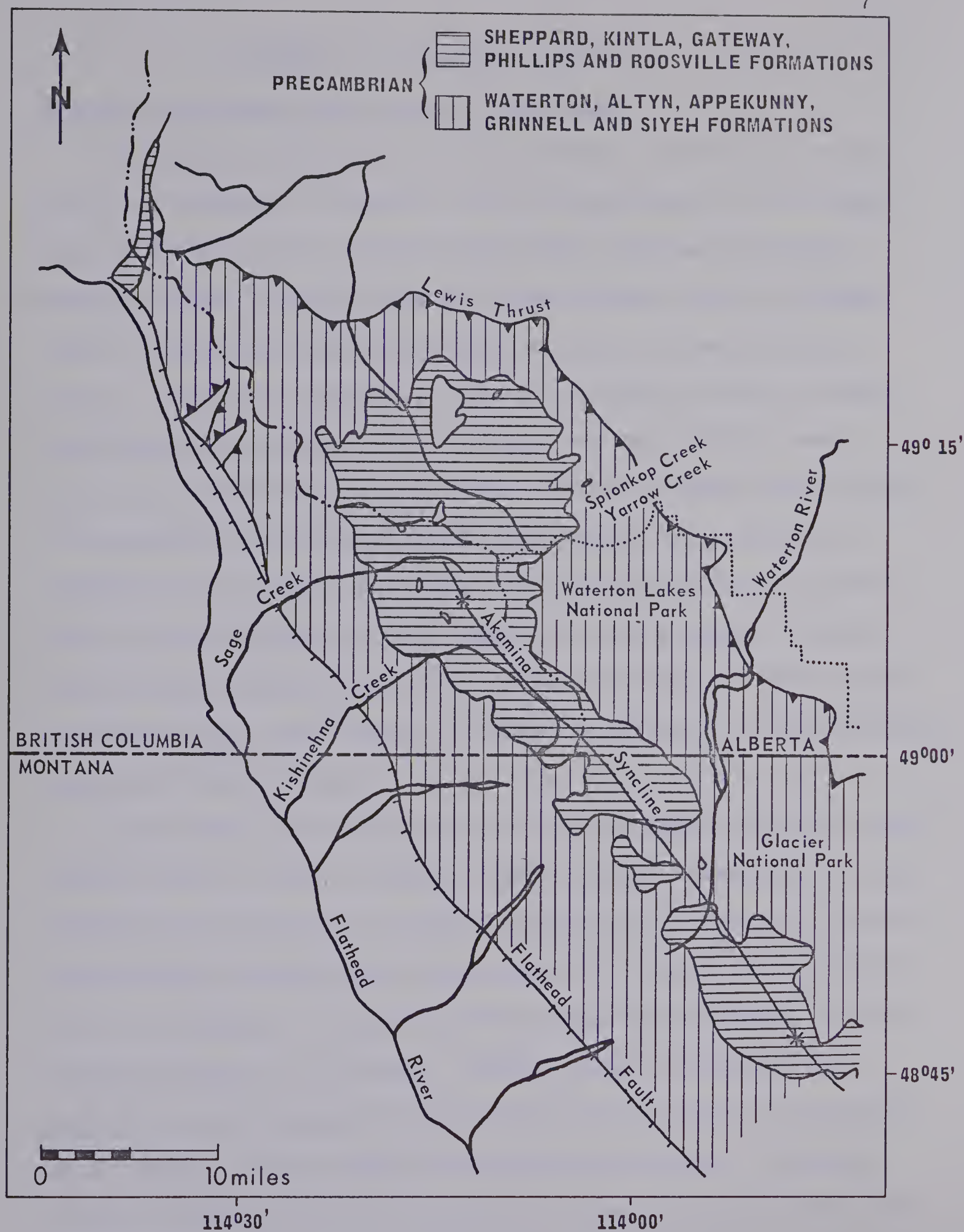


Fig.6. Regional geology of Lewis series (after PRICE, 1965).

CHAPTER II - GENERAL GEOLOGY

Regional geological and tectonic setting

The Lewis series and its equivalent, the Purcell supergroup, is exposed in Canada south of latitude 51°N in three major tectonic units, the Purcell Arch, the Western Rocky Mountain fault complex, and the Lewis thrust plate (BURWASH, 1968). The Lewis series outcrops within the Lewis thrust plate. The plate itself is a sheet of gently folded, almost horizontal Precambrian strata which has been thrust over Paleozoic and Mesozoic formations. It is folded into a series of en-echelon structures which trend south to southeast. BOSTOCK et al. (1957) conclude that the most dominant of the folds, the Akamina syncline, parallels the Purcell anticlinorium, formed west of the Rocky Mountain Trench. HUME (1932) concludes that this warping occurred subsequent to the movement along the Lewis thrust.

The Lewis thrust sheet is cut to the west by the Flathead fault, one of a set of normal faults formed subsequent to the thrusting. BALLY et al. (1966) believe that this is a listric normal fault formed after emplacement of the Lewis overthrust by 'back-slippage' along a pre-existing thrust during a phase of post-orogenic uplifting. JONES (1969) classifies the thrusting and subsequent normal faulting as part of the Laramide orogeny of the Middle Paleocene and Eocene. Movement on the Flathead fault is believed to have continued well into the Oligocene.

Regional metamorphism within the Lewis thrust sheet is

of low grade. LEECH (1962) found that in the western Rockies this metamorphism was near the transition from the quartz-albite-epidote-biotite subfacies to the quartz-albite-epidote-almandine subfacies of the greenschist facies. This metamorphism occurred during the East Kootenay orogeny at approximately 750 million years ago (BURWASH et al., 1965) and should have had little effect on the eastern Rockies.

Stratigraphy

As previously noted, the rocks of the Lewis thrust sheet belong to the Precambrian Lewis series and its equivalents, the Purcell and Belt supergroups. These rocks are for the most part shallow-water, subaerial and marine quartzites, argillites, and carbonates with minor submarine lava flows and deeper water sediments. The stratigraphic succession as given by PRICE (1962) is shown in Fig.7. Correlations with Purcell and Belt formations are shown in Fig.8. The formations of interest in this study, the Appekunny and Grinnell formations, were defined by FENTON and FENTON (1937) as follows:

Appekunny formation - argillite, interbedded with quartzite, conglomerate, and minor beds of argillaceous limestone; prevailing green, greenish-gray to brownish, with some dull red, white, and purplish beds. Thin-bedded to thick-bedded, with fine laminae; massive only in quartz conglomerates and quartzites. Grades into

adjacent formations.

Grinnell formation - red or purplish argillites and white to light-green quartzites, lying between the Appekunny and the succeeding Piegan group. Textures, colors, and bedding are highly variable; ripple marks, mud cracks, and current marks are abundant, as are rain or hail prints in some members.

It is possible, as WALDRON (1942) points out, that the Appekunny and Grinnell formations are differently coloured phases of one formation, with the line of distinction between them being one oblique to the stratification.

As JOHNS (1964) notes, the western boundary of the Rocky Mountain trench approximates the western limit of deposition of Grinnell-type rocks except where modified by local embayments. JOHNS (op.cit.) believes that a northeastern iron-rich source area was subjected to subaerial erosion, and that hematite formed during deposition produced the distinctive colour of Grinnell strata. The green discoloration in the Appekunny possibly represents reduction of ferric iron to ferrous iron after deposition in water, thereby producing the green tinge characteristic of beds in this unit. ADSHEAD (1963) from a study of the overlying Siyeh formation near the Yarrow Creek - Spionkop Creek deposit, concludes the source area for the Siyeh to have been southeast of the site of deposition. He concludes that the source rocks were low-lying fine grained, low-grade metamorphic schists and phyllites essentially

ERA	PERIOD OR EPOCH	GROUP FORMATION	LITHOLOGY	THICKNESS (feet)
PRECAMBRIAN	PURCELL (LEWIS)		EROSIONAL UNCONFORMITY	
		MOYIE INTRUSIONS	Diorite sills and dykes	
		ROOSVILLE FORMATION	Green argillite, siltstone, sandstone, stromatolitic dolomite	3500±
		PHILLIPS FORMATION	Red sandstone, siltstone, argillite	500-700
		GATEWAY FORMATION (upper member)	Argillite, argillaceous siltstone, dolomite dolomitic sandstone, and argillite	1150-3000
		SHEPPARD FORMATION	Quartzitic & dolomitic sandstone, dolomite, oolitic dolomite, argillite, siltstone, pillowed andesite	150-900
			EROSIONAL UNCONFORMITY IN PART	
		PURCELL LAVA	Chloritized andesite, & amygdaloidal andesite, pillowed andesite	00-600
		SIYEH FORMATION	Limestone, dolomite, argillite & sandy limestone & dolomite, argillite, stromatolitic limestone	1130-3000
		GRINNELL FORMATION	Red argillite, sandstone & siltstone; white, green & red quartzite	350-1700
		APPEKUNNY FORMATION	Green argillite; white, grey & green quartzite; sandy argillaceous dolomite & dolomitic argillite; siltstone	1500-2000
		ALTYN FORMATION	Argillaceous limestone & dolomite; sandy dolomite, argillite, & stromatolitic dolomite	500-4000
		WATERTON FORMATION	Limestone & dolomite, argillite, & argillaceous dolomite	1500+

Fig.7. Stratigraphic succession (after PRICE, 1962).

	Alberta & B.C. (PRICE, 1962)	B.C. (LEECH, 1962)	Glacier Park (ROSS, 1959)	Coeur d'Alene Mountains (JOHNS, 1961)	Lewis & Clarke Flathead Ranges (JOHNS, 1964)
MISSOULA GROUP	ROOSVILLE	ROOSVILLE	UNDIFFERENT- IATED MISSOULA GROUP	(Top eroded)	(Top eroded)
	PHILLIPS	PHILLIPS			AHERN
	GATEWAY	GATEWAY			HOADLEY
	SHEPPARD	GATEWAY	SHEPARD	STRIPED	CAYUSE
PIEGAN GROUP	PURCELL LAVA	Purcell lava mapped as top of SIYEH	PURCELL BASALT	PEAK	MILLER PEAK
	SIYEH	SIYEH KITCHENER	LOWER MISSOULA GROUP	WALLACE	HELENA
			SIYEH		SPOKANE
					GREYSON NEWLAND
RAVALLI GROUP	GRINNELL	CRESTON	GRINNELL	ST. REGIS	GRINNELL
	APPEKUNNY		APPEKUNNY	REVETT	APPEKUNNY
	ALTYN		ALTYN	BURKE	ALTYN
PRE-RAVALLI GROUP	WATERTON	ALDRIDGE	(base not exposed)	PRICHARD	(base not exposed)
	FORT STEELE				

Fig.8. Correlation chart of Belt-Purcell-Lewis formations.

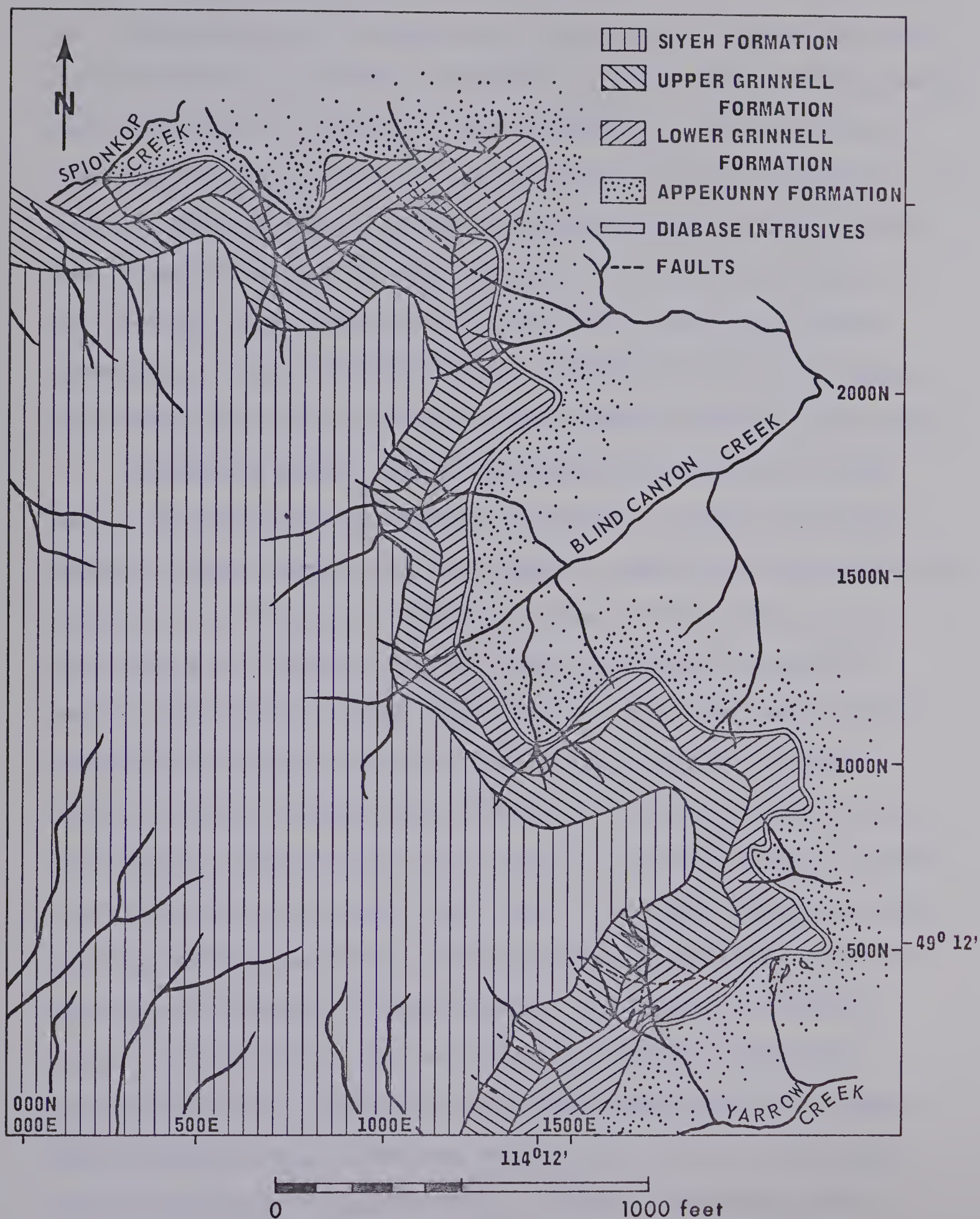


Fig.9. Geology of the Yarrow Creek - Spionkop Creek deposit (after STEVENSON, 1968).

composed of quartz and fine-grained micas.

Deposition of the Appekunny and Grinnell formations must have occurred, as noted in CHAPTER I, about 1300 million years ago according to OBRADOVICH and PETERMAN'S (1967) dates for the equivalents of the underlying and overlying formations of 1315 ± 35 million years. This is substantiated by HUNT (1961), who obtained an age of approximately 1100 million years for the Purcell lava found at the top of the overlying Siyeh formation, and by OBRADOVICH and PETERMAN'S (loc.cit.) ages of 1600-1850 million years for the basement rocks of the area.

SMITH and BARNES (1966) recognize two cycles of deposition in the Belt supergroup of Montana. These are represented by the Pre-Ravalli and Ravalli, and the Piegan-Missoula groups. The Sheppard formation forms a third minor cycle. Each cycle is characterized by deep, followed by shallow water, deposition. This gives rise to two contrasting fine grained rock types in each cycle. The first of these is a black to gray carbonaceous siltite (a slightly metamorphosed siltstone), thickest near the axis to the Belt-Purcell depositional trough, commonly very fine and evenly laminated and lacking mud-crack casts, intraformational mud-chip conglomerates and abundant stromatolites. Carbonate is commonly present as calcite. The second is a reddish, hematite-bearing siltite, thickest on the basin margins, with laminated sediments with abundant mud-crack casts and intraformational mud-chip conglomerates. Towards the axis of the trough this second type commonly passes laterally into

greenish siltite that contains similar but less abundant sedimentary features. Carbonate is usually absent but where present is in the form of dolomite. It is to this second, shallower-water type that the Appekunny and Grinnell formations belong, with the transition from the first to the second cycle of deposition taking place at the Grinnell-Siyeh contact.

REESOR (1957) states that deposition of the Lewis series occurred in a slowly subsiding basin or trough of relatively high stability. The rate of subsidence kept close pace with the quantity of supply, with some localities exposed to sub-aerial conditions while others were submerged below wave-base. REESOR (op.cit.) concludes that these conditions are those which would exist on the flood plain of a large subsiding delta. PRICE (1964) concludes that deposition was on or adjacent to the flood plain of a large subsiding delta with the very shallow water Grinnell sediments probably accumulating on a non-marine flood plain or in a brackish tidal flat environment. RICE (1937) found that most of the ripple marks in the Creston formation (the equivalent of the Grinnell-Appekunny formations) were of the symmetrical or wave-ripple type and concludes from this that deposition took place under fresh water conditions. The presence of salt crystal casts within the Kintla formation indicates however, that at times brackish water deposition did occur.

In the Yarrow Creek - Spionkop Creek vicinity the Appekunny formation consists mainly of argillites in the



Fig.10. Mottling of green argillite within red Grinnell argillites, Yarrow Creek.

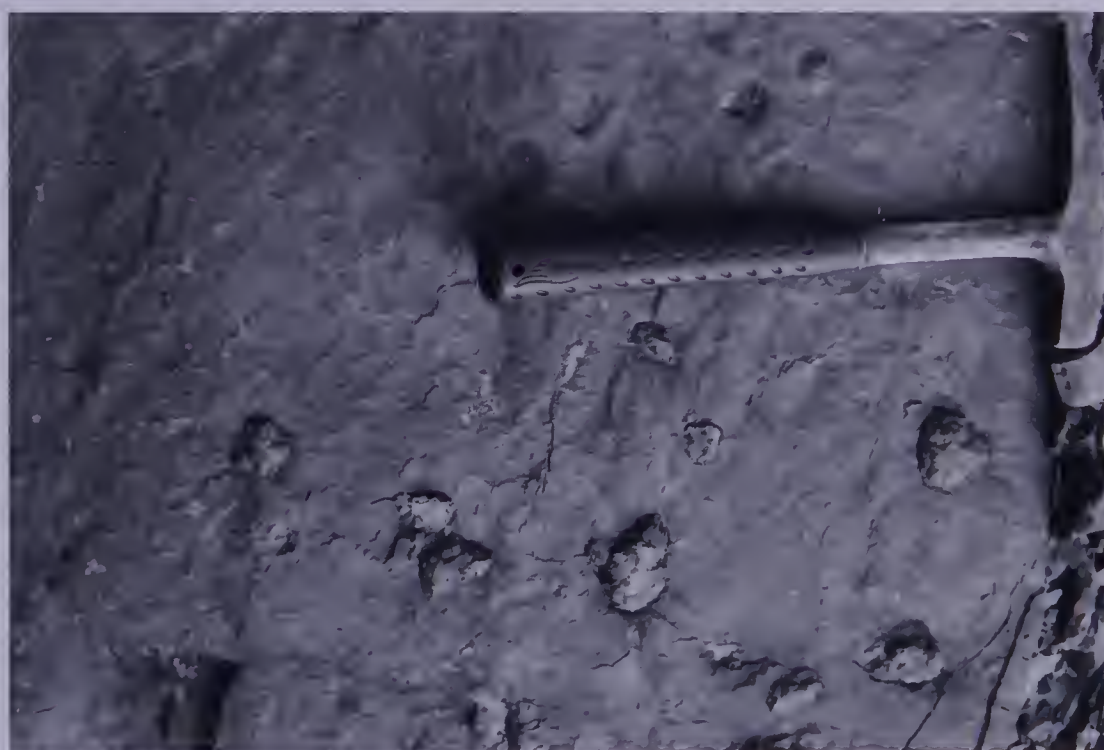


Fig.11. Mud balls within upper Appekunny argillites, Yarrow Creek.

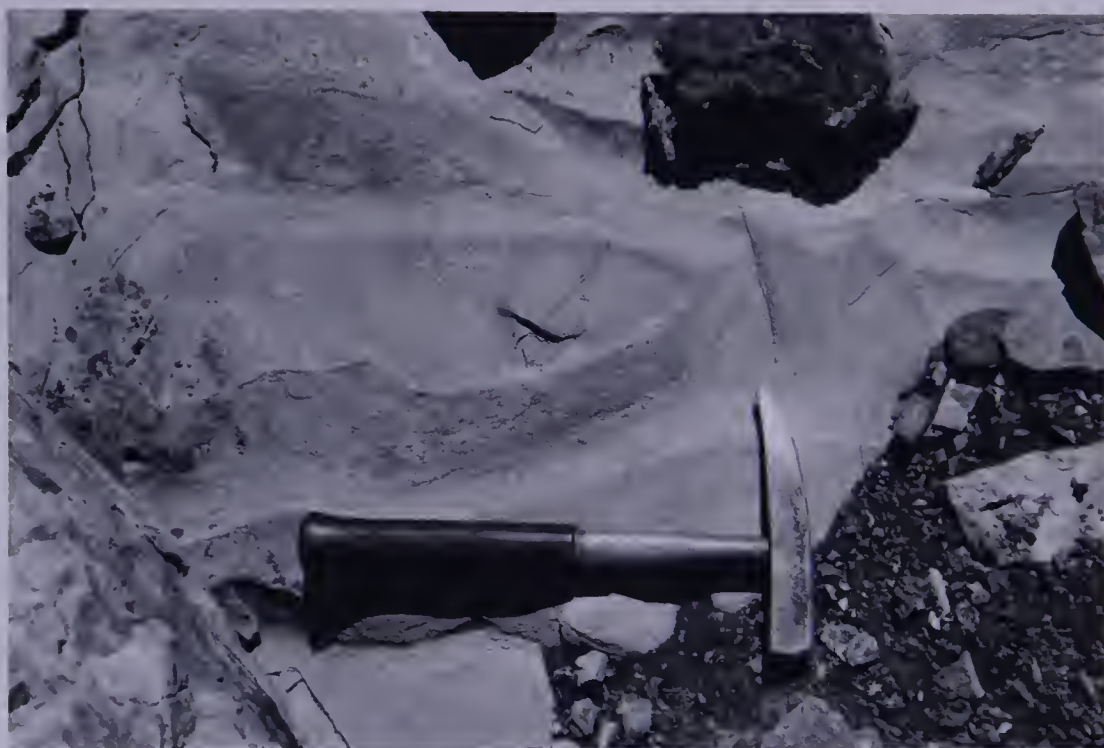


Fig.12. Current marks within upper Grinnell quartzites, Yarrow Creek.



Fig.13. Ripple marks in upper Grinnell quartzite, Yarrow Creek.



Fig.14. Cross-stratification within Grinnell quartzite, Yarrow Creek.

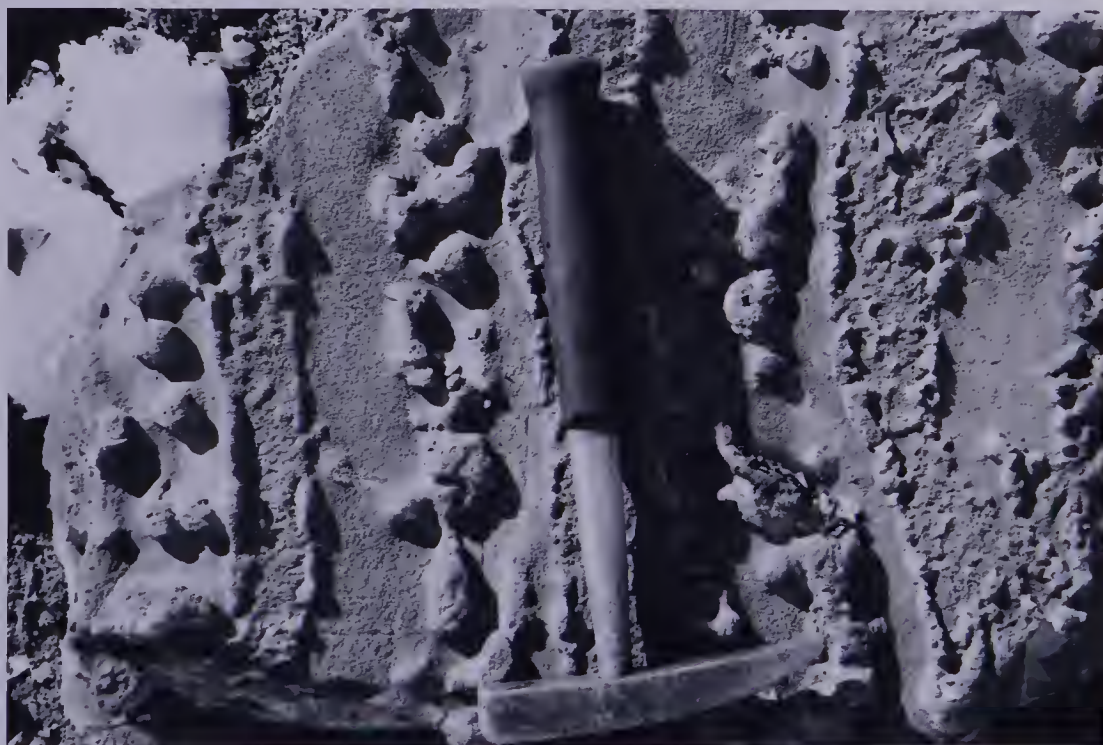


Fig.15. Sole markings (?) within lower Siyeh quartzite, Yarrow Creek.

lower part, but light greenish-gray, coarse-grained quartzites become dominant in the upper part. A gradational contact exists with the overlying Grinnell formation. The lower Grinnell contains approximately 300 feet of reddish argillite, mottled and interbedded with minor amounts of yellowish-green argillite. Thin bands (usually not more than a few inches thick) of white to brown, medium-grained quartzite, and reddish, fine-grained sandstone are present, increasing in abundance towards the upper Grinnell. The upper Grinnell consists of approximately 200 feet of red, and minor green argillite interbedded with white, green, and red quartzite. The quartzite beds range in thickness from a few inches to a few tens of feet. Mud cracks, ripple marks, and cross-bedding are commonly associated with the quartzite beds. STEVENSON (1968) noted that a high percentage of the Grinnell mud cracks are concave upwards and concludes that this indicates a fresh water environment. The upper Grinnell grades rapidly into the dark gray carbonaceous argillites and white to light green quartzites of the lower Siyeh. A few thin quartzite beds containing pyrite spheres occur about 30 feet above the base of the Siyeh formation throughout the Lewis thrust plate. STEVENSON (op.cit.) states that deposition of the Appekunny and Grinnell formations in the Yarrow Creek - Spionkop Creek area took place under either subaerial deltaic or valley-flat flood plain conditions.

Summary and conclusions

Deposition of the Grinnell and Appekunny quartzites and argillites took place under shallow water, subaerial, deltaic or tidal flat conditions around 1300 million years ago. The source area lay to the east. The sediments represent the end of a cycle of deep water sedimentation followed by shallow water sedimentation with the transition back to deeper water deposition occurring at the top of the Grinnell formation. Deposition was for the most part in fresh water.

Structure

PRICE (1962) outlined two distinct groups of structures within the Clarke Range. The first of these, a series of thrust faults and related folds, is generally cut by the second, a group of younger normal faults dipping towards the southwest or west. BALLY et al. (1966) suggest that this represents late Mesozoic and early Tertiary thrusting followed by late Tertiary normal faulting. They find that the normal faults, which are steep at the surface, also flatten at depth (listric normal faults) and may merge with older thrust faults.

The major examples of these structures within the Clarke Range are the Lewis thrust and related folds, and the Flat-head fault, truncating the Lewis thrust sheet to the west (see Fig.6). In the Clarke Range the Lewis thrust is essentially a bedding thrust relative to the stratigraphic layering of the thrust sheet. The thrust sheet itself is

bounded at the base by the Lewis thrust and above by thrust faults which are splays from the Lewis thrust. It is folded into a broad synclinorium extending from Cameron Lake in the south to Mount McCarty in the north (the Akamina syncline). As previously noted, the thrust sheet is truncated on the west by the Flathead fault, which PRICE (1962) concludes to be normal fault with the west side displaced downwards, giving a maximum stratigraphic separation of approximately 25,000 feet.

A third set of northeasterly trending transverse faults also occurs in the Clarke Range. PRICE (1967) concludes that these originated as gravity faults whose orientations were controlled by the anisotropy of the basement rocks underlying the region.

The Yarrow Creek - Spionkop Creek area is located within the Lewis thrust sheet on the east side of the Akamina syncline. The sediments in the area strike approximately N30°W and dip approximately 20°SW (STEVENSON, 1968). Dips vary from 10° to 40°. Numerous reverse faults, striking from N15°W to N45°W and dipping from 70° to 90° occur within the central part of the mineralized zone on Yarrow Creek. Displacements are from a few inches to 200 feet. A few thrust faults striking N45°E and dipping 15°-25° NW also occur. STEVENSON (op.cit.) noted that some of the faults cut the lower Grinnell formation but not the intrusive diabase sill in the Appekunny formation below it, and concludes from this that these faults are the result of intrusion of the

sill into the incompetent sediments. Several fault zones are occupied by dykes while others cut the sills and dykes in the area. This probably reflects two periods of faulting occurring prior to and during intrusion of the sills and dykes, and subsequent to the intrusion of the sills and dykes during the main periods of post-Precambrian thrusting and normal faulting.

Summary and conclusions

Faulting and related folding within the Clarke Range and, in particular, within the Yarrow Creek - Spionkop Creek area took place in four main episodes:

- 1) Precambrian gravity faulting related to the anisotropy of the basement rocks.
- 2) Precambrian normal and reverse faulting caused by intrusion of the diabase sills and dykes.
- 3) Late Mesozoic and early Tertiary thrust faulting.
- 4) Late Tertiary normal faulting.

The first two of these occurred on a minor scale but, as in the Yarrow Creek - Spionkop Creek area, may be locally important. Gravity faulting may be more widespread than noted since many of the creeks in the Clarke Range trend southwesterly and may reflect unmapped gravity faults. The later periods of thrust and normal faulting produced the dominant structures of the Clarke Range, however.

Igneous activity

Igneous activity within the Lewis thrust sheet was of three types. The first of these is represented by Moyie-type intrusives of Precambrian age. These are characterized by chloritized diorite and diabase sills and dykes concentrated within the Altyn, Appekunny, Grinnell, and Siyeh formations, although some do occur as high in the stratigraphic sequence as the Kintla formation. HUNT (1962) dates two periods of Purcell plutonism at 1580-1400 million years and 1110-1073 million years. This latter date is also that for the second type of igneous activity, the Purcell volcanism, which resulted in the extrusion of andesitic lavas which HUNT (1964) concludes to belong to the trachybasalt family. The third type of igneous activity consisted of the intrusion of leucocratic alkalic intrusives which PRICE (1962) states to be of Cretaceous and/or Tertiary age. These occur as narrow dykes and irregular anastomosing stock-like masses, trachyte being the most common rock type, with aegirine-augite and aegirine trachytes and syenites, latites, felsites, and intrusion breccias also present (PRICE, op.cit.).

Within the Yarrow Creek - Spionkop Creek area igneous activity is restricted to Moyie-type sills and dykes, the principle one of these being a diabasic sill varying from a few feet to 75 feet in thickness and occurring generally below or within the uppermost quartzite bed of the Appekunny formation. This diabase sill transgresses up through the Grinnell formation on the ridge between Blind Canyon and

Spionkop Creeks. HUNT (1958,1961) dated a sill occupying the same stratigraphic position on Blakiston Brook in Waterton Lakes National Park, believed by the author to be the same sill, at 1075 million years.

Diabasic sills and dykes also occur within the Grinnell formation in the Yarrow Creek - Spionkop Creek area, the dykes commonly occupying fault zones within the formation, while the sills generally are not cut by these same faults. This is believed to reflect movement of the magma into faults initiated by the intrusion of the diabasic sills. The largest and most extensive diabase sill itself intrudes some fault zones as a dyke while being cut by other faults.

The diabasic intrusives within the Yarrow Creek - Spionkop Creek area all show heavy alteration of the primary minerals. Alteration products accounted for up to 75% of the sample in those specimens studied. The most common of these secondary minerals are chlorite, sericite, serpentine, epidote, and carbonate. The primary minerals are plagioclase, augite, quartz, biotite, and chalcedony. Large radiating plagioclase phenocrysts (An_{50}) are common in the intrusives (Fig.17). HUNT (1961) argues that the textures of the Blakiston Brook and related Purcell intrusions can be related to deuteric alteration and autometamorphism of quartz diabase sills.

These diabase sills and dykes are believed by the author to have been essentially contemporaneous with the extrusion of the Purcell lava. HUNT'S (1958,1961) date for the Blakiston

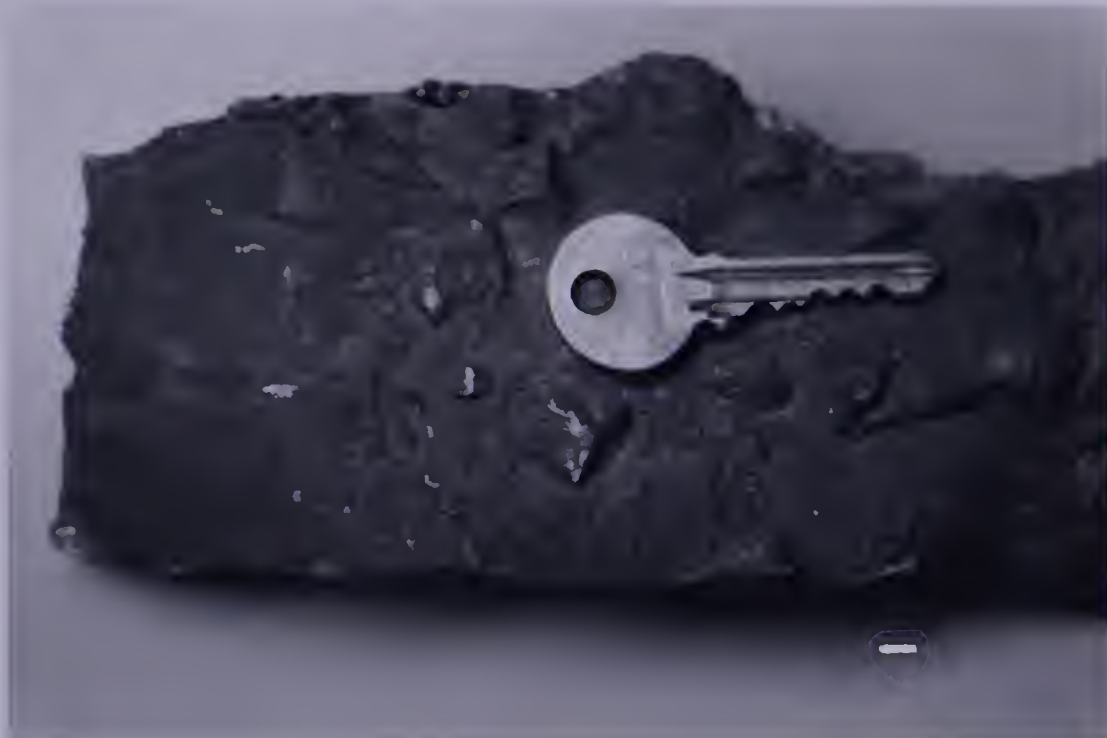


Fig.16. Salt crystal casts within Kintla formation argillites, Yarrow Creek.



Fig.17. Radiating plagioclase phenocrysts within a diabasic sill, Yarrow Creek.

Brook sill of 1075 million years corresponds closely with his date of 1100 million years for the extrusion of the Purcell lava within the Siyeh formation. Some of the faulting within the area seems to have been caused by the intrusion of the main diabase sill into unconsolidated and hence incompetent sediments. Amygdules found within many of the sills and dykes probably reflect a high gas pressure as compared to a lower external pressure and are therefore felt to reflect a shallow depth of burial. HUNT (1961) states that in the Waterton Lakes area the uralitization of the sills was arrested by more rapid cooling than in other areas, indicating a probable shallow depth of burial.

CHAPTER III - METALLIFEROUS DEPOSITS

Introduction

DAWSON (1886) first reported the occurrence of copper in the North Kootenay Pass region of the Lewis thrust sheet. This mineralization was in the form of chalcopyrite within the Purcell lavas and diabasic dykes. ROSS (1959) notes exploration activity within Glacier National Park around 1890 centered on copper ore near the heads of Quartz and Mineral Creeks. He also reports the staking of some one hundred claims around 1898 on two parallel veins associated with intrusive metagabbro dykes. These copper deposits were in veins and fracture zones, many of which occurred on the borders of metagabbro dykes. During the first decade of the 20th Century small scale mining was also undertaken within Waterton Lakes and Glacier National Parks. This was centered on two copper-bearing diabase dykes within Lewis series rocks on Blakiston Brook in Waterton Lakes National Park and on Chief Mountain in Glacier National Park. The Yarrow Creek deposit was initially staked during this same period.

Interest lapsed until the fall of 1963 when, with the rediscovery of copper-bearing quartzites in the Grinnell formation on Yarrow Creek, staking of the area began. By the time that Kennco Explorations (Western) Limited optioned these claims in the fall of 1966 some 150 mineral claims had been staked in the area and extensive leasing of Crown land had taken place. An exploration program was carried out on the Grinnell and the equivalent Creston formation by Kennco

Explorations (Western) Limited in the fall of 1966 and the summer of 1967. Further exploration has since been undertaken in the same area by Akamina Minerals Limited and Cominco Limited.

The Yarrow Creek - Spionkop Creek deposit

STEVENSON (1968) reports that in the Yarrow Creek - Spionkop Creek area chalcocite and bornite occur for 2500 feet laterally in quartzite beds on the north side of Yarrow Creek. A similar occurrence of cupriferous quartzites has since been noted on Spionkop Creek, and on the basis of traverses run in this area, is suspected to continue into the Blind Canyon. The mineralization occurs only in white and green quartzite beds and in associated green argillite. The thicknesses of the cupriferous beds vary from a few inches to a few feet with copper contents up to 5% Cu. Mineralization is in the form of copper sulphides and carbonates disseminated within the quartzites and, in many instances, localized within argillite pebbles within the quartzites.

The background copper content of unmineralized sections of the Grinnell formation was determined by STEVENSON (op.cit.) to be 5-10 ppm in the red argillites and 7-12 ppm in the quartzites. Copper mineralization is generally restricted to quartzites of the upper Grinnell but has been noted in small amounts in the quartzites of the upper Appekunny and in the quartzites and black argillites of the lower Siyeh.

The richer mineralized zones occur near fault zones and near intrusive diabasic sills and dykes. Minor sulphide veining occurs within the quartzites near diabase dykes.

The diabasic sills and dykes commonly exhibit sulphide mineralization on their borders, this mineralization being richest and most extensive in those portions of the intrusives within the upper Grinnell. One section of intrusive within the upper Grinnell on the ridge between Blind Canyon and Spionkop Creeks carries from 1.83% to 3.45% Cu over a possible volume of 10,000,000 cu. ft. but is essentially barren where the intrusive is within the lower Grinnell and upper Appekunny. However, copper has also been noted within some intrusives within the lower Grinnell, Appekunny, and Siyeh formations subsequently.

Related mineralization

Similar deposits have since been located within the Grinnell formation on Whistler Mountain, Grizzly Creek, and Commerce Creek, being associated with intrusive rocks only in the latter case. In this instance the area has been intruded by a series of syenite sills and dykes. Numerous smaller occurrences have also been noted, with copper having been detected at some horizon in the upper Grinnell on all traverses made by the author through this formation in the Lewis thrust sheet. The copper-bearing horizons occur, in nearly all cases, within the white and green quartzite beds of the upper Grinnell, and are most prevalent near intrusions

and zones of faulting or folding. Copper has been noted within red quartzites in only one instance, as a few disseminated specks of covellite within an upper Grinnell quartzite on Commerce Creek. Recent investigations have revealed similar stratiform copper occurrences within green quartzites and green and black argillites and siltstones at several stratigraphic horizons within the red sequences of the Gateway and Kintla formations.

Summary and conclusions

Copper mineralization occurs within the Lewis thrust sheet principally in the form of stratiform deposits associated with certain horizons within the red sedimentary sequences. In the case of the Grinnell formation the principle occurrences are located within the quartzites of the upper Grinnell. Other copper-bearing horizons have been noted, however, within the quartzites of the Appekunny, Siyeh, and Kintla formations. Mineralization is most prevalent near intrusions and zones of faulting and folding but has been noted where these are absent.

The widespread nature of the mineralization and its stratabound character at once lead one to suspect a syngenetic sedimentary origin for the copper. The localization of enriched cupriferous zones near zones of faulting and folding in this case probably reflects later, localized mobilization and redeposition of copper minerals by secondary fluids.

CHAPTER IV - ORE MICROSCOPY

Sedimentary suiteMineralogy

The copper sulphides noted, in the order of decreasing abundances, are covellite, bornite, chalcopyrite, chalcocite, chalcopyrrhotite, and cubanite. Other associated sulphides are pyrite, sphalerite, and galena. Magnetite, hematite, and spinel were the only oxides identified. Malachite is the dominant copper carbonate present, but azurite was found in some specimens.

The metallic mineral associations are of two types, depending upon the copper content of the sulphides present. The first of these is the 'low-copper' mineral assemblage of chalcopyrite or pyrite with other, non-copper-bearing minerals. The assemblages observed were:

- 1) Chalcopyrite
- 2) Pyrite + magnetite
- 3) Chalcopyrite + sphalerite
- 4) Chalcopyrite + hematite
- 5) Chalcopyrite + chalcopyrrhotite.

The simplest of these is that of chalcopyrite with no other associated metallics. Sphalerite and hematite are associated with chalcopyrite in some instances, however. None of the higher copper content sulphides were noted in any specimen in which chalcopyrite is the dominant copper sulphide. Pyrite was noted in only one sedimentary specimen. In this instance it was present as pseudo-oolitic pyrite

spheres within a bed of lower Siyeh quartzite. Minor magnetite was associated with the pyrite. Pyrrhotite was found in one specimen of upper Appekunny quartzite, however, it was in this case in solid solution with chalcopyrite as chalcopyrrhotite with exsolved chalcopyrite on planes at 60° to each other.

The 'high-copper' assemblages noted were:

- 1) Bornite + covellite
- 2) Bornite + covellite + chalcocite
- 3) Bornite + covellite + chalcocite + cubanite
- 4) Bornite + covellite + chalcopyrite
- 5) Bornite + covellite + galena
- 6) Bornite + covellite + magnetite.

The simplest of the 'high-copper' assemblages consists of bornite and covellite. Chalcocite, cubanite, magnetite, chalcopyrite, and galena were also noted in association with the bornite-covellite assemblage. Chalcocite was the most common of these, with chalcopyrite, galena, magnetite, and cubanite present only in minor amounts associated with the bornite and covellite. No pyrite or sphalerite were found within the 'high-copper' assemblages.

The gangue of the sedimentary ores consists of moderate- to very well-sorted quartz grains with minor chalcedony and carbonate and traces of microcline, perthite, gypsum, sphene, and alteration products of these. Quartz generally makes up approximately 95% of the rock with chalcedony and carbonate accounting for up to 45% in the more argillaceous specimens.

Very minor amounts of limonite, epidote, and sericite are present, mainly as alteration products of the feldspars.

Textural relationships

In the 'low-copper' assemblage there is no apparent relationship between the size of the metallics present and the size of the quartz grains of the quartzite. The quartz grains vary from 0.01 mm to 1.0 mm in diameter, with the average grain size being near 0.4 mm. The sulphide grains are from 0.01 mm to 2.0 mm in diameter but with the larger size crystals near the border between the fine grained argillite and the coarser grained quartzite. Where they are in contact the quartz and chalcopryrite generally exhibit smooth interfaces with evidence of solution of the quartz grains, giving 'inroads' of chalcopryrite into the quartz. The quartz grains themselves are very well rounded and highly spherical but show thick overgrowths of secondary quartz. The original arenites must therefore have been very porous prior to crystallization of these overgrowths.

Sphalerite, where present, occurs with the chalcopryrite and shows smooth regular interfaces with the chalcopryrite. Hematite is present as minute irregular grains within the argillites.

The pseudo-oolitic pyrite spheres occur in two forms. The first exhibits a colloform texture with layers of pyrite concentric around one or two nuclei in the sphere. The other is in the form of irregular pyrite grains approximately

0.05 mm in diameter aggregated into a sphere. The spheres range in size from 0.5 mm to 1.5 mm and average 0.9 mm in diameter as compared to 0.6 mm for the quartz grains of the groundmass. Minor pyrite crystals down to 0.01 mm in diameter were also noted, in most instances showing a subhedral to euhedral outline. The original quartz grains were very well rounded and moderately spherical but now exhibit thick overgrowths of secondary quartz. The pyrite spheres are generally in contact with the original quartz grain boundaries and have been overgrown by the secondary quartz. In some cases these overgrowths show signs of replacing the pyrite spheres, producing a rim of pyrite paralleling the pyrite sphere outline but within the quartz overgrowth. Minor pyrite was noted along both the original and the overgrown quartz grain boundaries.

An oolitic texture was noted in a specimen cut from a hematite-rich pebble within a quartzite bed in the upper Grinnell. In this case oolitic hematite was present both as individual ooliths and as aggregates of ooliths. The bulk of the hematite was present as cement between the rounded quartz grains. Quartz overgrowths were found only on those quartz grains outside the hematite-rich pebble.

Spherulitic chalcedony occurs within several of the quartzite beds sampled and is of approximately the same size as the surrounding quartz grains. One specimen showed a broken spherulite with quartz and sulphide replacing the outer layers, indicating that the spherulitic chalcedony was

derived from some other sedimentary environment.

In the 'high-copper' assemblages the sulphide grains tend to be somewhat smaller than the constituent quartz grains within the quartzites. This is not true within the argillite inclusions, however, where there is a tendency towards veining by sulphides. The quartz grains themselves are from 0.1 mm to 0.6 mm in diameter in the quartzites with the average grain size being near 0.4 mm. The average grain size of the argillite inclusions is less than 0.01 mm. The general range of sizes for the sulphides is 0.01 mm to 0.4 mm with some larger masses up to 1 mm in diameter. The average size for the disseminated sulphides would be close to 0.3 mm.

Bornite is generally present as irregular masses interstitial to and in some instances intergrown with and replacing the quartz grains (Fig.26). Usually a rim of covellite separates the bornite from the quartz grains.

Covellite occurs in two forms. The first of these is a pale to medium blue, weakly anisotropic variety associated with the bornite as irregular masses. The bornite-covellite interfaces in this instance are smooth and sharply defined. In the second form the covellite occurs as a dark blue, strongly anisotropic variety along fractures within the bornite and pale blue covellite. The interface between this and the other sulphides is somewhat more poorly defined and usually has an irregular outline, with rounded blebs of 'dark covellite' extending into the other minerals.

Chalcocite is frequently associated with the bornite

and covellite. It is present as irregular masses associated with the bornite in much the same manner as the 'pale covellite' and, in this form, contains 'dark covellite' along fractures in the same manner as the bornite and 'pale covellite.' It also occurs as small irregular masses with the bornite and 'pale covellite' and as veins within the same specimen as the bornite and 'pale covellite' but distinct from them.

Chalcopyrite and galena are also present in small quantities with the bornite and covellite in some cases. These minerals are restricted to those samples which are heavily mineralized and located adjacent to an intrusive. The chalcopyrite is present as minute blebs (<0.01 mm) associated with the bornite and covellite, as small needles and fracture fillings within the bornite, and as small veins along the cleavage in carbonate veins. Galena is present as small irregular grains associated with the bornite and covellite.

The other sulphide noted, cubanite, was found in only one specimen, in the form of small blebs at the bornite-'pale covellite' interface. Malachite is present in most specimens as coatings on the quartz and sulphide grains. Azurite is found in the same manner but in much lesser amounts.

Spinel and magnetite are the only two oxide minerals noted within the specimens examined. The spinel occurs as discrete detrital crystals having a triangular or rectangular shape, frequently surrounded or cut by sulphides. Magnetite

occurs as small irregular grains associated with the bornite and covellite in some specimens.

The gangue for the 'high-copper' assemblage is essentially the same as for the 'low-copper' assemblage. The quartz grains are generally very well sorted with thick overgrowths of secondary quartz on the original well rounded, spherical grains. In the more heavily mineralized of the specimens it is now nearly impossible to discern the contacts between the original quartz grains and the secondary overgrowths. Opaques tend to be intergrown with the overgrowths rather than with the original quartz grains and in some cases are present as a thin rim along the boundary between the two generations of quartz. Quartz grains with no visible overgrowths are occasionally found completely surrounded by sulphides.

Parageneses

The depositional sequence of the sedimentary suite must have been as follows:

- 1) Deposition of oolitic hematite and chalcedony.
- 2) Erosion and deposition of arenites and argillites.
- 3) Diagenesis involving the growth of pyrite spheres, secondary quartz overgrowths, and cogenetic bornite and 'pale covellite' (some chalcocite deposited instead of covellite).

Chalcopyrite and sphalerite precipitated.

- 4) Minor chalcopyrite, magnetite, galena exsolved from

bornite and covellite assemblage.

Exsolution of chalcopyrite - chalcopyrrhotite assemblage.

- 5) Replacement of bornite and 'pale covellite' by 'dark covellite' (also some replacement by chalcocite).
- 6) Weathering resulting in partial replacement of sulphides by malachite and azurite.

The pseudo-oolitic pyrite was almost certainly the earliest sulphide formed. The pseudo-oolitic nature of this pyrite, combined with the partial replacement of the outer shells of some of the spherulites and the very widespread occurrence within a limited stratigraphic horizon indicate that it was syngenetic or very early diagenetic in origin.

The bornite-covellite assemblages were obviously deposited after the burial of the quartzites. This is suggested by the fact that the sulphides commonly are intergrown with the quartz overgrowths rather than with the original quartz grains.

In the bornite-covellite assemblage itself, there seems to have been deposition of bornite and 'pale covellite', or of bornite and chalcocite in some instances, followed by alteration of these minerals to 'dark covellite' along fractures. Some replacement by a second generation of chalcocite is also indicated. The cubanite noted is probably a transition phase between the bornite and the 'pale covellite' caused by the unmixing of the latter two phases. The minor chalcopyrite, magnetite, and galena can be attri-

buted to exsolution of these phases from the bornite-covellite assemblage and would indicate a moderately high temperature of deposition for those few specimens containing such associations. The difference in colour and in the degree of anisotropism between the two covellite varieties is probably due to a varying Cu content or to submicroscopic mixing of covellite and chalcocite or digenite.

In the chalcopyrite-rich assemblages there seems to be a definite preference of the sulphides for deposition on quartzite-argillite contacts. This is probably due to a combination of ease of transport of dissolved ions through the quartzite during diagenesis with a favourable site of deposition in the carbonate-rich argillite. The chalcopyrite seems to have formed subsequent to the burial of the quartzites, since it is in many cases surrounding and intergrown with overgrowths on the quartz grains. The presence of the chalcopyrite-chalcopyrrhotite exsolution assemblage indicates a moderate to high temperature of deposition for one specimen. Sphalerite apparently formed at the same time as the chalcopyrite. Disseminated hematite within the argillites is probably due to remobilization of iron within the sediments after burial.

Intrusive suite

Mineralogy

Whereas the dominant copper minerals in the sedimentary suite were bornite and covellite, the only common copper

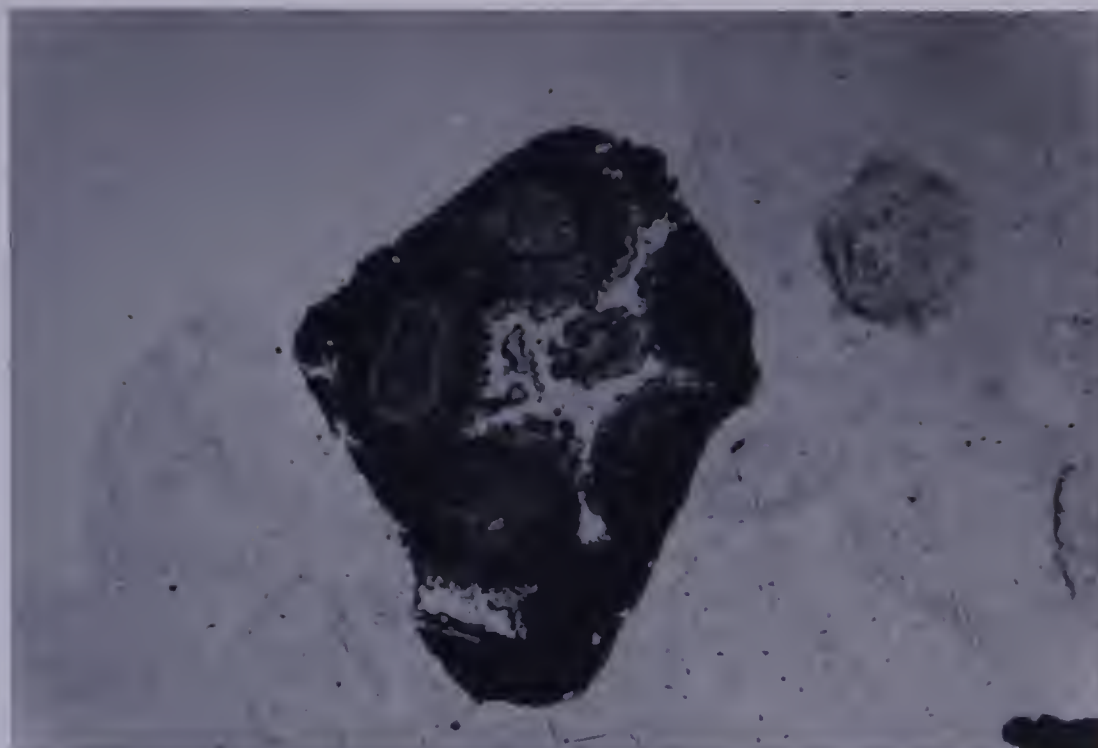


Fig.18. Fragment of oolitic hematite within upper Grinnell quartzite. (X16). RG - 36, Yarrow Creek (820N,3175E).

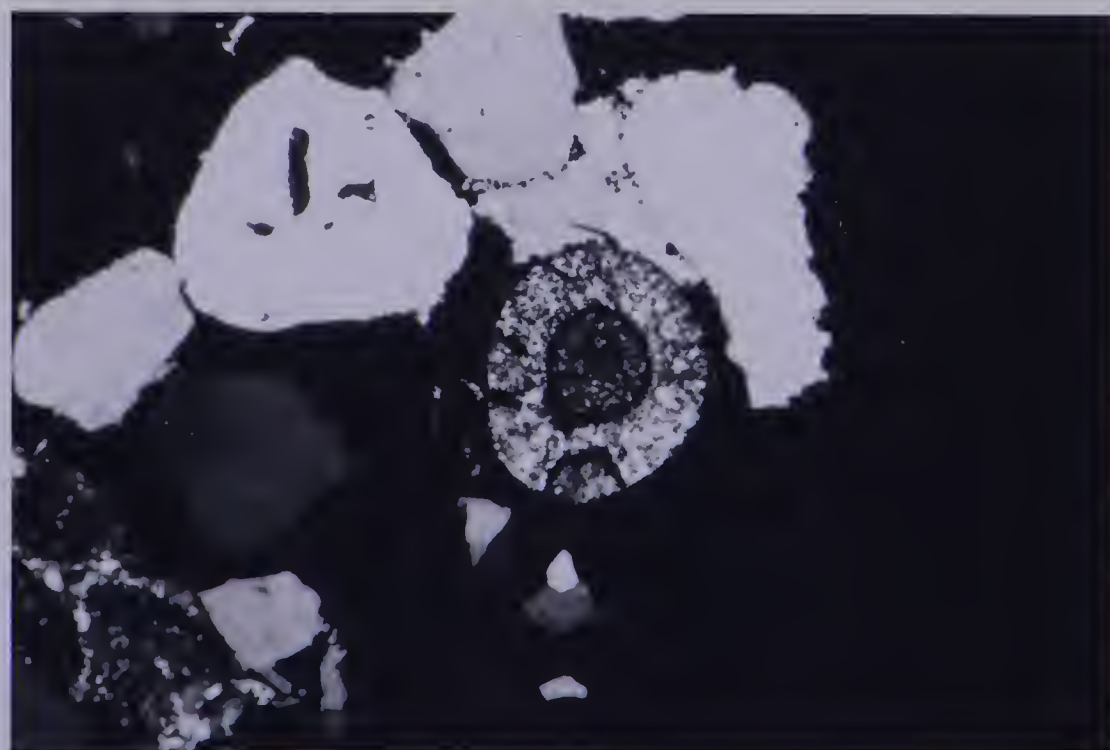


Fig.19. Fragment of oolitic chalcedony and hematite within upper Grinnell quartzite. (X16) X-nicols. RG - 36, Yarrow Creek (820N,3175E).



Fig.20. Chalcedony oololiths within upper Grinnell quartzite. (X16). RG - 10, Spionkop Creek (4475N,2120E).

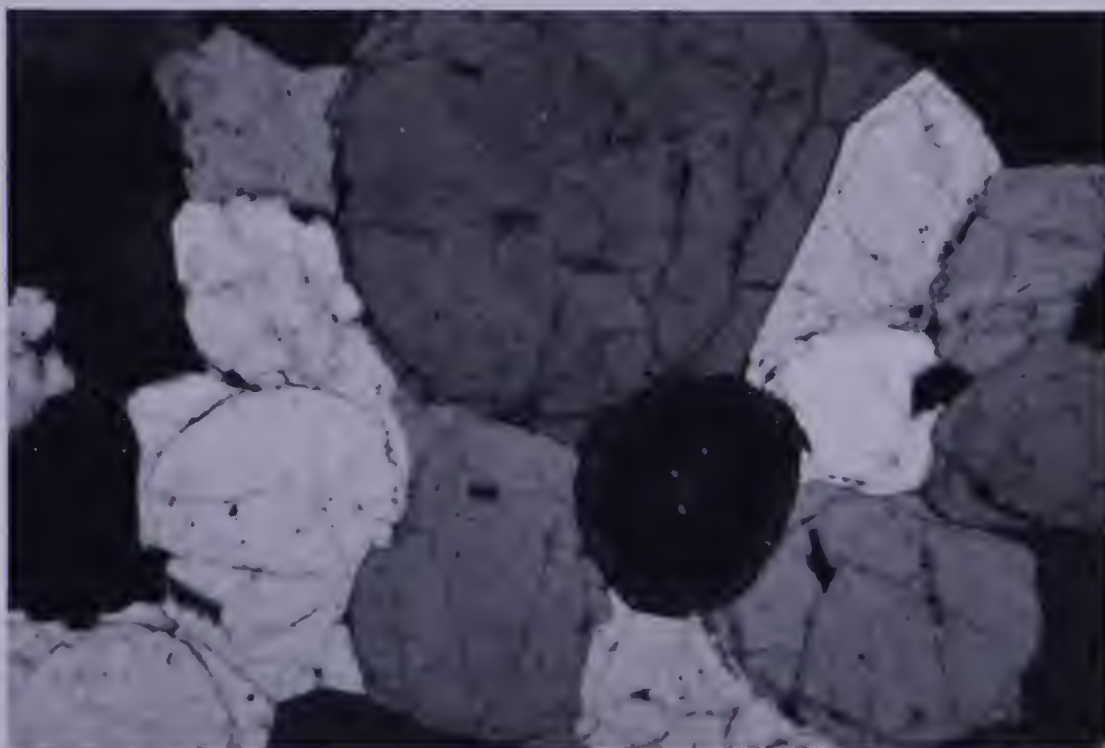


Fig.21. Chalcedony oololith and rounded quartz grains showing secondary overgrowths of quartz, upper Grinnell quartzite. (X16) X-nicols. RG - 4, Spionkop Creek (4775N,2265E).

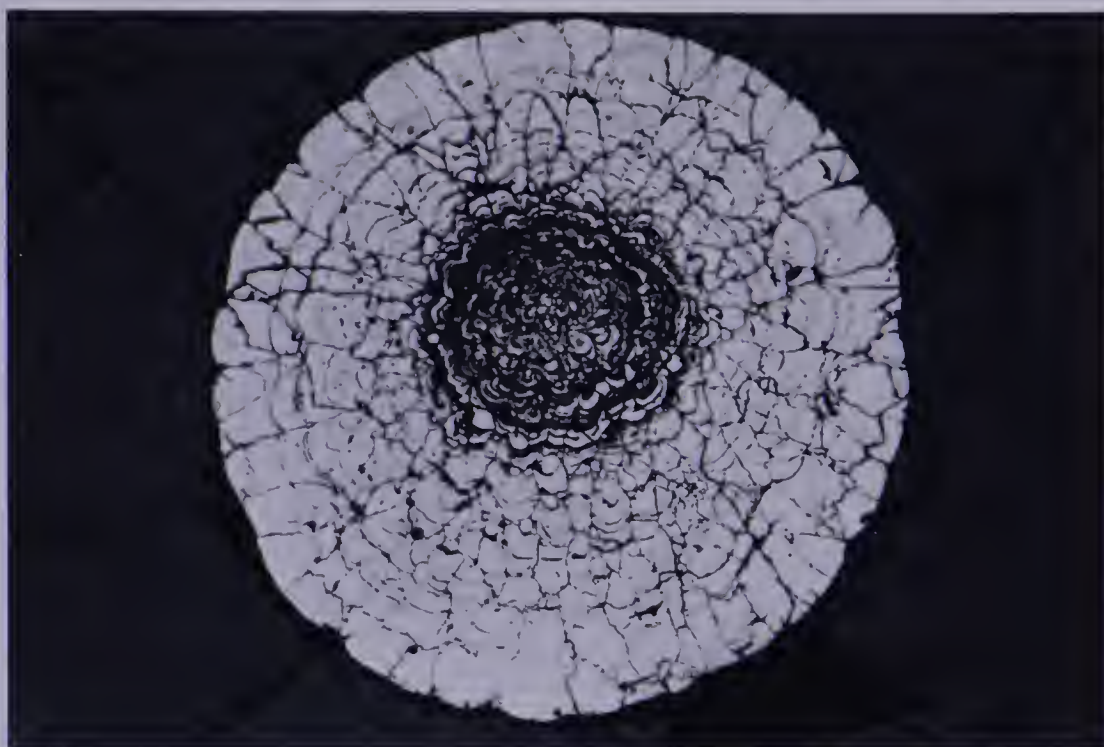


Fig.22. Pseudo-oolitic pyrite from lower Siyeh quartzite.
(X20). RG - 48, Yarrow Creek (500N,2670E).

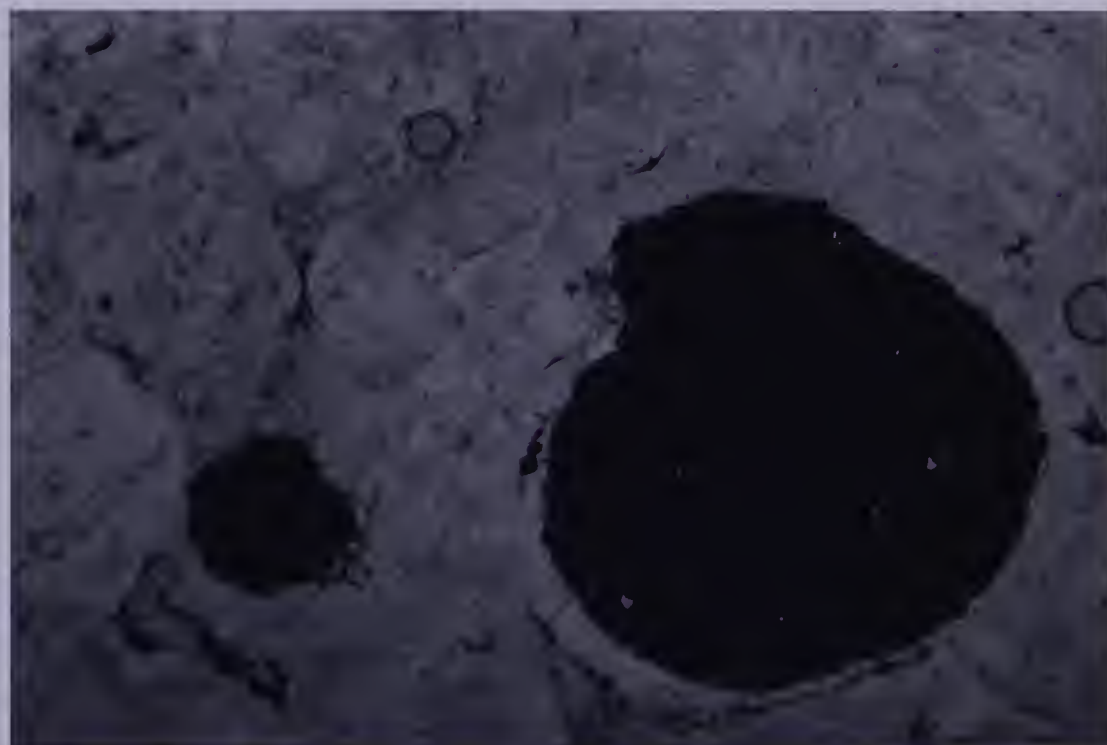


Fig.23. Pseudo-oolitic pyrite from lower Siyeh quartzite.
Shows rim of secondary pyrite within quartz overgrowth.
(X16). RG - 48, Yarrow Creek (500N,2670E).

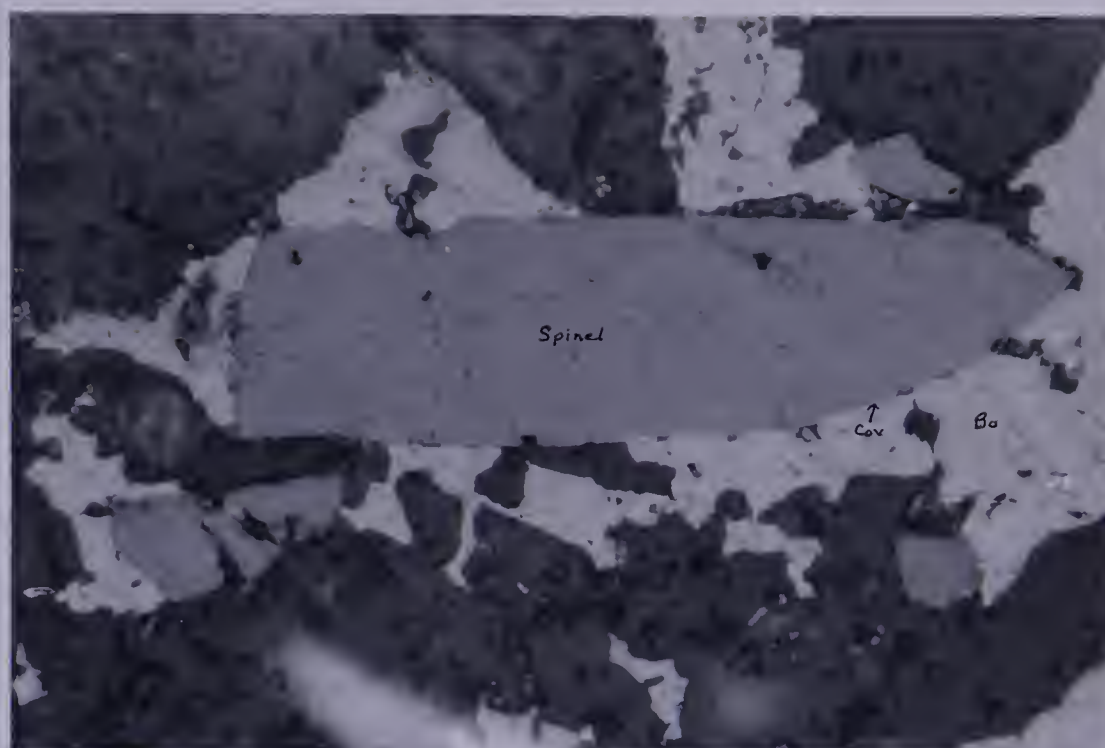


Fig.24. Detrital spinel surrounded by bornite and covellite in upper Grinnell quartzite. (X200). RG - 20, Yarrow Creek (1015N,3350E).



Fig.25. Detrital spinel within upper Grinnell quartzite. Showing conchoidal fracture. (X200). RG - 20, Yarrow Creek (1015N,3350E).

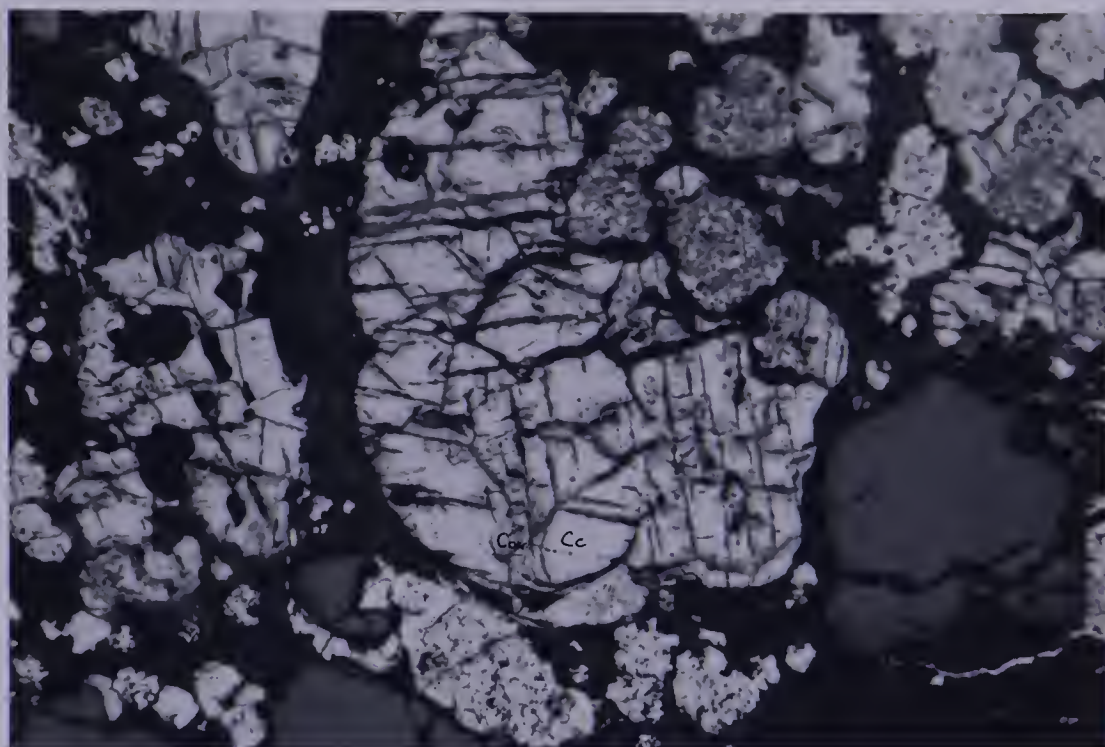


Fig.26. Bornite, covellite, chalcocite within upper Grinnell quartzite. (X16). RG - 4, Spionkop Creek (4775N,2265E).

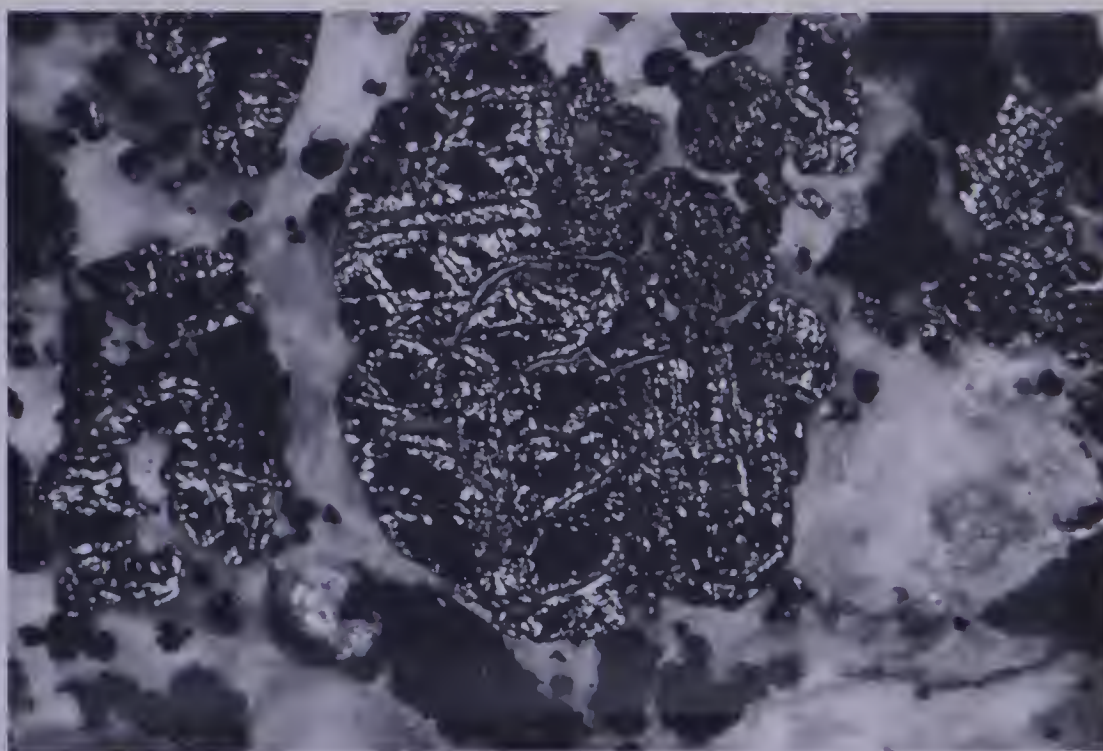


Fig.27. Same as Fig.26 above, X-nicols. (X16). RG - 4, Spionkop Creek (4775N,2265E).

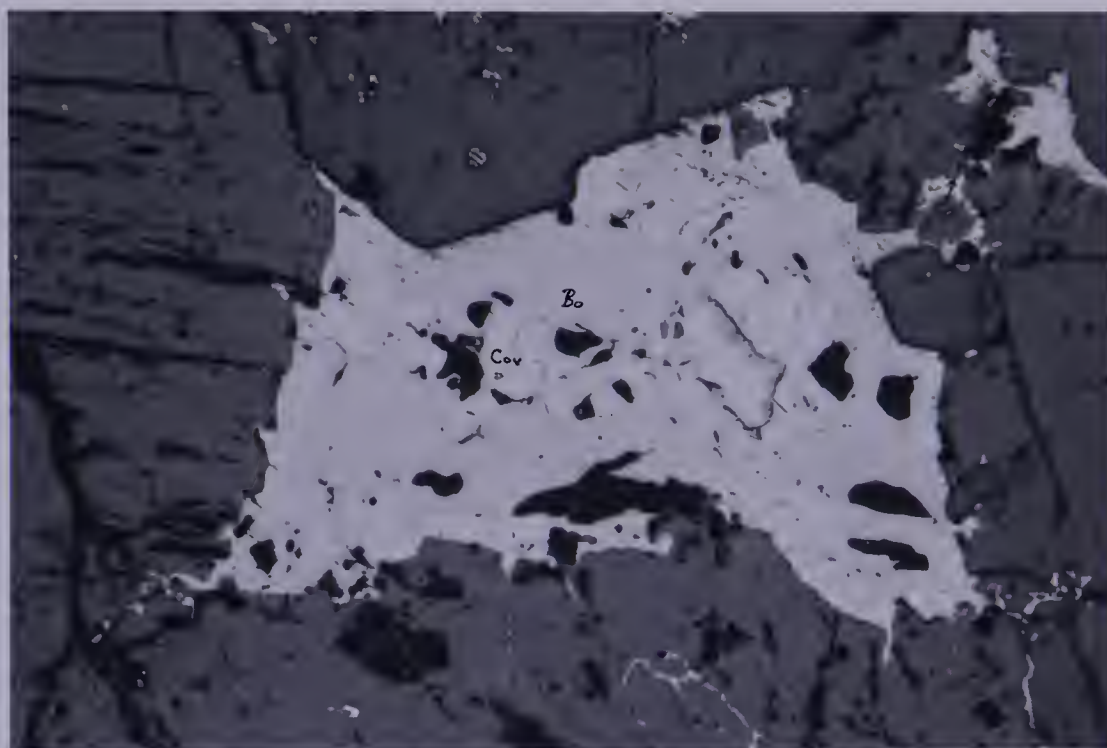


Fig.28. Bornite, covellite and chalcocite within carbonate vein in upper Grinnell argillite. (X16). RG - 21, Yarrow Creek (1015N,3330E).

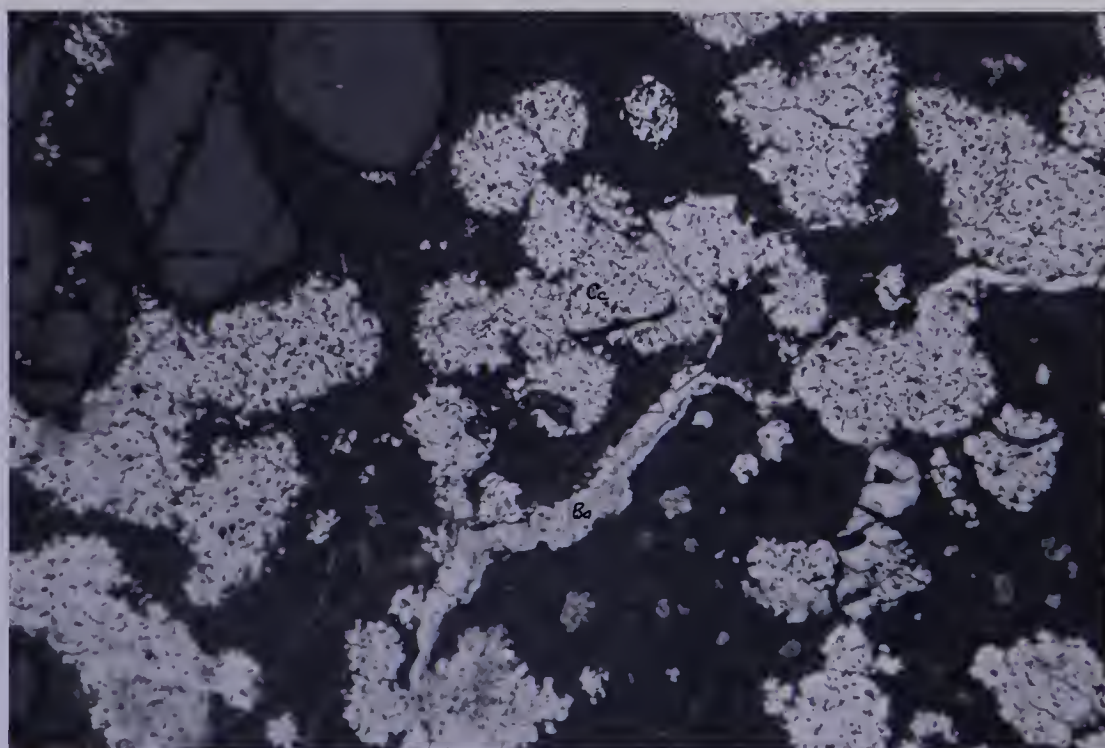


Fig.29. Bornite and chalcocite within upper Grinnell quartzite. (X16). RG - 4, Spionkop Creek (4775N,2265E).

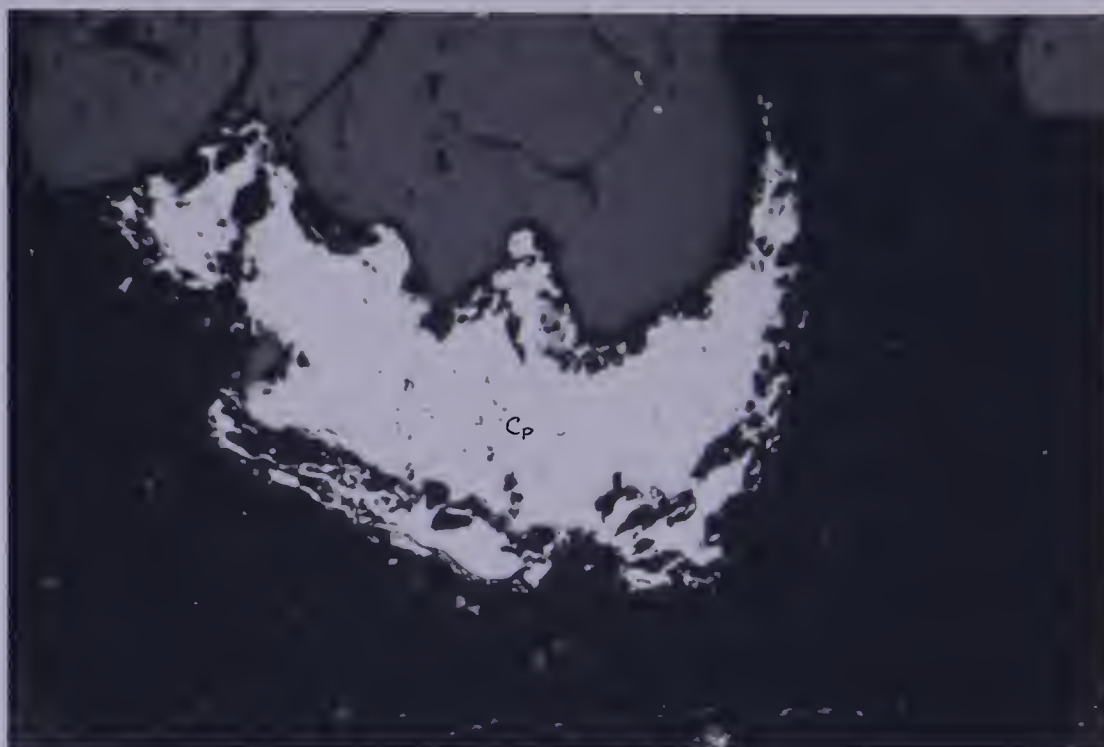


Fig.30. Chalcopyrite replacing quartz grain within upper Appekunny quartzite. (X25). RG - 17, Yarrow Creek (735N,3820E).

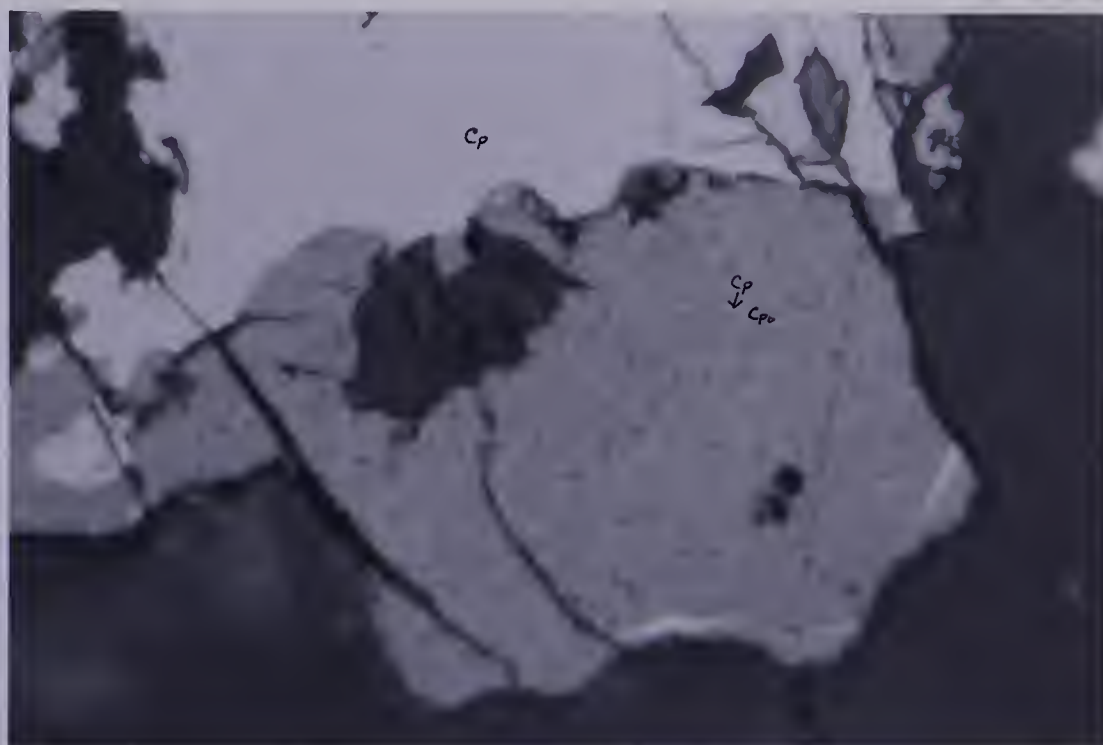


Fig.31. Chalcopyrite adjacent to and exsolved from chalcopyrrhotite. (X200). RG - 16, Yarrow Creek (655N,3415E).

mineral within the intrusive suite is chalcopyrite. This occurs in association with such minerals as magnetite, pyrite, arsenopyrite, sphalerite, and galena. Some of the dykes do contain bornite and covellite instead of the chalcopyrite, however; chalcocite and magnetite being generally associated with this assemblage. Those sectors of the sills and dykes apparently barren of copper sulphides were found to contain magnetite, pyrite, and hematite. Limonite and leucoxene exist as alteration products of the iron-bearing minerals. Minor malachite is associated with the copper sulphides.

The assemblages noted were:

- 1) Hematite
- 2) Magnetite + pyrite
- 3) Magnetite + pyrite + chalcopyrite ± sphalerite
- 4) Magnetite + chalcopyrite
- 5) Magnetite + arsenopyrite + chalcopyrite + sphalerite
- 6) Sphalerite + chalcopyrite + galena + magnetite
+ pyrite
- 7) Magnetite + chalcocite + covellite
- 8) Magnetite + bornite + covellite + chalcocite.

The intrusives themselves were highly altered in all sections studied. Up to 75% of the specimen was found to be composed of alteration products in some cases. The more common of these were chlorite, serpentine, epidote, sericite, and carbonate. The primary minerals present were plagioclase, augite, quartz, biotite, and chalcedony. The quartz content varied from less than 5% to more than 15%. Hematite was

found in place of magnetite in the quartz-rich specimens. This apparently reflects assimilation of quartz and hematite from the surrounding sediments. The chalcedony occurs chiefly as amygdules within some of the sills and dykes.

Textural relationships

In those specimens with chalcopryrite in the groundmass, the chalcopryrite is anhedral to subhedral. Silicate crystals are commonly seen growing into or enclosed by the chalcopryrite. Pyrite sometimes occurs within the chalcopryrite in line with magnetite needles in the surrounding silicate groundmass. Pyrite also occurs as large euhedral grains, occasionally badly fractured and resorbed. Sphalerite is often in association with the chalcopryrite, either in the form of irregular masses in contact with the chalcopryrite, or as small regular grains near the chalcopryrite grains. Magnetite is generally very heavily altered. Arsenopryrite is present in one specimen as stellate aggregates of euhedral crystals. Magnetite needles extend from the silicate groundmass into these crystals.

One dyke from the Siyeh formation is noteworthy in that it contains amygdules of chalcedony with sphalerite, galena, and chalcopryrite. Sphalerite is the dominant sulphide, with exsolved blebs of chalcopryrite randomly distributed throughout it. Galena is present as small irregular patches in some of those amygdules which do not contain sphalerite. Minor chalcopryrite, sphalerite, and pyrite are present in

the groundmass along with small magnetite needles.

In two of the specimens, one from Yarrow Creek and one from Spionkop Creek, bornite, covellite, and chalcocite were found to be the copper-bearing minerals. In the Spionkop Creek specimen chalcocite is disseminated throughout the sample in irregular masses up to 0.1 mm across. This chalcocite is interstitial to the silicates, with silicate crystals extending into the sulphide. Dark blue covellite occurs in place of the chalcocite along and near fractures within the intrusive. Magnetite needles are present but again have been heavily altered. In the Yarrow Creek specimen bornite and pale blue covellite are the dominant copper minerals with dark blue covellite along fractures within the bornite and 'pale covellite'. Chalcocite is also present as irregular patches within the edges of the bornite and covellite. Small rounded grains of magnetite were noted with the sulphides. Magnetite needles are again present in the groundmass. The sulphides are concentrated in carbonate veins along fractures within the intrusive, with minor disseminated 'dark covellite' in the groundmass near these fractures.

Those intrusives barren of copper sulphides contain pyrite and magnetite in the quartz poor specimens and hematite in the quartz-rich specimens. The pyrite occurs as random irregular grains up to 0.5 mm in diameter. Magnetite is present as heavily altered needles and skeletal grains. Hematite has a similar occurrence.

The sulphide grains within the intrusives are commonly

small and randomly oriented (an exception is the sulphide in the amygdaloidal dyke). Grain sizes for individual crystals range from approximately 0.01 mm to 4 mm. As previously noted, alteration of the silicates and oxides is very widespread.

Parageneses

The crystallization sequence for the intrusive suite was apparently as follows:

- 1) Deposition of sediments.
- 2) Intrusion of diabase sills and dykes.
- 3) Crystallization of silicates and magnetite needles.
- 4) Separation of immiscible sulphide phase.
- 5) Pyrite crystallized and partially resorbed.
- 6) Arsenopyrite crystallized, pyrite crystallized.
- 7) Chalcopyrite and sphalerite crystallized, chalcocite crystallized.
- 8) Magnetite needles react with chalcopyrite to give pyrite.
- 9) Bornite, covellite crystallized.
- 10) Bornite, covellite, chalcocite replaced by 'dark covellite' (possibly some replacement by chalcocite).
- 11) Alteration of silicates, oxides.
- 12) Alteration of sulphides.

Magnetite and hematite were the earliest metal oxides to form. These were followed by crystallization of sulphides from a later phase apparently immiscible with the silicate

phase. This is suggested by the interstitial nature of the sulphides, their rounded form, and by the inclusions of sulphide-rich material within the large plagioclase phenocrysts.

From this sulphide phase pyrite crystallized, to be fractured and partially resorbed by the solutions. Arsenopyrite then formed, followed by chalcopyrite and sphalerite, as well as a second generation of pyrite. Chalcocite probably crystallized during this same period. The bornite and pale blue covellite, apparently cogenetic, would seem to have been deposited later since they mainly occupy carbonate-filled fractures within the intrusive. Bornite, 'pale covellite', and chalcocite were then partially replaced by 'dark covellite' and possibly by a second generation of chalcocite. Alteration of the silicates and of the magnetite presumably took place at this or a later time.

Summary

From the above description it is envisaged that the paragenetic sequences for the sedimentary and intrusive suites were as summarized in Figures 36 and 37, respectively.

The similarities between these two sequences indicate that the copper sulphides within the two sequences probably crystallized during the same period. This would give the following overall paragenetic sequence for the Yarrow Creek - Spionkop Creek deposit:

- 1) Deposition of sediments.
- 2) Diagenesis.

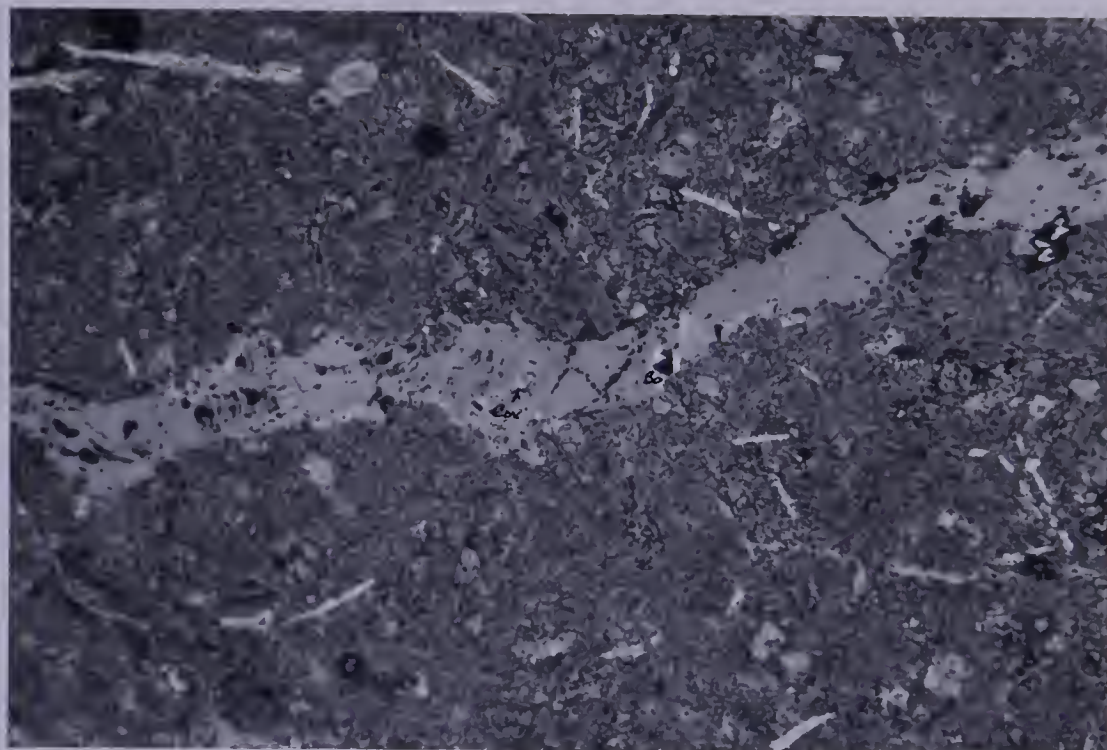


Fig.32. Bornite and covellite concentrated in and near carbonate vein in diabase dyke. (X20). RG - 31, Yarrow Creek (1005N,3345E).

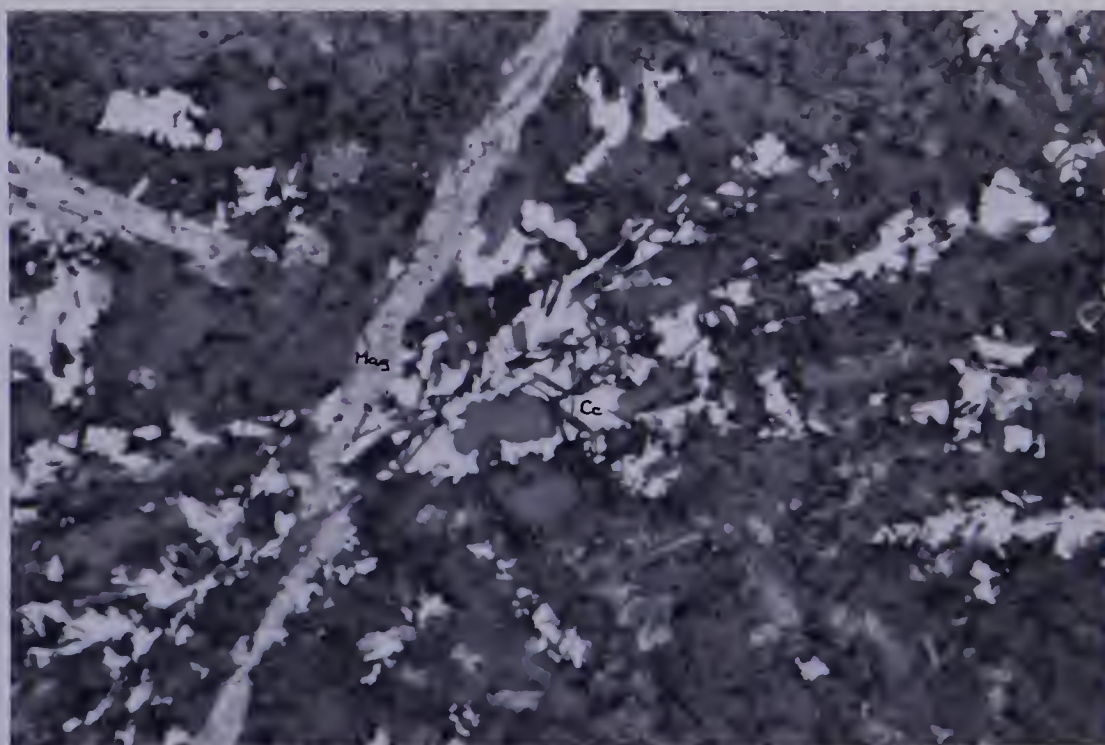


Fig.33. Chalcocite and magnetite within diabase sill. (X50). RG - 38, Spionkop Creek (4995N,2260E).

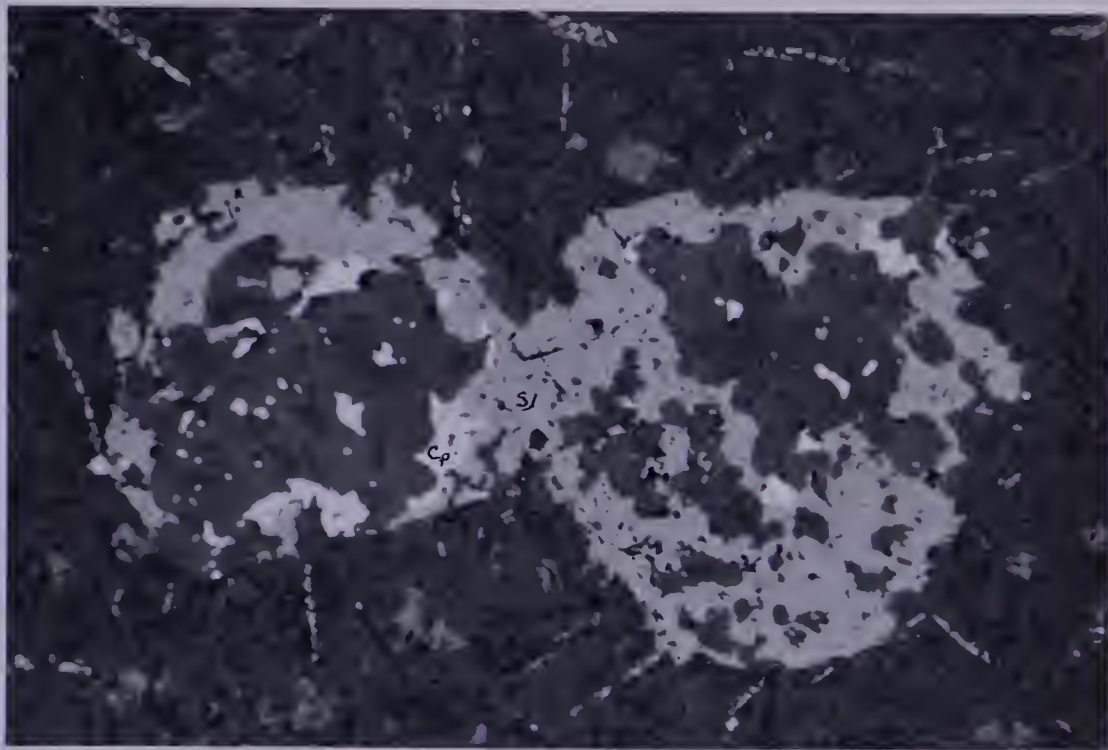


Fig.34. Late stage chalcopyrite and sphalerite within diabase sill. (X16). RG - 24, Yarrow Creek (950N,4155E).

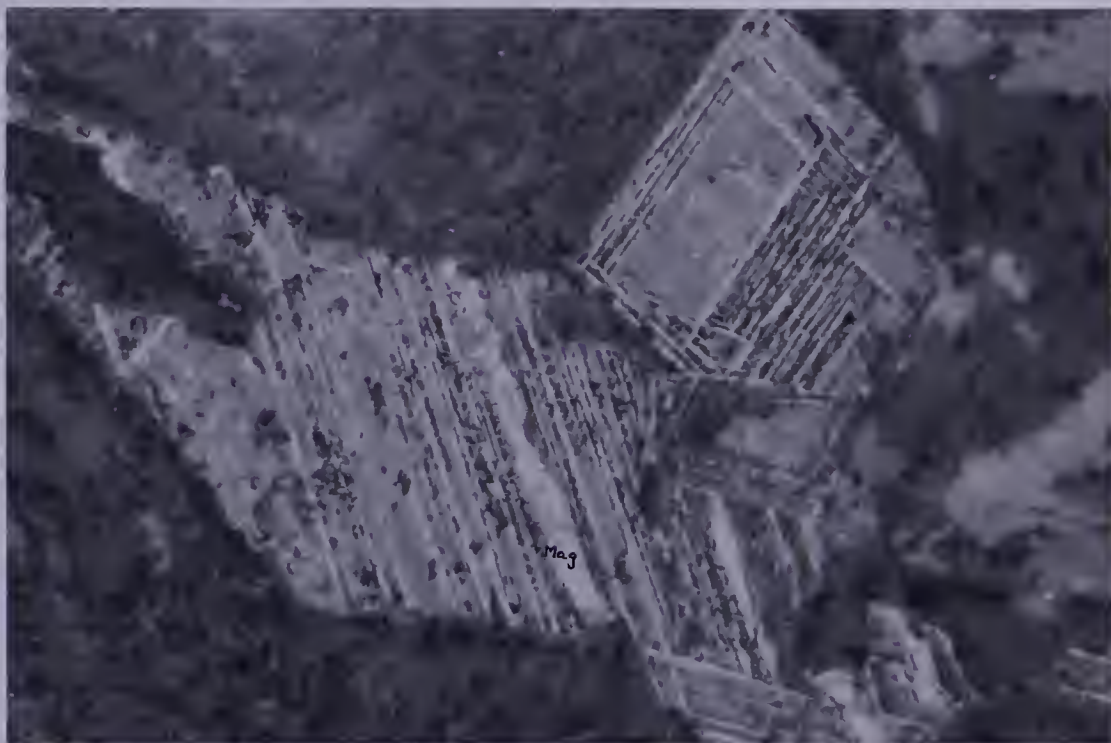


Fig.35. Skeletal magnetite. (X160). RG - 40, Yarrow Creek (200S,3000E).

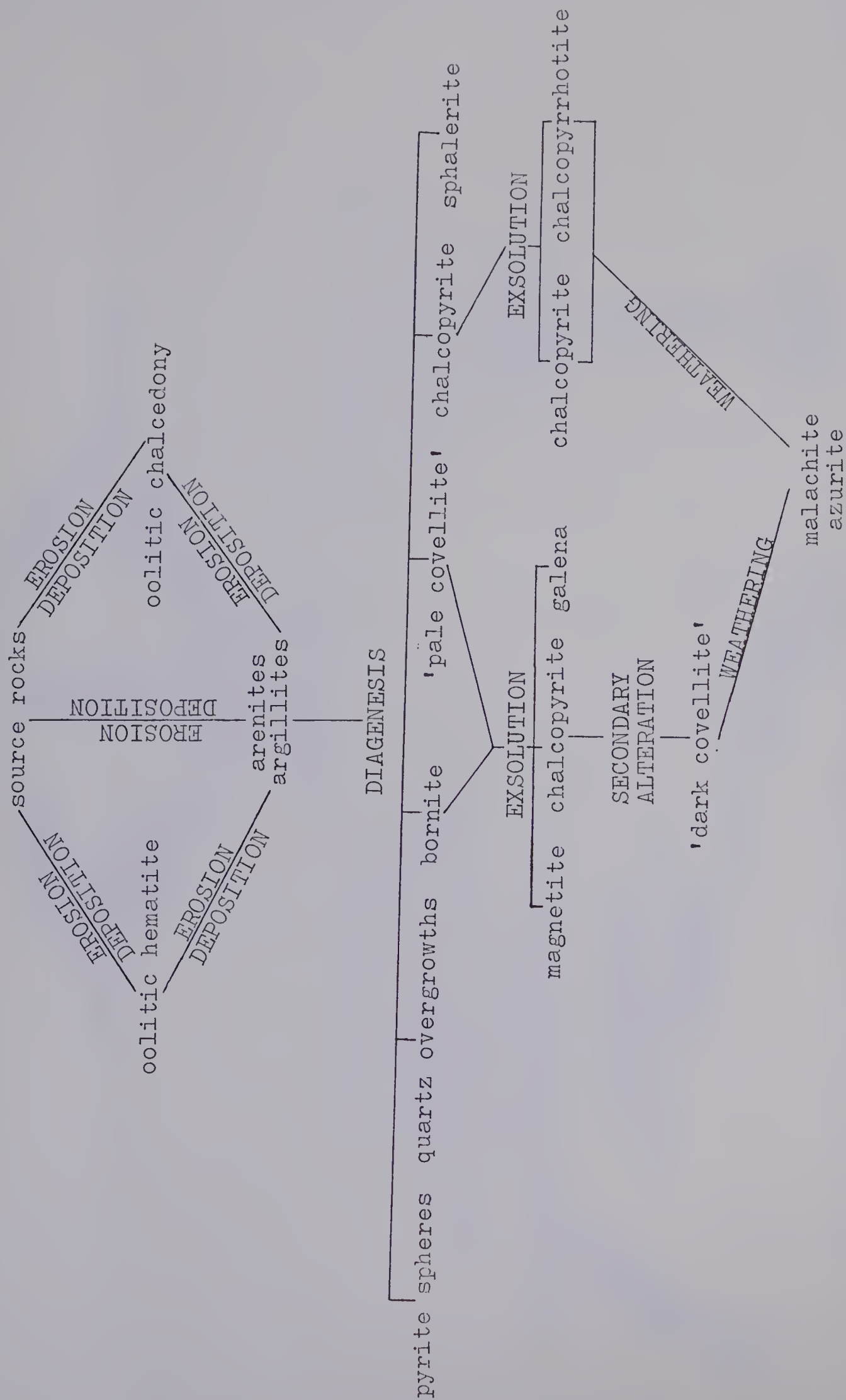


Fig.36. Paragenetic sequence of sedimentary suite, Yarrow Creek - Spionkop Creek.

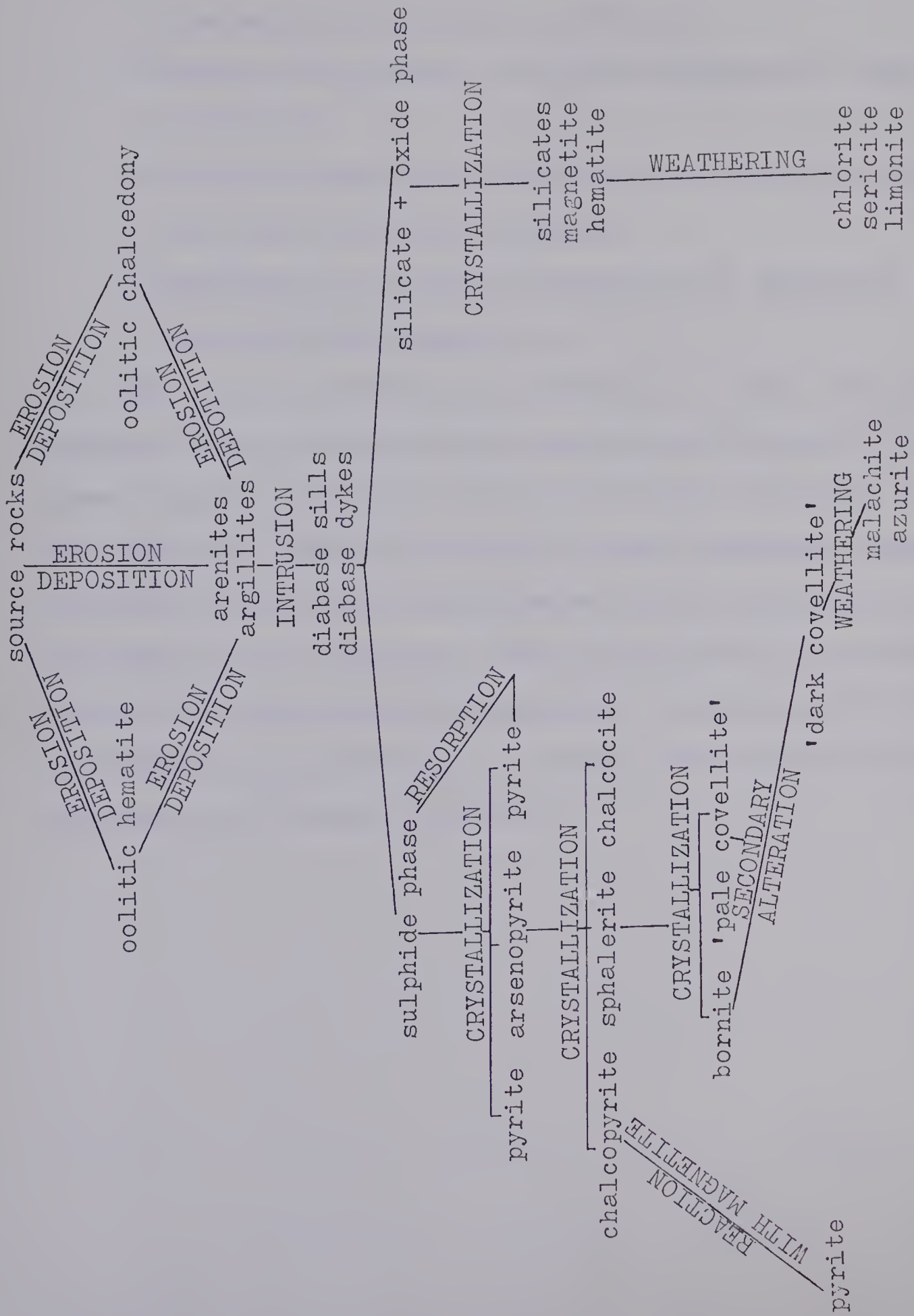


Fig.37. Paragenetic sequence of intrusive suite, Yarrow Creek - Spionkop Creek.

Intrusion of diabasic sills and dykes.

- 3) Crystallization of primary sulphides (pyrite, chalcopyrite, bornite, covellite).
- 4) Partial replacement of copper sulphides by 'dark covellite'.
- 5) Partial alteration of silicates to chlorite, sericite and other secondary minerals.
- 6) Weathering and partial alteration of sulphides to malachite and azurite.

The fact that within the intrusives we have two generations of pyrite and that the copper sulphides were a later phase than the magnetite and iron sulphides indicates that the copper was probably derived from the sediments themselves, probably transported by groundwater during diagenesis and intrusion of the diabases. This is supported by the similarities of the two sulphide paragenetic sequences and by the metallogenic specialization in copper shown by the intrusives breaching the Grinnell formation.

CHAPTER V - SULPHIDE GEOCHEMISTRY

Introduction

Many early attempts to use sulphur isotopes in the determination of the origin of sulphide deposits were based upon the supposition that sulphides of magmatic origin would have an isotopic composition, δS^{34} , close to 0‰, where δS^{34} (‰) is defined as:

$$\frac{(S^{34}/S^{32})_{\text{Sample}} - (S^{34}/S^{32})_{\text{Cañon Diablo Standard}}}{(S^{34}/S^{32})_{\text{Cañon Diablo Standard}}} \times 1000.$$

Sulphides showing δS^{34} values deviating markedly from 0‰ were generally interpreted as being of probable biogenic or sedimentary origin (e.g. BATEMAN and JENSEN, 1956). Recent investigations such as those carried out by BARNES and CZAMANSKE (1967), SAKAI (1968), and OHMOTO (1970), in the field of solution geochemistry, however, have revealed many other factors which enter into the determination of the isotopic composition of sulphides.

The geologically important sulphur-bearing species in aqueous solutions below 350°C are H_2S , HS^- , S^{2-} , SO_4^{2-} , HSO_4^- , and KSO_4^- (OHMOTO, op.cit.). SO_2 and SO_3 may become significant at higher temperatures. The isotopic composition of the sulphur in the mineralizing solutions can therefore be approximately expressed in terms of the isotopic composition of each of these species as follows:

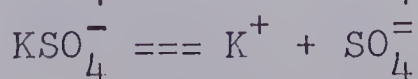
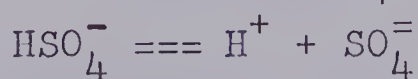
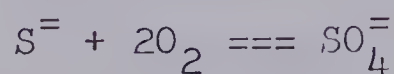
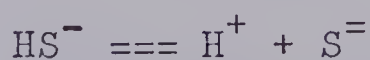
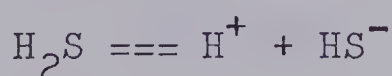
$$\begin{aligned} \delta S^{34}_{\text{solution}} = & \delta S^{34}_{H_2S} X_{H_2S} + \delta S^{34}_{HS^-} X_{HS^-} + \delta S^{34}_{S^{2-}} X_{S^{2-}} + \delta S^{34}_{SO_4^{2-}} X_{SO_4^{2-}} \\ & + \delta S^{34}_{HSO_4^-} X_{HSO_4^-} + \delta S^{34}_{KSO_4^-} X_{KSO_4^-} + \delta S^{34}_{SO_2} X_{SO_2} + \delta S^{34}_{SO_3} X_{SO_3} \end{aligned}$$

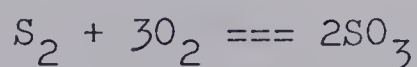
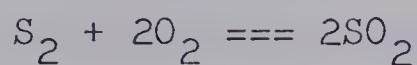
where δS^{34}_i is the isotopic composition of species i and X_i

is the mole fraction of this species present. Isotopic fractionation factors for the species H_2S , HS^- , $\text{SO}_4^{=}$, SO_2 , and SO_3 as compared to $\text{S}^{=}$ are recalculated from SAKAI'S (1968) data and plotted against temperature in Fig.38. Those for KSO_4^- and HSO_4^- , while not available, are believed by OHMOTO (1970) to be similar to the values for $\text{SO}_4^{=}$ since fractionation among various sulphate minerals is virtually nil. The isotopic composition of pyrite, chalcopyrite, and sphalerite precipitated from the solution, again compared with $\text{S}^{=}$, are also plotted on Fig.38.

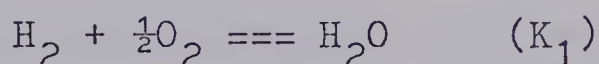
From this, we can see that, knowing the isotopic composition of our sulphides and knowing the temperature of deposition, we can determine by means of Fig.38 the isotopic composition of each of the sulphur-bearing species within the solution from which the sulphide was precipitated. To determine the isotopic composition of the total sulphur within the solution, however, we must first determine the mole fraction of each sulphur-bearing species within the solution.

The concentrations of the sulphur-bearing species H_2S , HS^- , $\text{SO}_4^{=}$, $\text{S}^{=}$, HSO_4^- , KSO_4^- , SO_2 , and SO_3 within the mineralizing solutions are dependent upon the degree to which these species have formed according to the following reactions:

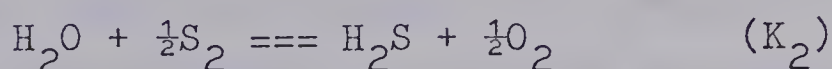




From these reactions one can calculate the concentration of the sulphur-bearing species within the solutions using the following equations:



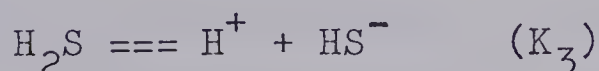
$$\log f_{\text{H}_2} = \log f_{\text{H}_2\text{O}} - \frac{1}{2}\log f_{\text{O}_2} - \log K_1$$



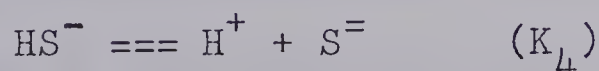
$$\log f_{\text{H}_2\text{S}} = \log K_2 + \log f_{\text{H}_2\text{O}} + \frac{1}{2}\log f_{\text{S}_2} - \frac{1}{2}\log f_{\text{O}_2}$$

$$f_{\text{H}_2\text{S}} = K_{\text{H}} a_{\text{H}_2\text{S}} / 55.5 \gamma_{\text{H}_2\text{S}}$$

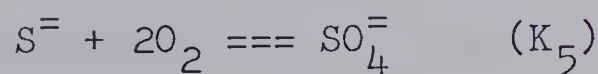
$$\log a_{\text{H}_2\text{S}} = \log f_{\text{H}_2\text{S}} - \log K_{\text{H}} + \log \gamma_{\text{H}_2\text{S}} + 1.7$$



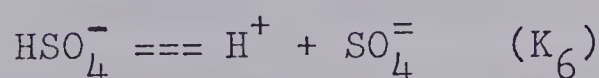
$$\log a_{\text{HS}^-} = \log K_3 + \log a_{\text{H}_2\text{S}} - \log a_{\text{H}^+}$$



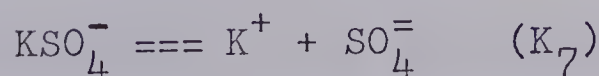
$$\log a_{\text{S}^{=2-}} = \log K_4 + \log a_{\text{HS}^-} - \log a_{\text{H}^+}$$



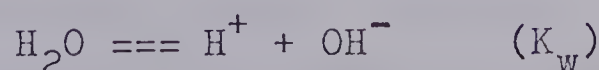
$$\log a_{\text{SO}_4^{=2-}} = \log K_5 + \log a_{\text{S}^{=2-}} + 2\log f_{\text{O}_2}$$



$$\log a_{\text{HSO}_4^-} = \log a_{\text{H}^+} + \log a_{\text{SO}_4^{=2-}} - \log K_6$$



$$\log a_{\text{KSO}_4^-} = \log a_{\text{K}^+} + \log a_{\text{SO}_4^{=2-}} - \log K_7$$



$$\log K_w = \log a_{\text{H}^+} + \log a_{\text{OH}^-} - \log a_{\text{H}_2\text{O}}$$

It can be seen from the above equations that the activity of each of the sulphur-bearing species within the solution is dependent upon the K_i (the equilibrium constant for the reaction involved), $\log f_{\text{H}_2\text{O}}$, $\log f_{\text{O}_2}$, $\log f_{\text{S}_2}$, $\log a_{\text{H}^+}$, and upon the activities of the other ions. Since K_i is dependent upon temperature, the basic variations in the activities of the sulphur species are caused by changes in temperature, pressure (fugacity of water), fugacity of sulphur (S_2), fugacity of oxygen (O_2), and pH ($-\log a_{\text{H}^+}$).

Once these are determined the molality of each sulphur species within the solution may be calculated from the relationship:

$$m_i = a_i / \gamma_i$$

where m_i is the molality of sulphur-bearing species i , a_i is the activity of sulphur-bearing species i , and γ_i is the activity coefficient of sulphur-bearing species i . Since γ_i , the activity coefficient of the sulphur-bearing species, is dependent upon both the temperature and the ionic concentration of the solution, we have another variable introduced.

In summary, therefore, to determine the original sulphur isotopic composition of the mineralizing solution we must first determine the isotopic composition of one of the sulphides present (or of the sulphate). We can then determine the isotopic composition of each sulphur-bearing species within the original solution, having first determined the temperature of deposition of the sulphide. To determine

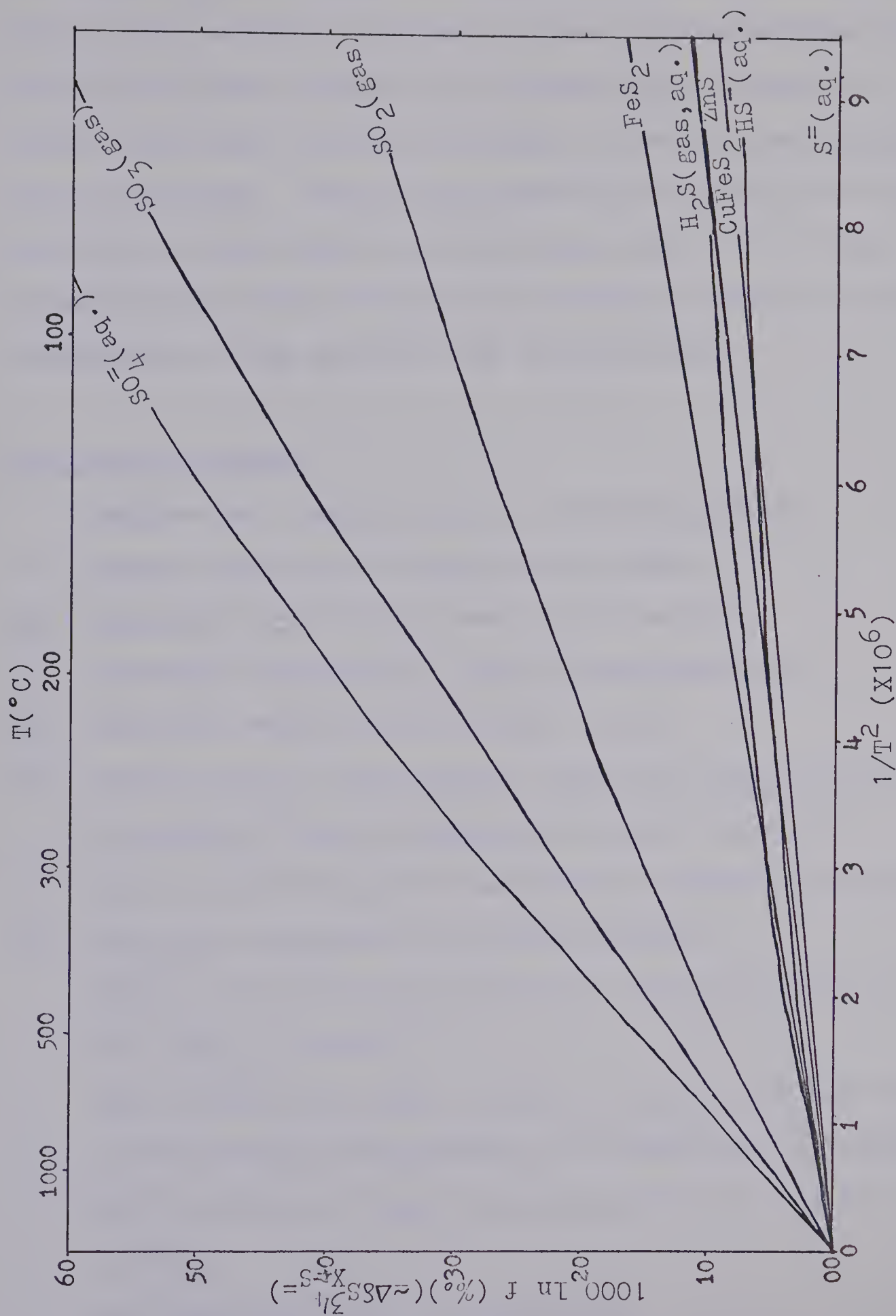


Fig.38. Sulphur-species composition versus temperature (after SAKAI, 1968).

NOTE: All values except CuFeS_2 based upon SAKAI'S Table 1, CuFeS_2 upon Fig.1. CuFeS_2 error due to error in Fig.1 less than 1%.

the original isotopic composition of the total sulphur present in the solution, however, we must also determine the fugacity of water, fugacity of sulphur (S_2), fugacity of oxygen (O_2), pH, and ionic strength of the original precipitating solution. From these values we can arrive at the molality of each sulphur species and, since the isotopic composition of each is known, the original sulphur isotopic composition of the solution may be determined.

Analytical methods

Samples were prepared by the following method:

- (1) Sample crushed and sieved to <100 mesh.
- (2) Magnetics separated by use of hand magnet.
- (3) 'Heavies' separated by use of tetrabromethane.
- (4) 'Heavies' washed with acetone, dried.
- (5) Bornite and/or chalcopyrite separated from covellite by means of Frantz isodynamic magnetic separator.
Pyrite and chalcopyrite purified by magnetic separation.
- (6) Sulphates converted to silver sulphide.
 - $BaSO_4$ reduced to H_2S utilizing a boiling mixture of HI, H_3PO_2 , and HCl.
 - H_2S flushed out with a stream of N_2 gas, washed with distilled H_2O and absorbed in a Cd-acetate solution.
 -CdS converted to Ag_2S and precipitated by addition of $AgNO_3$.
 - Ag_2S dried at $100^\circ C$ for one hour.
- (7) Sulphides burned in vacuum.

- Sulphides mixed with an excess of CuO and placed in quartz glass tube, ends sealed with quartz wool.
- Burned in vacuum at 1000°C for 10 minutes.
- Gas purified by freezing with liquid N₂, acetone-dry ice mixture, paste of methanol and liquid N₂.
- SO₂ gas sealed in glass break-seal.

(8) Mass spectrometer measurement of SO₂ gas performed using a 12 inch radius, 90° magnetic analyser equipped with a dual collector and a digital ratiometer and recorder (MCCULLOUGH and KROUSE, 1965). Samples run against YKS - GM1A reservoir standard ($\delta S^{34} = -1.9\%$).

The isotopic composition of the sample, δS^{34}_x , was calculated as:

$$\delta S^{34}_x = 1.0907((R_{st}/R_{cdt})(R_{xt}/R_{st}) - 1)1000$$

where:

$(R_{st}/R_{cdt}) = 0.99820$ (the ratio of the standard used to the Cañon Diablo standard),

and:

$$(R_{xt}/R_{st}) = (R_{xm} - \alpha)/(R_{sm} + \alpha) \quad (\text{when } R_{xm} < R_{sm})$$

$$(R_{xt}/R_{st}) = (R_{xm} + \alpha)/(R_{sm} - \alpha) \quad (\text{when } R_{xm} > R_{sm}).$$

R_{xm} , R_{sm} represent the measured ratios of the heights of the 34 to 32 peaks of the sample and standard (YKS - GM1A) respectively and:

$$\alpha = B|R_{xm} - R_{sm}|$$

where $B = 0.05$ and R_{xm} , R_{sm} are the same as above. These factors correct for the oxygen composition of the copper

oxide used in burning the sample and for memory and other factors within the mass spectrometer (equations after SASAKI, KAJIWARA, and OHMOTO, personal communications).

Two samples were rerun to check for procedural errors and two standards supplied by H. OHMOTO were also run for the same purpose. Those 'check-samples' with δS^{34} values below 20‰ checked within 0.3‰ of the expected result but those run with δS^{34} values above 20‰ gave results somewhat lower ($\sim 1.5\%$ for the OHMOTO standard) than expected. This is possibly due to an error within the oxygen correction factor.

Temperature of mineralizing solutions

Three temperatures were determined by barite-sulphide equilibria and three by fluid inclusion techniques (see Table 1). Two temperatures determined by both methods gave temperatures 50°-75° lower by fluid inclusion techniques than by isotope methods. In general, however, it would seem that the temperature of contact of the intrusives and the sediments was approximately 400°C. The temperature probably dropped off rapidly away from the contact since a value of approximately 250°C was obtained from a sample about 5 feet away from a dyke. One quartzite specimen contained chalcopyrite and sphalerite in equilibrium, the sphalerite being 1.8‰ heavier than the chalcopyrite. From Fig.38, this would give a temperature of about 110°C, indicating that the temperature of the sediments was near 100°C. This would check with the

SAMPLE NO.	LOCATION COORDINATES	DISTANCE FROM INTRUSIVE	FLUID INCLUSION TEMPERATURE	MINERAL ASSEMBLAGE**	SS ³⁴ (%)	ISOTOPE*
RG-12	985N, 3490E	15'	-----	sphalerite- chalcOPYrite	1.8	110°C
RG-44	950N, 4050E	0'	-----	barite- pyrite	17.7	400°C
RG-45	1020N, 3305E	0'	325°C	barite- bornite- covellite-	19.2	375°C
RG-46	920N, 4280E	5'	175°C	barite- pyrite	25.6	250°C
RG-47	900N, 5000E	?	225°C	-----	-----	-----

Table 1

*after SAKAI (1968).

**assumed to be equilibrium assemblages from specimen examination.

lack of any evidence of regional metamorphism in the area.

For all calculations, therefore, 400°C was taken as the contact temperature and 200°C and 600°C as the temperatures at an arbitrary distance (a few feet) on either side of the contact. A temperature as high as 600°C seems justified since plagioclase of An₅₀ such as that found in the intrusives of the area crystallizes at 1285°C (DEER et al., 1966). 100°C was taken as the temperature of the sediments away from the direct influence of the intrusives.

Pressure of mineralizing solutions

The sills and dykes were probably intruded at about the same time as the Purcell lava was extruded (a conclusion justified by data outlined in CHAPTER II). This suggests a depth of burial of 1000-1500 feet, the thickness of the Siyeh sediments overlying the Grinnell formation in this area, and a pressure of approximately 100 bars (assuming 250bars/3000 feet of depth).

Mineral stability relationships

Mineral stability diagrams were constructed for temperatures of 100°C, 200°C, 400°C, and 600°C using thermodynamic data summarized by HOLLAND (1959, 1965) to determine the probable values of f_{O_2} and f_{S_2} in the hydrothermal fluids (see Figs. 39, 40, 41, 42). The shaded areas indicate probable ranges of f_{O_2} and f_{S_2} of the fluids equilibrated with the observed mineral assemblages. The values of f_{O_2} and f_{S_2} predicted at the four temperatures are:

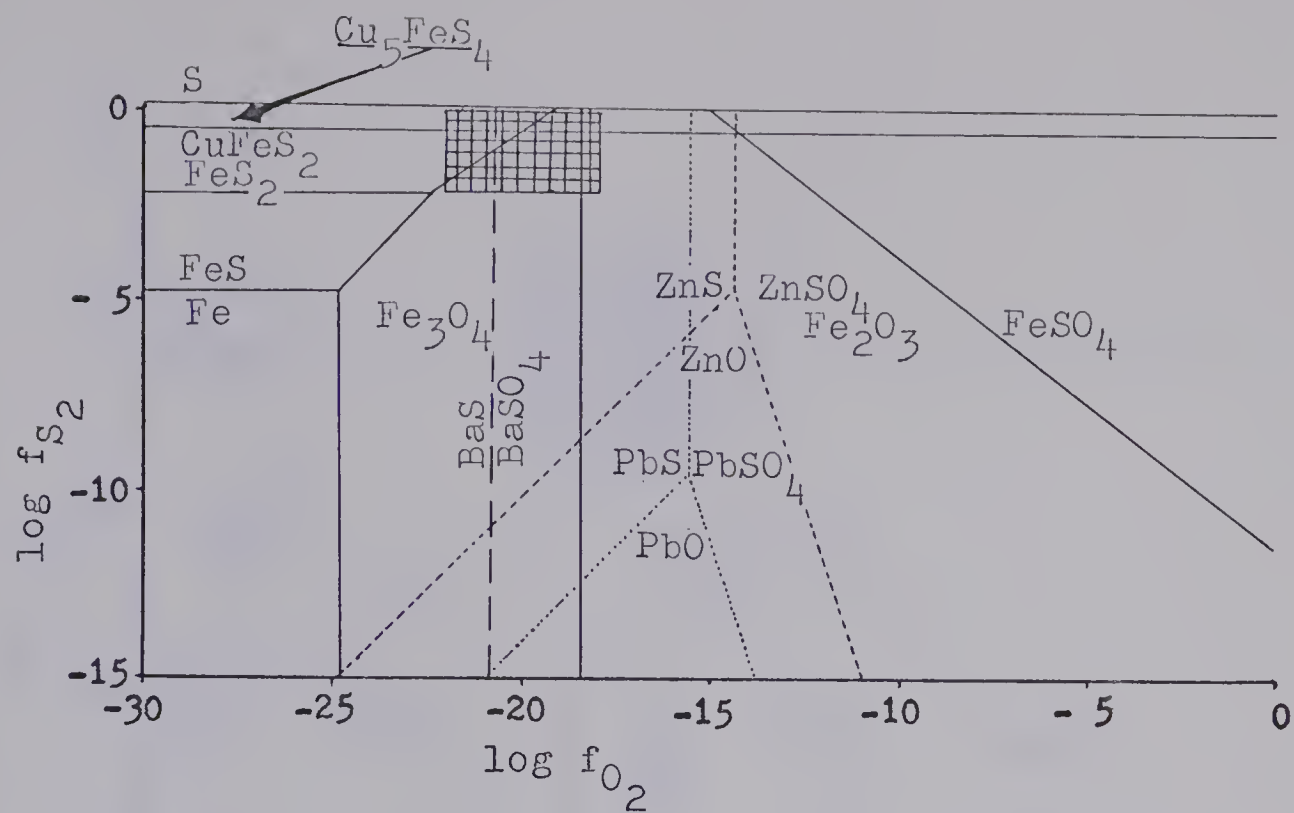


Fig.39. Mineral stabilities - 600°C.

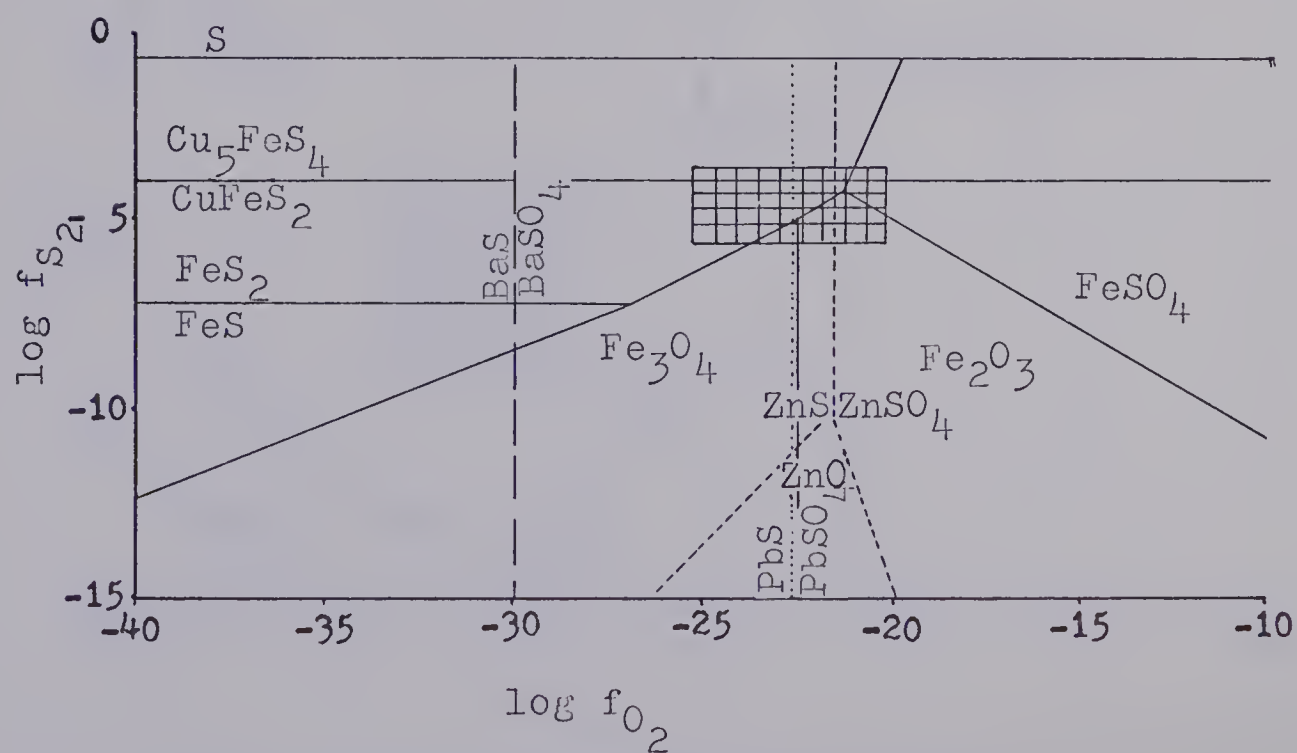


Fig.40. Mineral stabilities - 400°C.

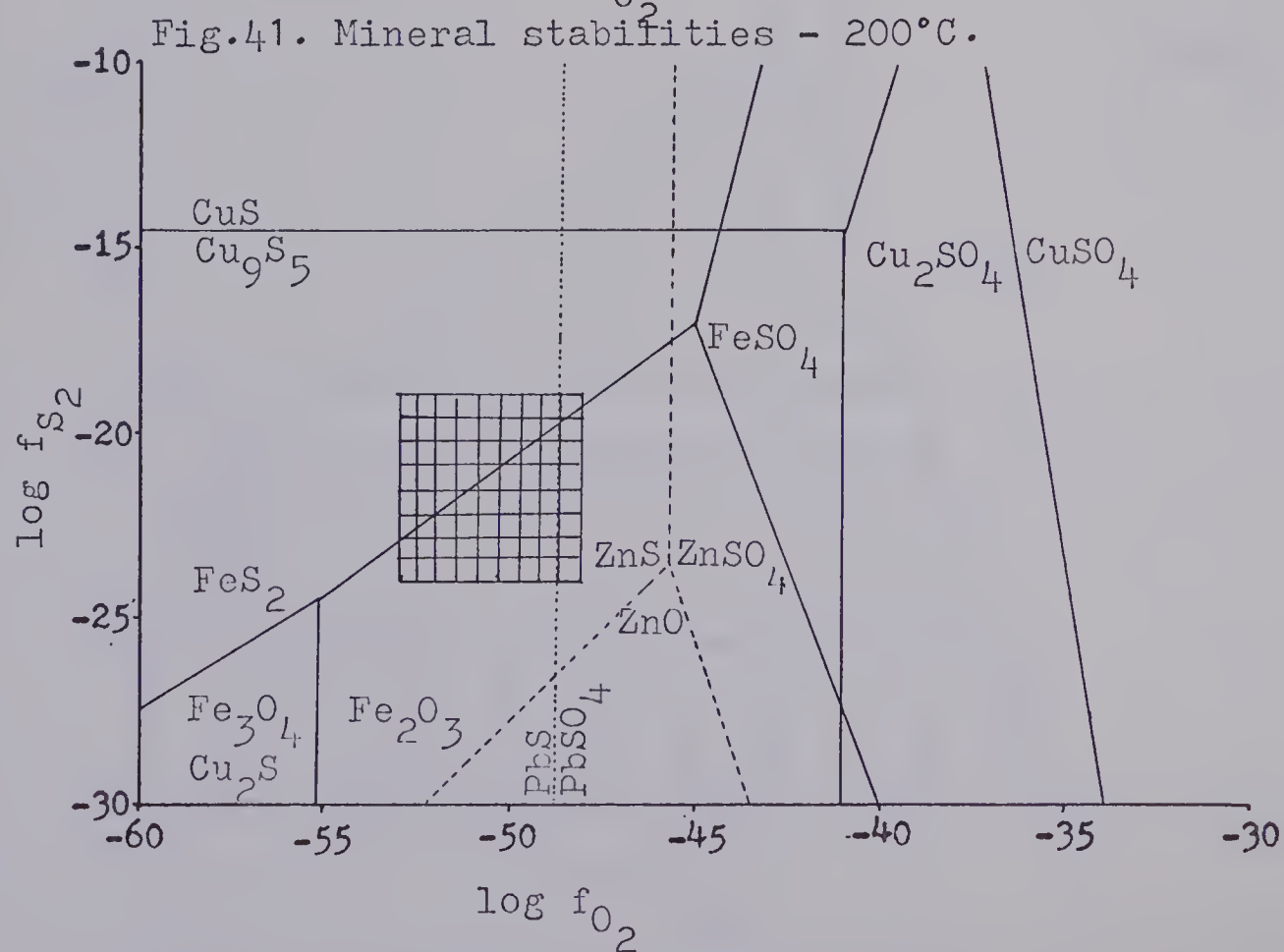
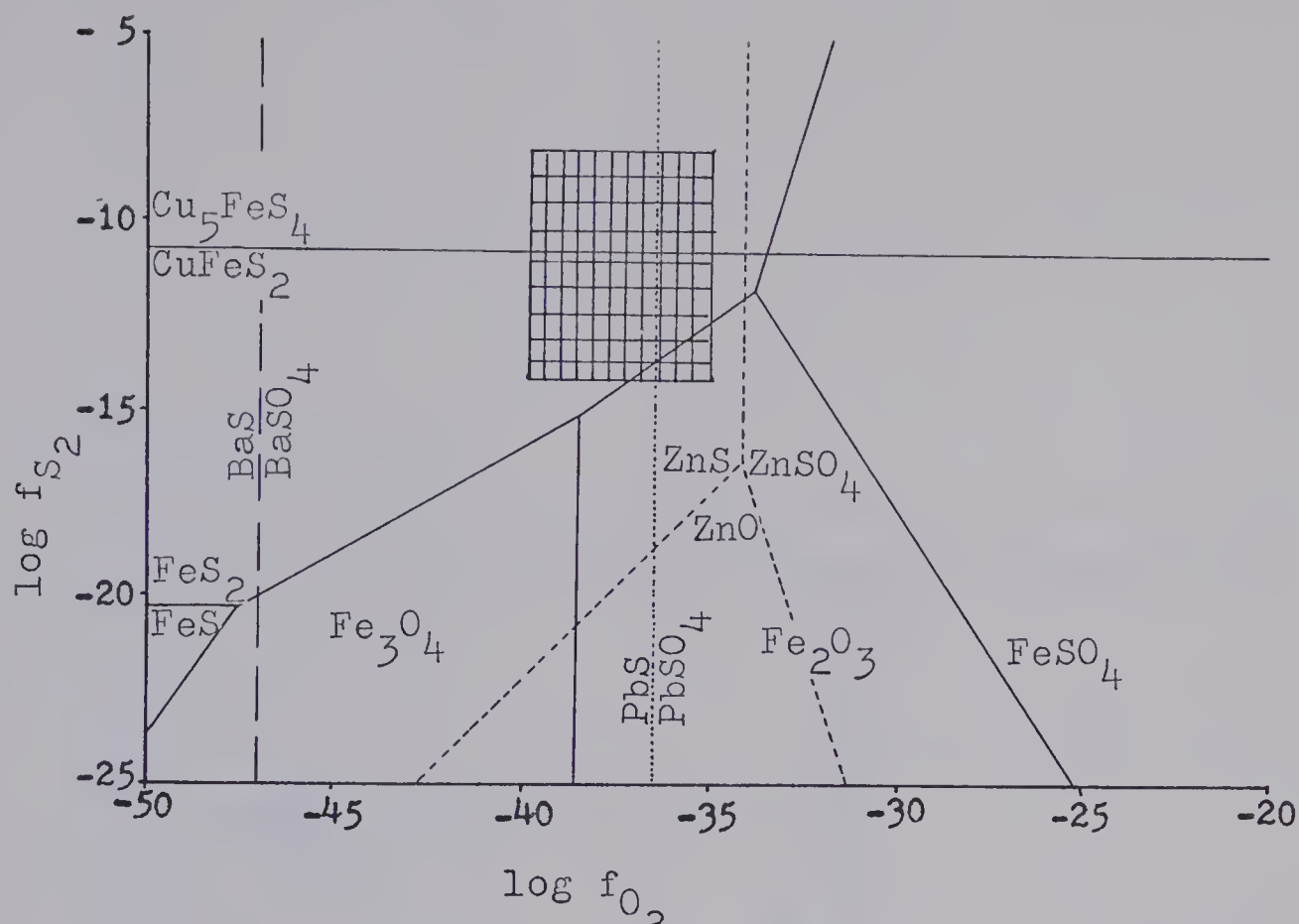


Fig. 42. Mineral stabilities - 100°C.

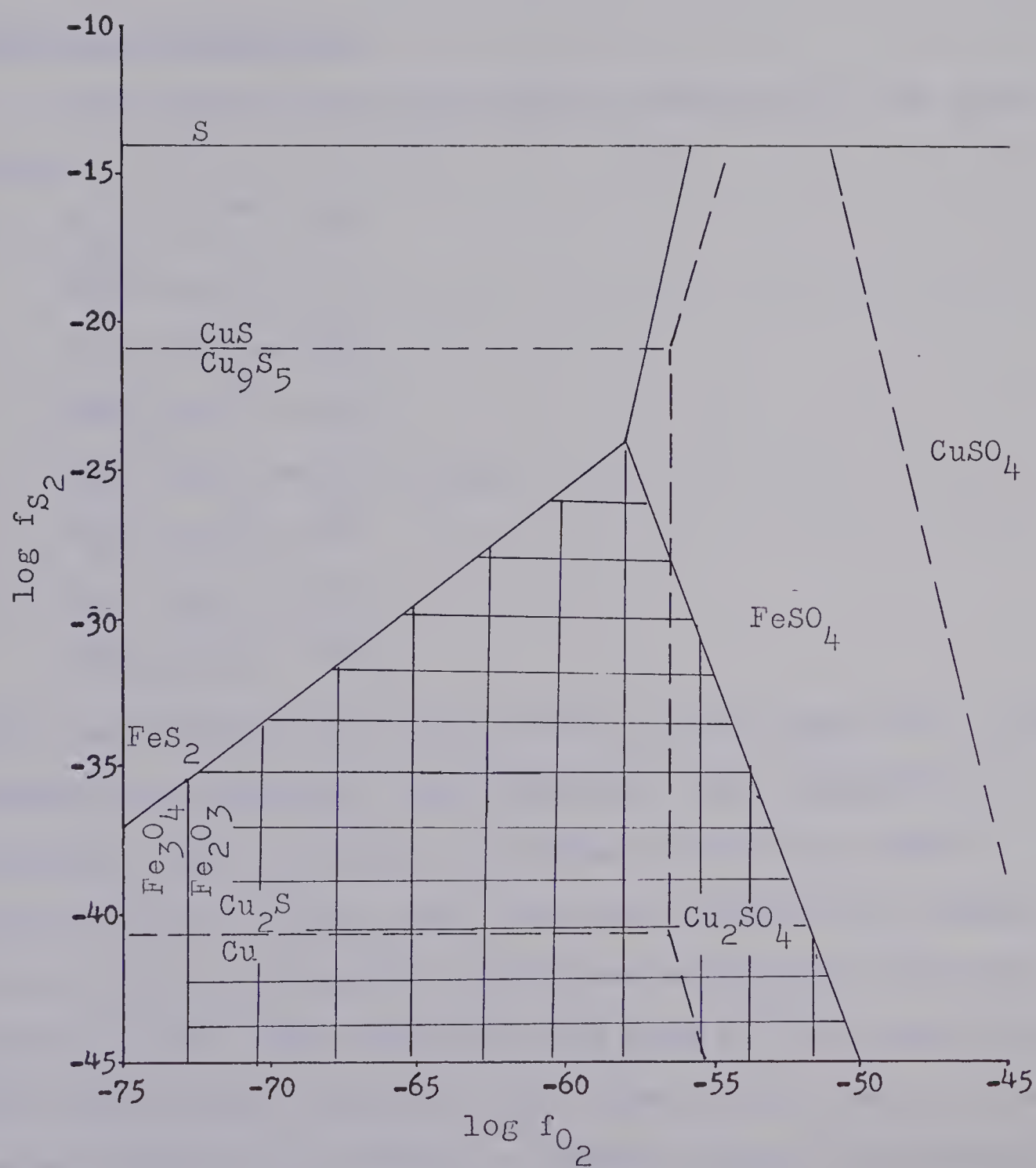
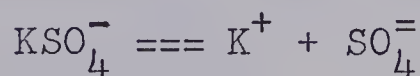
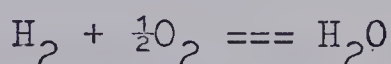
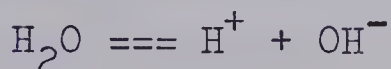
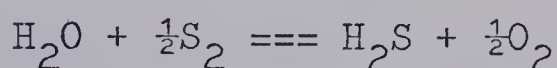
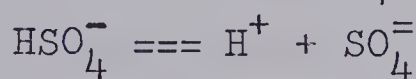
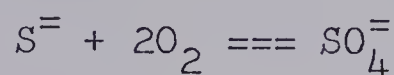
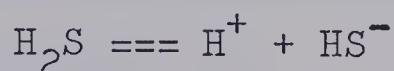


Fig.43. Mineral stabilities - 25°C.

$T^{\circ}\text{C}$	$\log f_{\text{O}_2}$	$\log f_{\text{S}_2}$
100	-50 (-53 to -48)	-22 (-24 to -19)
200	-37 (-40 to -35)	-11 (-14 to -8)
400	-23 (-25 to -20)	-5 (-5.5 to -3.5)
600	-20 (-22 to -18)	-1 (-2 to 00)

Solution geochemistry

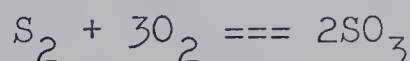
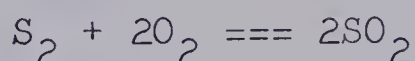
The values of the equilibrium constants for the reactions:



were extrapolated from known values in the range $25^{\circ}\text{C} - 350^{\circ}\text{C}$ (BARNES and HELGESON, 1966; HELGESON, 1967; HELGESON and GARRELS, 1968) to obtain the values at 400°C and 600°C (see Fig.44). In this case the ionic strength was assumed to be 1.0, i.e. slightly more concentrated than modern sea water (0.74). This assumption was made on the premise that the mineralizing solutions would essentially consist of sea water enriched in solubles by passage through the sediments and by mixture with solutions from the intrusives. Since deposition of the sediments took place in fresh water

(CHAPTER II) it is believed that these solutions would have been quite dilute. The fugacity of water at 100°C, 200°C, 400°C, and 600°C was calculated using BURNHAM et al's. (1968) data for the fugacity coefficients and the equation $f_{H_2O} = \gamma_{H_2O} P_{H_2O}$, taking the water pressure to be equal to the total pressure (100 bars). Henry's Law Constants for H_2S were likewise extrapolated (Fig.45) from KOZINTSEVA'S (1965) data, taking the NaCl content as 1.0N, and activity coefficients for the ions concerned were extrapolated in Fig.46 from data supplied by H. OHMOTO, again taking the ionic strength as 1.0.

Values of f_{SO_2} , f_{SO_3} were calculated using HOLLAND'S (1965) data for ΔH and ΔS for the reactions:



and using the values of f_{S_2} , f_{O_2} suggested by the mineral stability diagrams. An attempt was made to determine the values of m_{SO_2} , m_{SO_3} from the relation:

$$f_i = X_i \gamma_i P_T$$

where f_i is the fugacity of species i , X_i is the mole fraction of species i , γ_i is the fugacity coefficient of species i , and P_T is the total pressure. The result obtained by substituting the known values is:

$$f_i = \frac{m_i}{m_i + m_{H_2O}} \cdot 1 \cdot 100 = \frac{100m_i}{m_i + m_{H_2O}} \approx \frac{100m_i}{1000/18}$$

or:

$$\log m_i = -0.3 + \log f_i.$$

This value is unrealistic since when used with the H_2S species it gives values approximately three units higher than those obtained by calculating the value of m_{H_2S} using Henry's Law

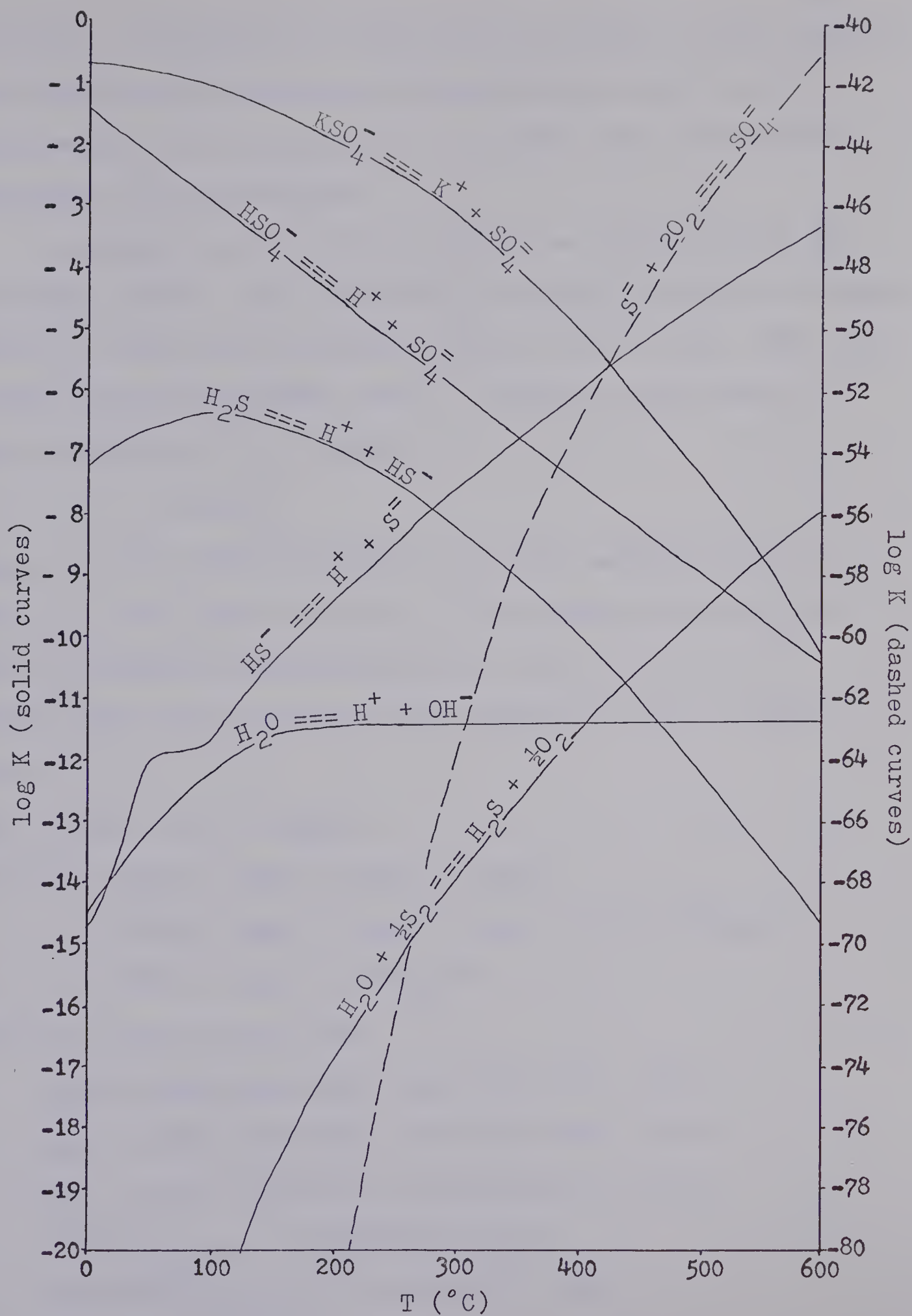


Fig.44. Equilibrium constants of sulphur-bearing species (after BARNES and HELGESON, 1966; HELGESON, 1967; HELGESON and GARRELS, 1968).

Constants. Therefore the value of K_H for SO_2 , SO_3 was assumed to be essentially the same as those values of K_H for CO_2 . These values are extrapolated from known values below $350^\circ C$ (HELGESON, 1967) in Fig.45.

An estimate of the value of $[K^+]$ was arrived at in the following manner. For the Purcell intrusive rocks the average calcium, sodium, and potassium contents are 7.74%, 1.30%, and 0.48% respectively (HUNT, 1961). Assuming a solution of ionic strength of 1.0, we have:

$$I = \frac{1}{2} \sum m_i z_i^2$$

where I is the ionic strength, m_i is the molality of ion i , and z_i is the charge on ion i . If we assume that the solution is composed essentially of the ions Cl^- , Na^+ , Ca^{++} , and K^+ , and that the cations are balanced by Cl^- we find that:

$$m_{Cl^-} = m_{Na^+} + m_{K^+} + \frac{1}{2}m_{Ca^{++}}$$

$$\begin{aligned} I = 1.0 &= \frac{1}{2}(m_{K^+} + m_{Na^+} + 4m_{Ca^{++}} + m_{Cl^-}) \\ &= \frac{1}{2}(m_{K^+} + m_{Na^+} + 4m_{Ca^{++}} + m_{Na^+} + m_{K^+} + \frac{1}{2}m_{Ca^{++}}) \\ &= (m_{K^+} + m_{Na^+} + 9/4m_{Ca^{++}}). \end{aligned}$$

From our data we know that:

$$m_{Ca^{++}} = \%Ca \cdot 10 / 40.08 = 7.74 \cdot 10 / 40.08 = 1.94$$

$$m_{Na^+} = \%Na \cdot 10 / 22.99 = 1.30 \cdot 10 / 22.99 = 0.57$$

$$m_{K^+} = \%K \cdot 10 / 39.10 = 0.48 \cdot 10 / 39.10 = 0.12$$

$$(K/Na)_{\text{silicate}} = 0.12 / 0.57 = 0.21$$

$$(Ca)/(Na)_{\text{silicate}}^2 = 1.94 / 0.57^2 = 5.97$$

and:

$$(m_{K^+}/m_{Na^+})_{\text{aq.}} = 0.74(m_{K^+}/m_{Na^+})_{\text{sil.}} \quad (\text{GAMMON et al., 1969})$$

$(m_{Ca^{++}})/(m_{Na^+})_{aq.}^2 = k'_{Ca,Na} (m_{Ca^{++}})/(m_{Na^+})_{sil.}^2$ where
 $k' = 0.6$ to 0.7 (HOLLAND, unpublished).

Therefore:

$$(m_{K^+})_{aq.} = 0.74 \cdot 0.21 \cdot (m_{Na^+})_{aq.} = 0.16(m_{Na^+})_{aq.}$$

$$(m_{Ca^{++}})_{aq.} = 0.6 \cdot 5.97 \cdot (m_{Na^+})_{aq.}^2 = 3.6(m_{Na^+})_{aq.}^2$$

or $(m_{Ca^{++}})_{aq.} = 0.7 \cdot 5.97 \cdot (m_{Na^+})_{aq.}^2 = 4.2(m_{Na^+})_{aq.}^2$

$$\begin{aligned} I = 1.0 &= (m_{K^+} + m_{Na^+} + 9/4 m_{Ca^{++}}) \\ &= 8.1 m_{Na^+}^2 + 1.2 m_{Na^+} \quad \underline{\text{or}} \quad 9.5 m_{Na^+}^2 + 1.2 m_{Na^+} \end{aligned}$$

Solving this:

$$m_{Na^+} = 0.28 \quad \underline{\text{or}} \quad 0.27$$

and:

$$m_{K^+} = 0.16 m_{Na^+} = 0.04$$

If $I = 3.0$,

$$m_{K^+} = 0.08.$$

From this 0.01 and 0.1m are taken as the minimum and maximum probable values of K^+ within the solutions. The results obtained by these calculations are summarized in Table 2 below. $K_1 - K_7$ and K_w here represent equilibrium constants for the reactions listed on page 59 of this chapter.

The composition of the sulphur-bearing solutions was then determined using these values at each of the four temperatures and for pH two units above neutral (basic), neutral, and two and four units below neutral (acidic). The results are summarized in Tables 3, 4, 5, and 6 below.

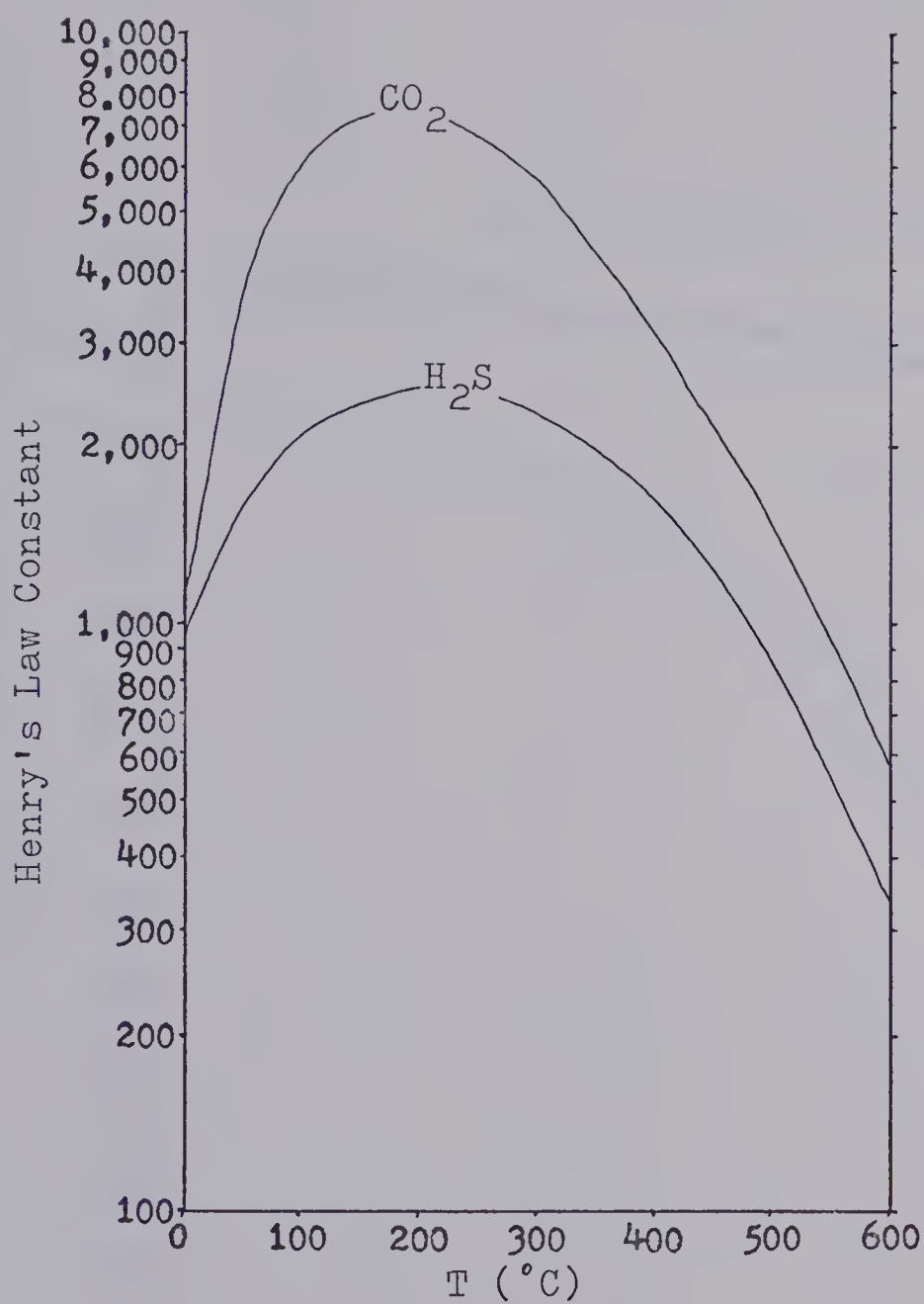


Fig.45. Henry's Law Constants of H₂S, CO₂ with 1.0 N NaCl (after HELGESON, 1967; KOZINTSEVA, 1965).

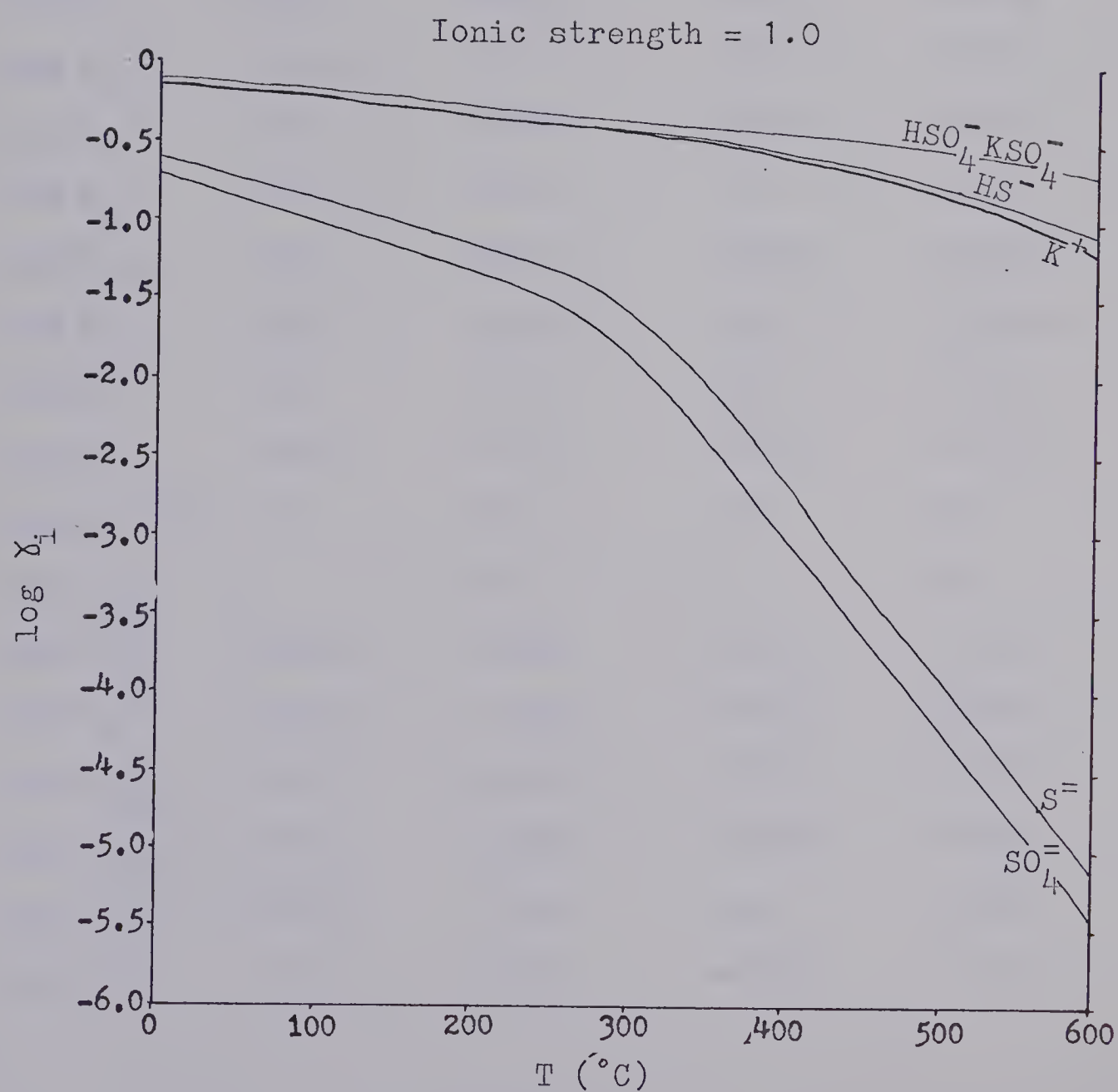


Fig.46. Variations of activity coefficients of sulphur-bearing species with temperature.

	<u>100°C</u>	<u>200°C</u>	<u>400°C</u>	<u>600°C</u>
γ_{H_2O}	0.016	0.153	0.873	0.955
$\log f_{H_2O}$	+0.2	+1.2	+1.9	+2.0
$\log f_{S_2}^*$	-22	-11	-5	-1
$\log f_{O_2}^*$	-50	-37	-23	-20
$K_H(H_2S)$	2200	2500	1600	340
$K_H(CO_2)$	6000	7600	3000	560
$\log K_1$	+31.5	+24.3	+16.3	+11.9
$\log K_2$	-21.6	-17.0	-11.7	-8.0
$\log K_3$	-6.6	-7.0	-10.0	-14.6
$\log K_4$	-11.8	-9.5	-6.1	-3.2
$\log K_5$	+112	+84	+53.2	+40.8
$\log K_6$	-3.0	-4.5	-7.5	-10.4
$\log K_7$	-1.1	-2.0	-5.0	-10.2
$\log K_w$	-12.2	-11.5	-11.4	-11.3
neutral pH	6.1	5.8	5.7	5.6
$\log \gamma_{H_2S}$	0	0	0	0
$\log \gamma_{HS^-}$	-0.22	-0.27	-0.53	-1.02
$\log \gamma_{S^{2-}}$	-0.84	-1.07	-2.72	-5.10
$\log \gamma_{HSO_4^-}$	-0.19	-0.25	-0.38	-0.68
$\log \gamma_{KSO_4^-}$	-0.19	-0.25	-0.38	-0.68
$\log \gamma_{SO_4^{2-}}$	-0.98	-1.24	-4.2	-5.32
$\log \gamma_{K^+}$	-0.23	-0.31	-0.57	-1.16

Table 2

	<u>100°C</u>	<u>200°C</u>	<u>400°C</u>	<u>600°C</u>
$\log f_{H_2}$	-6.3	-4.6	-2.9	+0.1
$\log f_{H_2S}$	-7.4	-2.8	-0.8	+3.5
$\log a_{H_2S}$	-9.0	-4.5	-2.3	+2.7
$\log f_{SO_2}$	-14.0	-6.2	-1.2	-2.6
$\log m_{SO_2}$	-16.1	-8.4	-3.0	-3.6
$\log f_{SO_3}$	-30.4	-14.0	-10.0	-15.3
$\log m_{SO_3}$	-32.5	-16.2	-11.8	-16.3
$\log a_{HS^-}$	-15.6+pH	-11.5+pH	-12.3+pH	-11.9+pH
$\log a_{S=}$	-27.4+2pH	-30.0+2pH	-18.4+2pH	-15.1+2pH
$\log a_{SO_4^{=}}$	-15.4+2pH	-11.0+2pH	-11.2+2pH	-14.3+2pH
$\log a_{HSO_4^-}$	-3.2+pH	-6.5+pH	-3.5+pH	-3.9+pH
$\log a_{KSO_4^-}$	-14.3+2pH + a_{K^+}	-9.0+2pH + a_{K^+}	-6.2+2pH + a_{K^+}	-4.1+2pH + a_{K^+}

Table 2 (continued)

*For the purpose of these calculations, one value of f_{S_2} , f_{O_2} was used. A check was run by computer for the complete range of values listed on page 70 of this chapter. These results are summarized in Appendix B.

		<u>100 °C</u>		
	pH = <u>2.1</u>	<u>4.1</u>	<u>6.1(n)</u>	<u>8.1</u>
log a _{H₂S}	- 9.0	- 9.0	- 9.0	- 9.0
log a _{HS⁻}	-13.5	-11.5	- 9.5	- 7.5
log a _{S=}	-23.2	-19.2	-15.2	-11.2
log a _{HSO₄⁻}	- 1.1	+ 0.9	+ 2.9	+ 4.9
log a _{SO₄⁼}	-11.4	- 7.4	- 3.4	+ 0.6
log a _{KSO₄^{-*}}	-11.3	- 7,3	- 3.3	+ 0.7
log a _{SO₂}	-16.1	-16.1	-16.1	-16.1
log a _{SO₃}	-32.5	-32.5	-32.5	-32.5
log m _{H₂S}	- 9.0	- 9.0	- 9.0	- 9.0
log m _{HS⁻}	-13.7	-11.7	- 9.7	- 7.7
log m _{S=}	-24.0	-20.0	-16.0	-12.0
log m _{HSO₄⁻}	- 1.3	+ 0.7	+ 2.7	+ 4.7
log m _{SO₄⁼}	-12.4	- 8.4	- 4.4	- 0.4
log m _{KSO₄⁻}	-11.5	- 7.5	- 3.5	+ 0.5
log m _{SO₂}	-16.1	-16.1	-16.1	-16.1
log m _{SO₃}	-32.5	-32.5	-32.5	-32.5
dominant ion	HSO ₄ ⁻	HSO ₄ ⁻	HSO ₄ ⁻	HSO ₄ ⁻

Table 3

*maximum probable concentration of K^+ taken at 0.1m.

		<u>200°C</u>			
pH = <u>1.8</u>		<u>3.8</u>	<u>5.8(n)</u>	<u>7.8</u>	
log a_{H_2S}	- 4.5	- 4.5	- 4.5	- 4.5	
log a_{HS^-}	- 9.7	- 7.7	- 5.7	- 3.7	
log $a_{S=}$	-17.4	-13.4	- 9.4	- 5.4	
log $a_{HSO_4^-}$	- 4.7	- 2.7	- 0.7	+ 1.3	
log $a_{SO_4^{=}}$	- 7.4	- 3.4	+ 0.6	+ 4.6	
log $a_{KSO_4^{=*}}$	- 7.7	- 3.7	+ 0.3	+ 4.3	
log a_{SO_2}	- 8.4	- 8.4	- 8.4	- 8.4	
log a_{SO_3}	-16.2	-16.2	-16.2	-16.2	
log m_{H_2S}	- 4.5	- 4.5	- 4.5	- 4.5	
log m_{HS^-}	-10.0	- 8.0	- 6.0	- 4.0	
log $m_{S=}$	-18.5	-14.5	-10.5	- 6.5	
log $m_{HSO_4^-}$	- 4.9	- 2.9	- 0.9	+ 1.1	
log $m_{SO_4^{=}}$	- 8.5	- 4.5	- 0.5	+ 3.5	
log $m_{KSO_4^{=*}}$	- 8.0	- 4.0	0.0	+ 4.0	
log m_{SO_2}	- 8.4	- 8.4	- 8.4	- 8.4	
log m_{SO_3}	-16.2	-16.2	-16.2	-16.2	
dominant ion	H_2S, HSO_4^-	HSO_4^-	$KSO_4^-, SO_4^{=}$	$KSO_4^-, SO_4^{=}$	

Table 4

*maximum probable concentration of K^+ taken at 0.1m.

		<u>400°C</u>			
pH = <u>1.7</u>		<u>3.7</u>	<u>5.7(n)</u>	<u>7.7</u>	
log a_{H_2S}	- 2.3	- 2.3	- 2.3	- 2.3	
log a_{HS^-}	-10.6	- 8.6	- 6.6	- 4.6	
log $a_{S=}$	-15.0	-11.0	- 7.0	- 3.0	
log $a_{HSO_4^-}$	- 1.8	+ 0.2	+ 2.2	+ 4.2	
log $a_{SO_4^{=}}$	- 7.8	- 3.8	+ 0.2	+ 4.2	
log $a_{KSO_4^{=*}}$	- 4.4	- 0.4	+ 3.6	+ 7.6	
log a_{SO_2}	- 3.0	- 3.0	- 3.0	- 3.0	
log a_{SO_3}	-11.8	-11.8	-11.8	-11.8	
log m_{H_2S}	- 2.3	- 2.3	- 2.3	- 2.3	
log m_{HS^-}	-11.1	- 9.1	- 7.1	- 5.1	
log $m_{S=}$	-17.7	-13.7	- 9.7	- 5.7	
log $m_{HSO_4^-}$	- 2.2	- 0.2	+ 1.8	+ 3.8	
log $m_{SO_4^{=}}$	-12.0	- 8.0	- 4.0	0.0	
log $m_{KSO_4^{=*}}$	- 4.8	- 0.8	+ 3.2	+ 7.2	
log m_{SO_2}	- 3.0	- 3.0	- 3.0	- 3.0	
log m_{SO_3}	-11.8	-11.8	-11.8	-11.8	
dominant ion	HSO_4^- , H_2S^+ , SO_2	HSO_4^- , KSO_4^-	KSO_4^-	KSO_4^-	

Table 5

*maximum probable concentration of K^+ taken at 0.1m.

		<u>600°C</u>			
pH = <u>1.6</u>		<u>3.6</u>	<u>5.6(n)</u>	<u>7.6</u>	
log a_{H_2S}	+ 2.7	+ 2.7	+ 2.7	+ 2.7	
log a_{HS^-}	-10.3	- 8.3	- 6.3	- 4.3	
log $a_{S=}$	-11.9	- 7.9	- 3.9	+ 0.1	
log $a_{HSO_4^-}$	- 2.3	- 0.3	+ 1.7	+ 3.7	
log $a_{SO_4^{=}}$	-11.1	- 7.1	- 3.1	+ 0.9	
log $a_{KSO_4^{=*}}$	- 3.1	+ 0.9	+ 4.9	+ 8.9	
log a_{SO_2}	- 3.6	- 3.6	- 3.6	- 3.6	
log a_{SO_3}	-16.3	-16.3	-16.3	-16.3	
log m_{H_2S}	+ 2.7	+ 2.7	+ 2.7	+ 2.7	
log m_{HS^-}	-11.3	- 9.3	- 7.3	- 5.3	
log $m_{S=}$	-17.0	-13.0	- 9.0	- 5.0	
log $m_{HSO_4^-}$	- 3.0	- 1.0	+ 1.0	+ 3.0	
log $m_{SO_4^{=}}$	-16.4	-12.4	- 8.4	- 4.4	
log $m_{KSO_4^{=*}}$	- 3.8	+ 0.2	+ 4.2	+ 8.2	
log m_{SO_2}	- 3.6	- 3.6	- 3.6	- 3.6	
log m_{SO_3}	-16.3	-16.3	-16.3	-16.3	
dominant ion	H_2S	H_2S	KSO_4^-	KSO_4^-	

Table 6

*maximum probable concentration of K^+ taken at 0.1m.

The calculations indicate that at 100°C HSO_4^- is the dominant sulphur-bearing ion at all pH's between 2.1 and 8.1. The solution will therefore have essentially the same sulphur isotopic composition as the HSO_4^- ion. At 200°C the sulphate ions (HSO_4^- , SO_4^{2-} , and KSO_4^-) are dominant above pH of about 3.0. Below 3.0 H_2S becomes significant within the solution. Thus, the isotopic composition of the solution is approximately equal to the δS^{34} value of the sulphate ion at pH above about 3.0, and is nearer to the δS^{34} value of the H_2S at pH much below 3.0. At 400°C the sulphate ions are again dominant at pH above 3.0, but below 3.0 SO_2 becomes of minor importance, as well as H_2S , in the composition of the sulphur-bearing species within the solution.

At 600°C the dominant sulphur-bearing ion at pH of 1.6 and of 3.6 is H_2S , while at pH of 5.6 and of 7.6 it is KSO_4^- . Thus the sulphur isotopic composition of the solution at pH below about 4.0 is similar to that of the H_2S species, and at pH above 4.0 similar to that of the KSO_4^- species.

The measured δS^{34} values of minerals as well as the descriptions and the locations of the specimens in relation to the geology are shown in Fig.47, Fig.48, and Table 7. Assuming that the sulphur isotopic composition of the solutions remained reasonably constant throughout ore deposition and knowing that the δS^{34} value of the sulphate at 400°C was approximately +25‰ from our measurements on barite (Table 7), we find that at the temperatures considered we have the following results:

<u>SAMPLE NO.</u>	<u>$\delta S^{34}(\text{‰})$</u>	<u>MINERAL</u>	<u>DESCRIPTION</u>
RG - 1	+20.7	chalcopyrite	Sill. 4330N, 2550E.* +0'‡
RG - 4	+ 1.4	chalcocite	Quartzite. 4775N, 2265E.* +465'‡.
RG - 7	+12.5	pyrite	Dyke. 4800N, 2630E. +50'.
RG - 8	- 3.6	covellite	Dyke. 4825N, 2505E. +200'.
RG - 11	- 7.3	bornite	Quartzite, dyke beneath. 700N, 3520E. +350'.
RG - 12	+11.6	sphalerite	Quartzite, dyke beneath. 985N, 3490E. +505'.
RG - 13	+ 5.7	chalcopyrite	Quartzite. 1045N, 3340E. +520'.
RG - 14	+ 6.2	covellite	Quartzite. 1045N, 3340E. +520'.
RG - 15	+12.5	bornite	Quartzite, near dyke. 1015N, 3330E. +520'.
RG - 17	+ 4.6	chalcopyrite	Quartzite. 735N, 3820E. -35'.
RG - 18	+10.5	chalcopyrite	Quartzite. 730N, 3830E. -45'.
RG - 19	+ 4.8	chalcopyrite	Quartzite. 720N, 3840E. -60'.
RG - 20	- 4.6	covellite	Quartzite. 1015N, 3350E. +510'.
RG - 22	+13.7	bornite	Sill. 650N, 3415E. +10'.
RG - 23	+ 0.6	chalcopyrite	Quartzite. 1065N, 3200E. +540'.
RG - 24	+ 0.6	bornite	Sill. 950N, 4155E. +0'.
RG - 30	+27.0	arsenopyrite	Supergene (?) covellite from sill. 660N, 3350E. +135'.
RG - 38	+10.8	covellite	Sill. 4995N, 2260E. +415'.
RG - 39	-11.5	chalcocite	Dyke. 5365N, 2285E. +125'.
RG - 44	+ 6.2	chalcopyrite	Vein at edge of sill. 950N, 4050E. +0'.
RG - 45	+26.8	barite	Lens at edge of dyke. 1020N, 3305E. +525'.
	+ 9.1	pyrite	
	+23.0	barite	
	+ 3.8	bornite, covellite	
RG - 46	+25.3	barite	Vein at top of dyke. 920N, 4280E. -10'.
RG - 48	- 0.3	pyrite	Pseudo-oolitic pyrite in lower Siyeh quartzite. 500N, 2670E. +620'.
	+10.9	pyrite	

Table 7

*distance in feet North and East of point marked 000N, 000E on Fig.9.

‡height above base of Grinnell Formation(- if in Appekunny Formation).

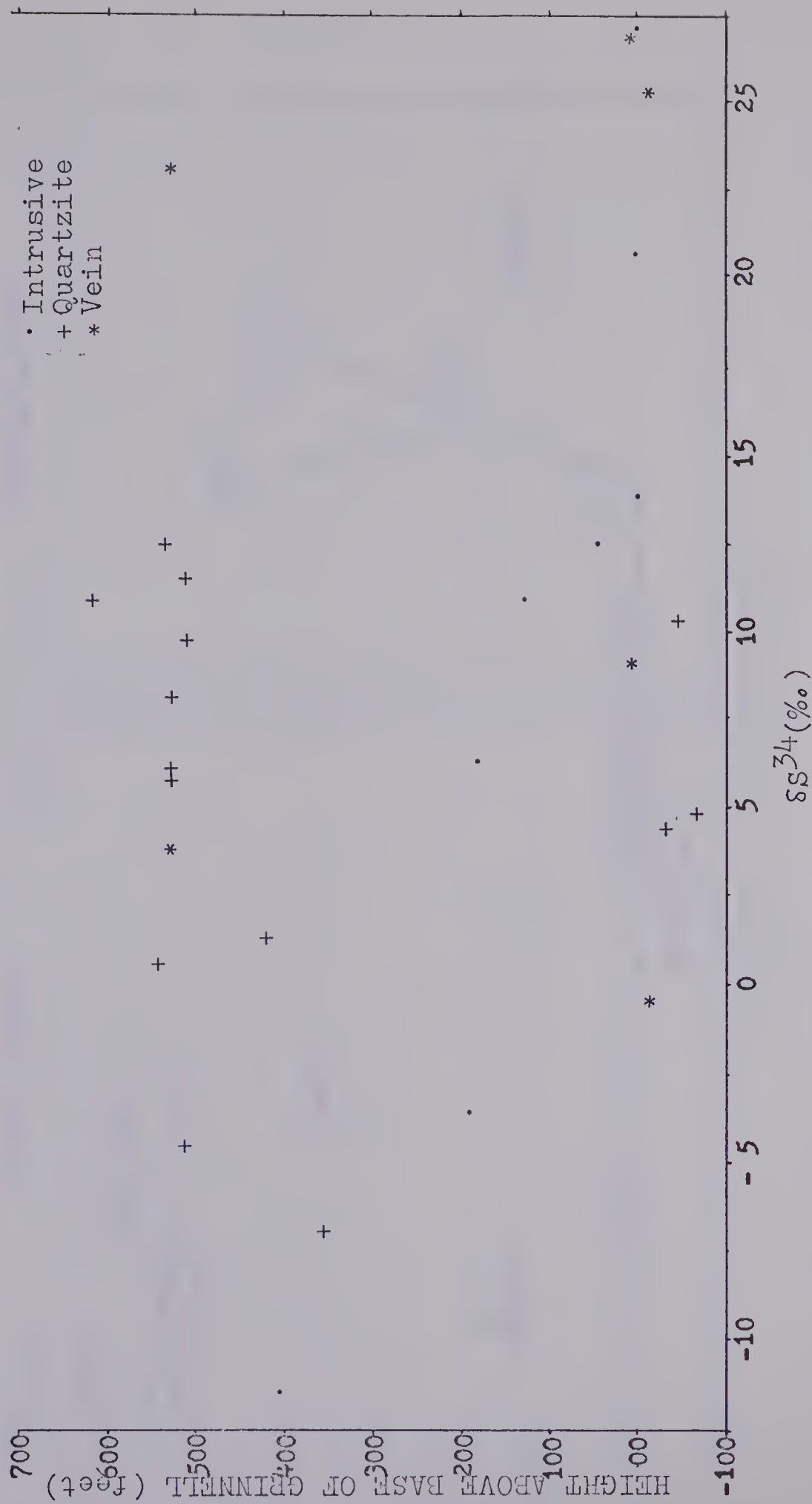


Fig. 47. Sulphur isotopic composition versus height above base of Grinnell Formation.

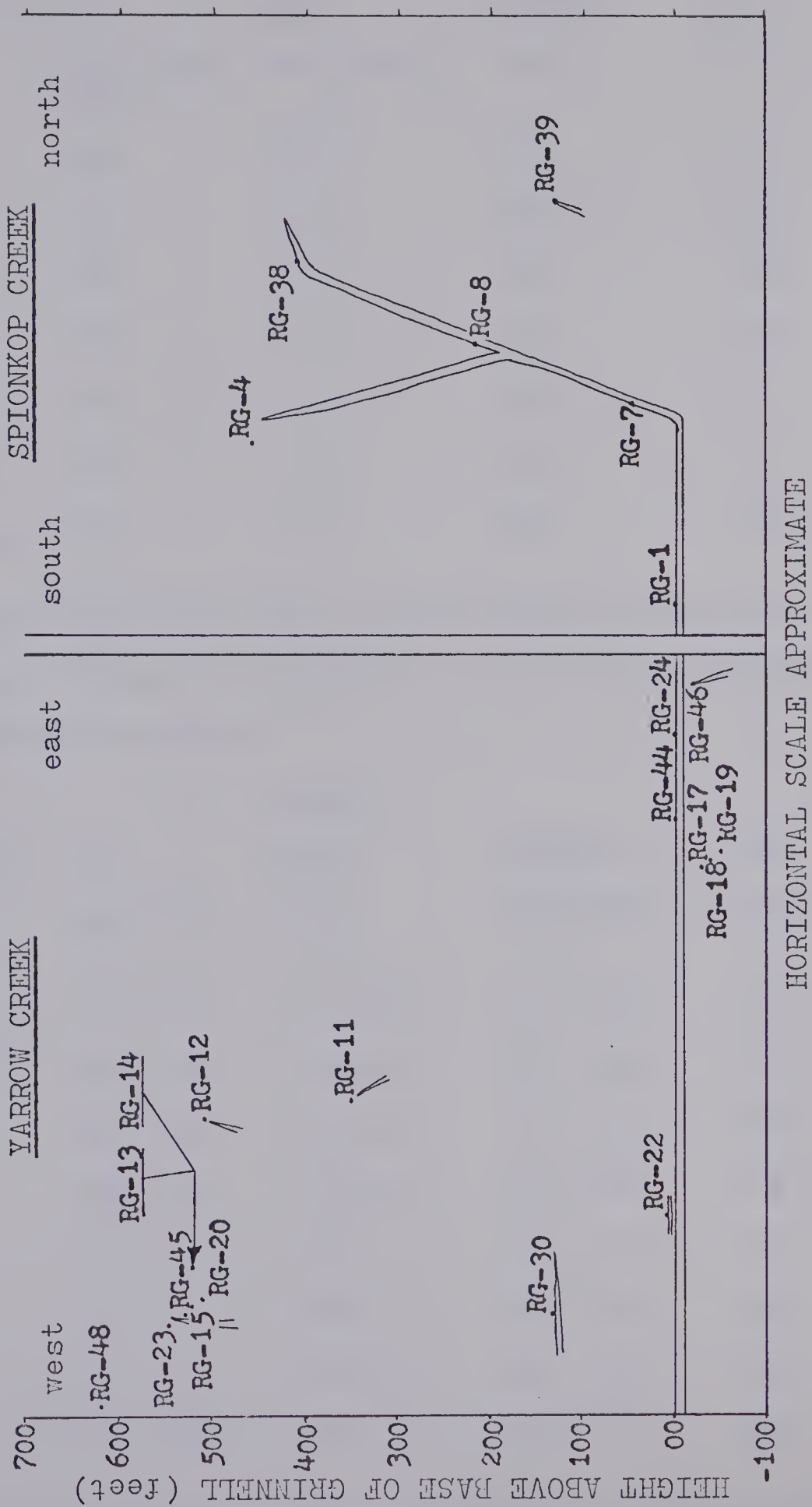


Fig.48. Sample position within Yarrow Creek - Spionkop Creek deposit versus geology.

		<u>400°C</u>			
pH = <u>1.7</u>		<u>3.7</u>	<u>5.7(n)</u>	<u>7.7</u>	
dominant ion	$\text{HSO}_4^-, \text{H}_2\text{S}, \text{SO}_2$	$\text{HSO}_4^-, \text{KSO}_4^-$	KSO_4^-	KSO_4^-	
$\delta\text{S}_{\text{SO}_4}^{34=}$	+25	+25	+25	+25	
$\delta\text{S}_{\text{HSO}_4}^{34-}$	+25	+25	+25	+25	
$\delta\text{S}_{\text{KSO}_4}^{34-}$	+25	+25	+25	+25	
$\delta\text{S}_{\text{H}_2\text{S}}^{34}$	+10	+10	+10	+10	
$\delta\text{S}_{\text{HS}}^{34-}$	+ 9	+ 9	+ 9	+ 9	
$\delta\text{S}_{\text{S}}^{34\pm}$	+ 6	+ 6	+ 6	+ 6	
$\delta\text{S}_{\text{solution}}^{34}$	+18	+25	+25	+25	

Taking +18‰ and +25‰ as the possible range of $\delta\text{S}_{\text{solution}}^{34}$ (+25‰ more probable), we have the following compositions at 200°C:

		<u>200°C</u>			
pH = <u>1.8</u>		<u>3.8</u>	<u>5.8(n)</u>	<u>7.8</u>	
dominant ion	$\text{H}_2\text{S}, \text{HSO}_4^-$	HSO_4^-	$\text{KSO}_4^-, \text{SO}_4^{=}$	$\text{KSO}_4^-, \text{SO}_4^{=}$	
$\delta\text{S}_{\text{solution}}^{34}$	+18 +25	+18 +25	+18 +25	+18 +25	
$\delta\text{S}_{\text{SO}_4}^{34=}$	+37 +44	+18 +25	+18 +25	+18 +25	
$\delta\text{S}_{\text{HSO}_4}^{34-}$	+37 +44	+18 +25	+18 +25	+18 +25	
$\delta\text{S}_{\text{KSO}_4}^{34-}$	+37 +44	+18 +25	+18 +25	+18 +25	
$\delta\text{S}_{\text{H}_2\text{S}}^{34}$	+ 5 +12	-14 - 7	-14 - 7	-14 - 7	
$\delta\text{S}_{\text{HS}}^{34-}$	+ 4 +11	-15 - 8	-15 - 8	-15 - 8	
$\delta\text{S}_{\text{S}}^{34\pm}$	- 2 + 5	-21 -14	-21 -14	-21 -14	
$\delta\text{S}_{\text{FeS}_2}^{34}$	+ 7 +14	-12 - 5	-12 - 5	-12 - 5	

Since no values of -12‰ were found in the sulphides in

the sediments, a solution composition of +18‰ was discarded in favour of the +25‰ value for the remainder of the calculations. At 600°C we then have:

		<u>600°C</u>			
pH = <u>1.6</u>		<u>3.6</u>	<u>5.6(n)</u>	<u>7.6</u>	
dominant ion	H_2S	H_2S	KSO_4^-	KSO_4^-	
$\delta\text{S}_{\text{solution}}^{34}$	+25	+25	+25	+25	
$\delta\text{S}_{\text{SO}_4}^{34} =$	+35	+35	+25	+25	
$\delta\text{S}_{\text{HSO}_4^-}^{34}$	+35	+35	+25	+25	
$\delta\text{S}_{\text{KSO}_4^-}^{34}$	+35	+35	+25	+25	
$\delta\text{S}_{\text{H}_2\text{S}}^{34}$	+25	+25	+15	+15	
$\delta\text{S}_{\text{HS}^-}^{34}$	+24	+24	+14	+14	
$\delta\text{S}_{\text{S}^\pm}^{34}$	+22	+22	+12	+12	

and at 100°C we have:

		<u>100°C</u>			
pH = <u>2.1</u>		<u>4.1</u>	<u>6.1(n)</u>	<u>8.1</u>	
dominant ion	HSO_4^-	HSO_4^-	HSO_4^-	HSO_4^-	
$\delta\text{S}_{\text{solution}}^{34}$	+25	+25	+25	+25	
$\delta\text{S}_{\text{SO}_4}^{34} =$	+25	+25	+25	+25	
$\delta\text{S}_{\text{HSO}_4^-}^{34}$	+25	+25	+25	+25	
$\delta\text{S}_{\text{KSO}_4^-}^{34}$	+25	+25	+25	+25	
$\delta\text{S}_{\text{H}_2\text{S}}^{34}$	-22	-22	-22	-22	
$\delta\text{S}_{\text{HS}^-}^{34}$	-26	-26	-26	-26	
$\delta\text{S}_{\text{S}^\pm}^{34}$	-32	-32	-32	-32	

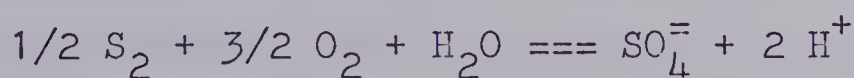
It can be seen that if we disregard a pH of 1.7 at

400°C as unrealistic both from a solution geochemistry point of view and from the standpoint of results obtained, the isotopic composition at each temperature is unaffected by a pH range of two pH units on either side of the neutral point (an exception is pH of 3.6 at 600°C). Using the values obtained we have the following pyrite and chalcopyrite isotopic compositions at each temperature:

	<u>100°C</u>	<u>200°C</u>	<u>400°C</u>	<u>600°C</u>
Pyrite	-19‰	-5‰	+10‰	+15.5‰, +25.5‰
Chalcopyrite	-24‰	-9‰	+ 8‰	+14‰, +24‰

The above calculations indicate that a range of δS_{pyrite}^{34} from +25‰ in the intrusives to -19‰ in the sediments can be explained on the basis of a temperature gradient. Similarly we can account for a chalcopyrite range from +24‰ to -24‰. From this we would expect the sulphides to be strongly 'positive' in the center of the intrusives and strongly 'negative' in the sediments away from the intrusives. This is not always the case, however, since we have values as low as -11.5‰ in the intrusive itself, and since most of our values in the sediments are positive rather than negative.

If we next consider the reaction:



where:

$$K = (a_{SO_4^{=2}})(a_{H^+})^2 / (f_{S_2})^2 (f_{O_2})^{3/2} (f_{H_2O})$$

we see that:

$$a_{SO_4^{2-}} = K(f_{S_2})^{1/2}(f_{O_2})^{3/2}(f_{H_2O})/(a_{H^+})^2.$$

In the case of the dyke on the ridge between Blind Canyon and Spionkop Creeks the temperature can be assumed to be essentially constant, and we can probably assume that the f_{H_2O} , f_{S_2} , and pH are nearly constant within the intrusive. In this case:

$$a_{SO_4^{2-}} = (f_{O_2})^{3/2} \times \text{Constant}.$$

Some assimilation of hematite must have occurred as the dyke transgressed up through the Grinnell argillites, and the mineral is present in polished samples from this area of the intrusive (CHAPTER IV). From the above equation we can see that this would result in an increase in the oxygen fugacity and a corresponding increase in $a_{SO_4^{2-}}$. Since the total sulphur content is assumed to be constant, any increase in $a_{SO_4^{2-}}$ must result in a decrease in $a_{S^{2-}}$ for f_{S_2} to remain constant. Since SO_4^{2-} is enriched in S^{34} relative to S^{32} , this results in a decrease in the δS^{34} value of the S^{2-} . A corresponding decrease in δS^{34} values of the other ions would occur along with a decrease in the δS^{34} values of the sulphides precipitated. This would be further accentuated by crystallization of S^{34} -enriched sulphide from the solutions. This probably accounts for the decrease in the δS^{34} values as the dyke transgresses up through the Grinnell argillites.

Evaluation of results

The principle sources of error in the results of the

foregoing section lie in the basic assumptions made for calculation purposes. The temperature values, since no attempt is made to assign positions to the temperatures other than a contact temperature, would introduce no error into the calculations other than the one in the determination of the 'contact' temperature of 400°C. The pressure of 100 bars is again a basic assumption but would seem to be justified for the reasons outlined in CHAPTER II.

The major source of error, therefore, lies in the extrapolation of the equilibrium constants and other values (e.g. activity coefficients and Henry's Law Constants) from 350°C to 600°C. However, since only one of the two temperatures taken above 350°C required a great deal of extrapolation (to 600°C) those values for 100°C, 200°C, and 400°C should be acceptable. Errors due to the ionic strength differing from the assumed 1.0 value and by the NaCl content differing from the assumed 1.0 value would tend to affect all species. Since we are interested in the ratio of the abundances of these species, rather than in the absolute abundances of the species, the uncertainty in the ionic strength should have little effect on our results. Errors in the estimated value of the Henry's Law Constant for SO_2 , SO_3 would again have little effect since they are unlikely to be of more than one power of magnitude and since an error of two powers of magnitude would be of effect only at pH of 1.7 at 400°C.

Finally, small errors in the estimation of f_{O_2} and f_{S_2}

from our mineral stability diagrams would be of concern principally at pH outside the range of those expected in our solutions (i.e. strongly acid, see APPENDIX B), since the abundances of all the sulphur-bearing species are dependent partially upon the abundances of the other sulphur-bearing species and such an error would tend to be lessened in magnitude. A change in the f_{O_2} value would have its principle effect upon the sulphate ions, as previously noted, and may be the cause of some of the values found in the intrusives. A change in the f_{S_2} value would be of effect only when considering the absolute abundances of the ions and would not affect the relative abundances.

Summary and conclusions

From our calculations it is evident that the sulphides within the Grinnell formation in the Yarrow Creek - Spionkop Creek deposit were deposited from a solution containing isotopically S^{34} -enriched sulphur (δS^{34} of the solutions at the contact between the sediments and intrusives being approximately +25%). A simple deposition of the sulphides from this solution as it moved out from the intrusions would have resulted in a range of δS^{34} from +25.5% to -24% from the intrusives to the sediments. The predicted high δS^{34} values in the intrusives were found in the samples run, but the low δS^{34} values in the sediments were not found.

Variations of the sulphur isotope values from the predicted high values within the intrusives can be explained

by assimilation of hematite from the Grinnell argillites. This would cause an increase in the oxygen fugacity and an increase in the amount of sulphate in solution, coupled with a decrease in the S^{34} -content of the sulphides precipitated.

The relatively S^{34} -enriched sulphides in the sediments as compared to the predicted strongly negative values is best explained by attributing the source of the sulphur to the sediments themselves. In this way we would have 'heavy' sulphur (enriched in S^{34}) picked up by the intrusives from the sediments; 'heavy' sulphides precipitated in the intrusives (complicated by local variation in the oxygen fugacity); and ' S^{34} -depleted' sulphur moving out from the intrusive in solution mixing with ' S^{34} -enriched' sulphur in the sediments to precipitate sulphides of 'intermediate' isotopic composition.

The presence of heavy sulphur within the sediments is shown by the sulphur isotope value found for a sample of the pseudo-oolitic pyrite from the base of the Siyeh formation (see CHAPTER IV). This diagenetic pyrite gave a δS^{34} value of +10.9%.

The major source of the sulphur within the Yarrow Creek - Spionkop Creek deposit would seem, therefore, to have been the sediments themselves. Such sulphur was probably present in the form of sulphate ions in formation water circulating through the sediments. Also, it should be noted that at 25°C and conditions conducive to the deposition of hematite-bearing 'red-bed' deposits, Cu_2SO_4 is stable as well as

Cu_2S (see Fig.43). Therefore a possibility exists that when the sediments were deposited Cu_2SO_4 and FeSO_4 were precipitated along with the Fe_2O_3 and that with burial and intrusion of the diabases, these were mobilized to form a solution of Fe, Cu, and $\text{SO}_4^{=}$ with a 'heavy' sulphur isotopic composition due to the original 'heavy' FeSO_4 and Cu_2SO_4 .

CHAPTER VI - COMPARISONS WITH OTHER AREAS

Introduction

BOGDANOV (1967), proposes the following classification of stratified copper deposits, based upon a twofold division on the basis of sedimentary and metasedimentary deposition:

A. Sedimentary

- i. Cupriferous shale type (sedimentary diagenetic) (e.g. Mansfield).
- ii. Cupriferous sandstone type (cata-diagenetic)
 1. Dzhezkazgan (paralic (lagoonal to deltaic)) subtype (e.g. Dzhezkazgan).
 2. Ural (continental (alluvial)) subtype (e.g. Colorado Plateau).

B. Metasedimentary

- i. Regionally metamorphosed (e.g. Zambian-Congolese belt).
- ii. Contact metamorphosed (e.g. deposits in the Dlekma-Vitim highlands).

Comparison of the Yarrow Creek - Spionkop Creek deposit is first made with other deposits within the Purcell-Belt series. Then, since the Yarrow Creek - Spionkop Creek deposit is of the cupriferous sandstone type, comparison is made with similar deposits within Russia. Finally, notice is made of certain similarities between this and other Lewis series deposits and deposits of the cupriferous shale type in the Kupferschiefer and related formations, and the deposits of the Zambian-Congolese Copperbelt.

Comparisons with other deposits in the Belt-Purcell series

The principle ore deposits encountered within the Belt-Purcell series are the Pb, Zn, Ag deposits of Kimberley, British Columbia and those of the Coeur d'Alene district in Idaho. Numerous smaller deposits of copper, lead, zinc, and related metallics are found throughout the series in Montana, Idaho, and British Columbia.

The ore deposit of Kimberley, British Columbia is a stratabound deposit located near the transition zone between the lower and middle members of the Aldridge formation. Host rocks are argillites, silty argillites, and impure argillaceous quartzites. Several northeasterly-trending reverse or thrust faults and northeasterly to northwesterly trending normal faults and fractures, which FREEZE (1966) considers to be pre-ore, occur in the mine and its general vicinity. Sills and dykes of dioritic composition occur below and within the ore zone. KANASEWICH (1968) dated the Sullivan Mine lead at 1340 ± 50 million years.

The deposits of the Coeur d'Alene district occur as replacement veins within the Pre-Ravalli and Ravalli groups of the Belt Series, but are mainly enclosed in the Prichard, Burke, and Revett formations. UMPLEBY and JONES (1923) determined that these deposits are roughly grouped around the intersection of an axis of uplift and igneous intrusion with a broad zone of extensive faulting. The axis of uplift and igneous intrusion lies along a northeast-southwest line marked in part by Cretaceous monzonite stocks. The zone of

extensive faulting is part of the 'Lewis and Clarke' line running from Coeur d'Alene, Idaho to Superior, Montana. KANASEWICH (1968) dated the Coeur d'Alene lead at 1340-1500 million years. ANDERSON (1967) proposes that the structures of the Coeur d'Alene district were developed by slumping along a N85°W trending rift graben that formed during late Precambrian time.

JOHNS (1961,1964) reports minor occurrences of copper in the Kootenai-Flathead region of Montana. These consist of chalcopyrite in metadiorite sills within the Prichard and Piegan formations, and of chalcopyrite associated with fissure-filled veins within rocks of the Ravalli group. PARDEE (1911) reports disseminated specks and crystals of pyrite and chalcopyrite within the equivalents of the Burke and Revett quartzites in the Upper St. Joe River Basin. CROWLEY (1963) found disseminated pyrite and pyrrhotite within the Prichard formation as well as mineralization near sills intruded into the Prichard, Ravalli, and Wallace groups.

These deposits are of interest for they illustrate several points in common with the deposit studied:

- 1) They are mostly concentrated within the first cycle of deposition of the Belt-Purcell series (i.e. Pre-Ravalli and Ravalli groups).
- 2) They are commonly associated with quartzites and argillaceous sediments rather than with the carbonaceous sediments.
- 3) Mineralization is commonly noted in association

with diorite or diabase sills and dykes but examination (of the Canadian outcrops) reveals that some mineralization is generally present where these are absent.

- 4) Where dated, the dates show deposition of the sulphides during or soon after sedimentation (e.g. 1340 million years for lead compared to 1315 million years for sediments).
- 5) KANASEWICH (1968) has postulated that deposition of the ores at the Sullivan Mine at Kimberley, British Columbia and possibly of those of the Coeur d'Alene district (and of the Yarrow Creek - Spionkop Creek deposit) as well took place within the boundaries of a rift valley which he has identified cutting across the Churchill province of southern Alberta and southeastern British Columbia (see Fig.49).
- 6) LANDWEHR (1967) is of the opinion that the mineralizing fractures, as well as the centers of the three main metallogenic epochs, of the western United States are aligned in belts which trend northeasterly (see Fig.50). He concludes that the belts of mineralization reflect zones of deep rupture in the earth's crust, all of which formed simultaneously in response to a common regional stress. It should be noted that one of these belts corresponds roughly to Kanasewich's rift

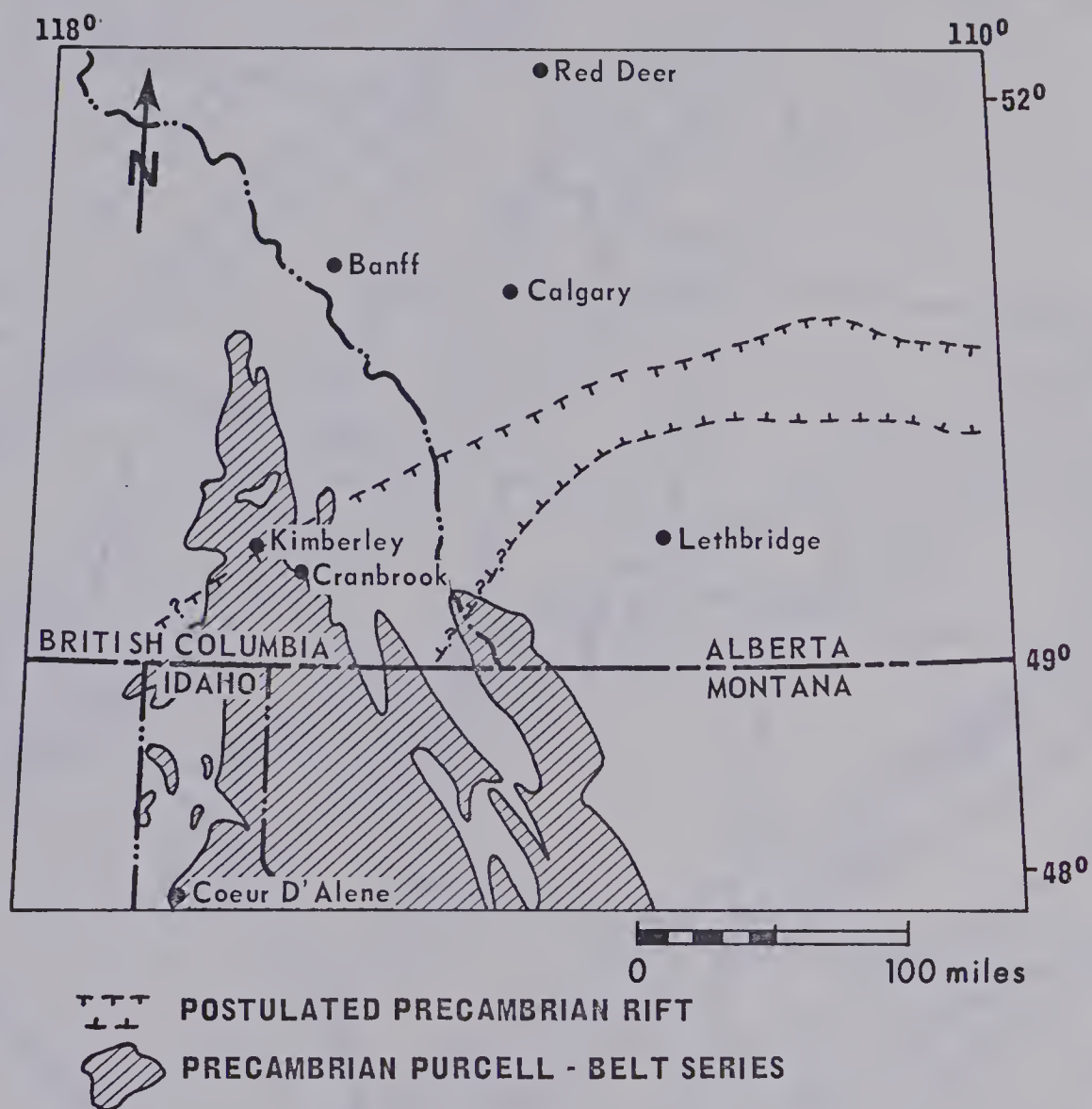


Fig.49. Postulated Precambrian rift valley in relationship to the Purcell-Belt series (after KANASEWICH, 1968).



Fig.50. Belts of mineralization in western United States
(after LANDWEHR, 1967).

valley and runs near both the Sullivan Mine and the Yarrow Creek - Spionkop Creek deposit.

Comparisons with deposits outside North America

Tables 8, 9, and 10 list pertinent features of the geology of the Russian Udokan, Dzhezkazgan, and Donbass deposits; the Kupferschiefer - Rotliegende deposits; and the Zambian - Congolese Copperbelt deposits; as outlined by BOGDANOV (1964), DEANS (1950), DRUZHININ (1965), DUNHAM (1964), FEDEROVSKAYA and BESPALOV (1968), GARLICK (1969), HIRST and DUNHAM (1963), MENDELSON (1961), NARKELYUN and YURGENSON (1968), and POPOV (1962) together with a comparison of these features to similar features of the Yarrow Creek - Spionkop Creek and related deposits.

Mode of deposition

Deposition of the metallics within stratiform copper deposits has probably occurred through a combination of the modes described by BOGDANOV (1967) and NOBLE (1963). BOGDANOV (loc.cit.) determined that in arid zones of the Soviet Union copper flows into sedimentation basins chiefly in a suspended state (basic carbonate suspensions etc.) and subordinately in dissolved form. These suspensions of basic carbonates and other copper compounds settle principally in fine sediments. The bulk of the ore deposits apparently originated during diagenesis as interstitial waters bearing copper moved into coarser sediments. Cu was apparently

(i) Russian deposits

<u>Feature</u>	<u>Udokan</u>	<u>Dzhezkazgan</u>	<u>Donbass</u>	<u>Yarrow - Spionkop</u>
Age:	Proterozoic	Carboniferous	?	Proterozoic
Structural setting:	Brachysyncline	----	----	Lewis thrust sheet
Cu-bearing rock type:	Arenite	Arenite	Arenite	Quartzite
Facies:	Deltaic	Deltaic	Deltaic	Deltaic
Ore zonation:	Present	Present	Present	Present (?)
Ore-controlling structures:	None	None	None	Faults (?), intrusives
Special features of intrusives:	Metallogenic specialization	None	None	Metallogenic specialization
Classification:	Dzhezkazgan subtype	Dzhezkazgan subtype	Dzhezkazgan subtype	Dzhezkazgan subtype
Host rock type:	Red beds	Red beds	Gray beds	Red beds

Table 8

(ii) Kupferschiefer - Rotliegende deposits

<u>Feature</u>	<u>Kupferschiefer</u>	<u>Rotliegende</u>	<u>Kintla*</u>	<u>Yarrow - Spionkop</u>
Age:	Permian	Permian	Proterozoic	Proterozoic
Structural setting:	----	----	Lewis thrust sheet	Lewis thrust sheet
Cu-bearing rock type:	Dolomitic shale	Sandstone	Shale	Quartzite
Facies:	Lagoonal	Aeolian	Deltaic (?)	Deltaic
Ore zonation:	Present	Present	?	Present (?)
Ore-controlling structures:	None	None	?	Faults (?), intrusives
Special features of intrusives:	None	None	Metallogenic specialization	Metallogenic specialization
Classification:	Cupriferous shale type	Dzhezkazgan subtype	Cupriferous shale type	Dzhezkazgan subtype
Host rock type:	Black shale	Red beds	Black shale, green shale, limestone, red beds.	Red beds
Special features:	Spheroidal pyrite	----	----	Spheroidal pyrite

Table 9

*refers to deposits in the Kintla formation of the Lewis thrust sheet.

(iii) Zambian - Congolese Copperbelt

<u>Feature</u>	<u>Zambian</u>	<u>Congolese</u>	<u>Kintla*</u>	<u>Yarrow - Spionkop</u>
Age:	Proterozoic	Proterozoic	Proterozoic	Proterozoic
Structural setting:	Anticlines, synclines	----	Lewis thrust sheet	Lewis thrust sheet
Cu-bearing rock type:	Quartzite, shale	Dolomite	Shale	Quartzite
Facies:	Deltaic	Reef & lagoonal	Deltaic (?)	Deltaic
Ore zonation:	Present	Present	?	Present (?)
Ore-controlling structures:	Fracture of basement	Fracture of basement	Fracture of basement (?)	Fracture of basement(?) Faults (?), intrusives
Special features of intrusives:	Metallogenic specialization	----	Metallogenic specialization	Metallogenic specialization
Classification:	Regionally metamorphosed	Regionally metamorphosed	Cupriferous shale type	Dzhezkazgan subtype
Host rock type:	Black shale	Dolomite	Black shale, green shale, limestone, red beds	Red beds

Table 10

*refers to deposits in the Kintla formation of the Lewis thrust sheet.

derived by the 'sucking' of ore matter from sediments of nearby lagoons and by the movement of copper compounds from different kinds of coarse sediments.

This diagenetic process involves two possible methods of deposition. In the first case sulphides were formed in fine sediments from suspensions of copper carbonates and other copper compounds accumulated in them during sedimentation. Copper migrated in interstitial water principally in the ionic form together with the bicarbonate ion (BOGDANOV, 1967). The deposition of copper compounds had a stratiform character, so sulphides were formed in the organic matter-rich seams and lenses deposited in the reducing environment of authigenic minerogenesis (cupriferous shale-type deposits).

The second case involved the migration of cupriferous interstitial solutions from fine to coarse sediment during compaction and lithification. This occurred when reducing conditions necessary for sulphide deposition were absent from the original, fine, cupriferous sediment and reducing barriers existed within the coarse detritus (cupriferous sandstone-type deposit).

NOBLE (1963) has proposed a similar origin by deposition from formation water but believes that the formation water picks up metals from the enclosing sediments as well as containing those metals already in solution. Deposition would probably be accentuated by bacterial reduction of ions in solution. BAAS BECKING and MOORE (1961) have prepared covellite, digenite, and iron sulphides by this method but

were unable to obtain bornite or chalcopyrite.

With respect to the ultimate origin of the metallic ions within the Yarrow Creek - Spionkop Creek and related deposits, some exhalation of metallic ions from the mantle by ascending solutions may have occurred along fractures such as those proposed by KANASEWICH (1968), and LANDWEHR (1967) for Canada and the western United States, and by MENDELSON (1961) for the Zambian Copperbelt. Such exhalations would be similar to those proposed by BOSTROM and PETERSON (1966) for the East Pacific Rise.

A modification of this theory may be necessary to account for the mineralization within and adjacent to sills and dykes within the Purcell-Belt series. LEWIS (1955), in discussing the importance of the structural controls of pre-ore dykes and sills on ore localization, states that such dykes and sills commonly are competent, brecciated bodies that act as host rocks or as channelways for ore solutions. Incompetent dykes and sills serve as dams, ponding ore solutions at their contacts. Fracturing at dyke contacts is also believed to be of importance since it creates channelways and loci for deposition, while intersections of dykes and sills with fault zones, formation contacts, and other planar structures (i.e. porous quartzites enclosed within the non-porous argillites of the Grinnell formation) also provide excellent sites for ore deposition.

SUMMARY AND CONCLUSIONS

Field and laboratory studies carried out by the author and previous workers in the Yarrow Creek - Spionkop Creek and related areas indicate the following sequence of geologic events:

- 1) Deposition of Grinnell and Appekunny sediments under shallow water subaerial deltaic or tidal flat conditions around 1300 million years ago; the source area for the sediments lying to the east and deposition occurring under fresh water conditions at the end of a cycle of deep- followed by shallow-water conditions.
- 2) Precambrian gravity faulting controlled by the anisotropy of the basement rocks.
- 3) Diagenesis involving the deposition of secondary quartz within the primary arenites; and intrusion of diabasic sills causing:
- 4) Precambrian normal and reverse faulting with subsequent movement of basaltic magma into the fault zones to form dykes.
- 5) Continuing diagenesis and deposition of secondary quartz and of primary sulphides within the sediments and the intrusives from fluids moving through them.
- 6) Late Mesozoic and early Tertiary thrust faulting resulting in the formation of the Lewis thrust sheet.
- 7) Late Tertiary normal faulting.

- 8) Weathering resulting in:
- 9) Partial replacement of primary sulphides by secondary sulphides and in:
- 10) Partial alteration of primary minerals to secondary carbonates, oxides, and silicates.

Petrographic and isotopic studies indicate that the source of most of the copper probably lay in the sediments themselves. This copper consisted of a mixture of copper eroded from the source area and deposited with the sediments and of primary copper and sulphur released from the mantle along fractures of the basement outlined by KANASEWICH (1968) and LANDWEHR (1967). Some enrichment was undoubtedly brought about by copper picked up by the formation waters from surrounding sediments and by copper brought in with the basaltic magma.

Deposition occurred under favourable reducing conditions within the quartzites. Concentration of copper sulphides on the borders of sills and dykes was caused by damming of the formation waters at these points and by the action of the dykes as channelways for the movement of copper-bearing solutions.

BIBLIOGRAPHY OF CITED REFERENCES

- ADSHEAD, J.A. (1963): Petrology of the carbonate rocks of the Siyeh formation, southwestern Alberta. M.Sc. thesis. Univ. of Alberta. 108 p.
- ANDERSON, R.A. (1967): Graben structure in the Coeur d'Alene district. Econ. Geol. 62, 1092-1094.
- BAAS BECKING, L.G.M. and MOORE, D. (1961): Biogenic sulphides. Econ. Geol. 56, 259-272.
- BALLY, A.W., GORDY, P.L., and STEWART, G.A. (1966): Structure, seismic data, and orogenic evolution of the Southern Canadian Rocky Mountains. Bull. Can. Petrol. Geol. 14, 337-381.
- BARNES, H.L. and CZAMANSKE, G.K. (1967): Solubilities and transport of ore minerals in Geochemistry of hydrothermal ore deposits, 334-381.
-HELGESON, H.C., and ELLIS, A.J. (1966): Ionization constants in Handbook of physical constants. G.S.A. Mem. 97, 401-413.
- BATEMAN, A.M. and JENSEN, M.L. (1956): Notes on the origin of Rhodesian copper deposits. Isotope composition of sulphides. Econ. Geol. 51, 555-564.
- BOGDANOV, Yu.V. (1964): Geology and genesis of cupriferous sandstones in the Udokan region (eastern Siberia). Dokl. Acad. Sci. USSR, Earth Sci. Sect. 145, 110-111.
-(1967): The role of sedimentation (interstitial) water in the formation of stratified copper deposits. Dokl. Acad. Nauk SSSR 176, 70-72.
- BOSTOCK, H.S., MULLIGAN, R. and DOUGLAS, R.J.W. (1957): Geol. Surv. Can. Geology and Economic Minerals of Canada. Econ. Geol. Series No. 1, 4th ed., 283-392.

- BOSTROM, K. and PETERSON, M.N.A. (1966): Precipitates from hydrothermal exhalations on the East Pacific Rise. Econ. Geol. 61, 1258-1265.
- BURNHAM, C.W., HOLLOWAY, J.R., and DAVIS, N.F. (1968): Thermodynamic properties of water to 1,000°C and 10,000 bars. Contri. No. 68-19, College of Earth and Mineral Sciences, The Pennsylvania State University.
- BURWASH, R.A. (1968): East Kootenay - British Columbia: Field guide for the East Kootenay field trip. Dept. of Geol. Univ. of Alberta.
-BAADSGAARD, H., PETERMAN, Z.E., and HUNT, G.H. (1965): Precambrian in Geological history of Western Canada, Chapter 2. Alberta Soc. Petrol. Geol., 14-19.
- CHEMICAL RUBBER CO. (ed.) (1964): Handbook of chemistry and physics.
- CLAPP, C.H. (1932): Geology of a portion of the Rocky Mountains of Northwestern Montana. Mont. Bur. Mines and Geol. Mem. No. 4.
-and DEISS, C.F. (1931): Correlation of Montana Algonkian formations. Geol. Soc. Amer. Bull. 42, 673-696.
- CLARK, L.M. (1954): Cross-section through the Clarke Range of the Rocky Mountains of southern Alberta and southern British Columbia. Guide book, Alta. Soc. Petrol. Geol., Fourth Annual Field Conference, 105-109.
-(1964): Cross section of Flathead Valley in vicinity of Sage Creek, B.C. Bull. Can. Petrol. Geol. 12, 345-349.
- CLARK, S.P. (1966): Handbook of physical constants. G.S.C. Mem. 97.

- CROWLEY, F.A. (1963): Mines and mineral deposits (except fuels) Sanders County, Montana. Mont. Bur. of Mines and Geol. Bull. 34.
- DALY, R.A. (1912): Geology of the North-American Cordillera at the 49th Parallel. Geol. Surv. Can. Mem. 38.
- DAWSON, G.M. (1886): Preliminary report on the physical and geological features of that portion of the Rocky Mountains between Latitudes 49° and 51° 30'. Geol. Surv. Can. Ann. Rept. 1, pt. B.
- DEANS, T. (1950): The Kupferschiefer and associated Lead-Zinc mineralization in the Permian of Silesia, Germany, and England. 18th Int. Geol. Cong. 7, 340-352.
- DEER, W.A., HOWIE, R.A., and ZUSSMAN, J. (1966): An introduction to the rock-forming minerals. John Wiley and Sons Inc. New York.
- DOUGLAS, R.J.W. (1953): Preliminary map, Waterton, Alberta. Geol. Surv. Can. Paper 52-10.
- DRUZHININ, I.P. (1965): Cyclic type of copper ore zoning at the Dzhezkazgan deposit. Dokl. Acad. Sci. USSR, Earth Sci. Sect., 160, 25-28.
- DUNHAM, K.C. (1964): Neptunist concepts in ore genesis. Econ. Geol. 59, 1-21.
- FEDEROVSKAYA, L.I., and BESPALOV, I.M. (1968): Secondary alterations in copper sandstones of the Donbass. Inst. of Mineral Resources, Dnepropetrovsk, 559-565.
- FENTON, C.L. and FENTON, M.A. (1937): Belt series of the North; stratigraphy, sedimentation, paleontology. G.S.A. Bull. 48, 1873-1969.

- FREEZE, A.C. (1966): On the origin of the Sullivan orebody.
C.I.M.M. Spec. Vol. No. 8, 263.
- GAMMON, J.B., BORCSIK, M., and HOLLAND, H.D. (1969):
Potassium-sodium ratios in aqueous solutions and coexist-
ing silicate melts. Science 163, 179-181.
- GARLICK, W.G. (1969): Geology of the Zambian Copperbelt.
Horizon, Sept. 1969, 7-11.
- GARRELS, R.M. and THOMPSON, M.E. (1962): A chemical model
for sea water at 25°C and one atmosphere total pressure.
Am. J. of Sci., 260, 57-66.
- HELGESON, H.C. (1967): Thermodynamics of complex dissociation
in aqueous solution at elevated temperatures. Jour.
Phys. Chem. 71, 3121-3136.
-and GARRELS, R.O. (1968): Hydrothermal transport and
deposition of gold. Econ. Geol. 63, 622-635.
- HIRST, D.M. and DUNHAM, K.L. (1963): Chemistry and petro-
graphy of the Marl Slate of S.E. Dunham, England.
Econ. Geol. 58, 912-940. (abstract)
- HOLLAND, H.D. (1959): Some applications of thermochemical
data to problems of ore deposits. I. Stability relations
among the oxides, sulfides, sulfates, silicates, and
carbonates of ore and gangue minerals. Econ. Geol. 54,
185-233.
-(1965): Some applications of thermochemical data to
problems of ore deposits. II. Mineral assemblages and
the composition of ore forming fluids. Econ. Geol. 60,
1101-1166.

- HUME, G.S. (1932): Waterton Lakes-Flathead Valley area, Alberta and B.C.. Geol. Surv. Can. Sum. Rept. part B, 1-20.
- HUNT, G.H. (1958): Petrology of the Purcell sills in the St. Mary Lake Area, B.C.. M.Sc. thesis. Univ. of Alta.
-(1961): The Purcell eruptive rocks. Ph.D. thesis. Univ. of Alta. 139 p.
-(1962): Time of Purcell eruption in Southeastern British Columbia and Southwestern Alberta. Jour. Alta. Soc. Petrol. Geol. 10, 438-442.
-(1964): Chemical correlation of the Purcell igneous rocks. Bull. Can. Petrol. Geol. 12, 544-555.
- JOHNS, W.M. (1961): Progress report on geologic investigations in the Kootenai-Flathead area, Northwest Montana. 3. Northern Lincoln County. Mont. Bur. Mines and Geol. Bull. 23.
-(1964): Progress report on geologic investigations in the Kootenai-Flathead area, Northwest Montana. 6. Southeastern Flathead County and Northern Lake County. Mont. Bur. Mines and Geol. Bull. 42.
- JONES, P.B. (1969): The Tertiary Kishenehn formation, British Columbia. Bull. Can. Petrol. Geol. 17, No. 2, 234-246.
- KANASEWICH, E.R. (1968): Precambrian rift: genesis of strata-bound ore deposits. Science, 161, 1002-1005.
- KOZINTSEVA, T.N. (1965): The solubility of hydrogen sulphide in water and solutions under higher temperatures in Geochemical investigation in the field of higher pressures and temperatures Nauka Publications Office.
- LANDWEHR, W.R. (1967): Belts of major mineralization in western United States. Econ. Geol. 62, 494-501.

- LEECH, G.B. (1962): Metamorphism and granitic intrusions of Precambrian age in Southeastern British Columbia. Geol. Surv. Can. Paper 62-13.
- LEWIS, D.V. (1955): Relationships of ore bodies to dikes and sills. Econ. Geol. 50, 495-516.
- MCCULLOUGH, H. and KROUSE, H.R. (1965): Application of digital recording to simultaneous collection in mass spectrometry. Rev. Sci. Inst. 36, 1132-1134.
- MENDELSON, F. (1961): The geology of the Northern Rhodesian Copperbelt. London, Macdonald.
- NARKELYUN, L.F. and YURGENSON, G.A. (1968): Copper sources in the formation of deposits of the cupriferous sandstone type. Transbaikal Combined Scientific-Research Institute, Chita, 739-747.
- NOBLE, E.A. (1963): Formation of ore deposits by water of compacting. Econ. Geol. 58, No. 7, 1145-1156.
- OBRADOVICH, J.D. and PETERMAN, Z.E. (1967): Geochronology of the Belt Series, Montana. Proc. Conf. Geochronology of Precambrian Stratified Rocks. Univ. of Alta., 75.
- OHMOTO, H. (1970): Isotopic and chemical equilibria among sulfur species in hydrothermal solutions. Unpublished paper, Univ. of Alta.
- PARDEE, J.T. (1911): Geology and mineralization of the Upper St. Joe River Basin, Idaho. U.S.G.S. Bull. 470, 39-61.
- POPOV, V.M. (1962): Geologic regularities in the distribution of cupriferous sandstones in central Kazakhstan. Inter. Geol. Review, 4, 393-411.

- PRICE, R.A. (1959): Flathead, B.C. and Alberta. Geol. Surv. Can. Map 1-1959.
-(1962): Fernie map-area, east half, Alberta and British Columbia. Geol. Surv. Can. Paper 61-24.
-(1964): The Precambrian Purcell System in the Rocky Mountains of Southern Alberta and British Columbia. Bull. Can. Petrol. Geol. 12, 399-426.
-(1965): Flathead map area, British Columbia and Alberta. G.S.C. Mem. 336.
-(1967): The tectonic significance of mesoscopic sub-fabrics in the Southern Rocky Mountains of Alberta and British Columbia. Can. Jour. Earth Sci. 4, 39-70.
- REESOR, J.E. (1957): The Proterozoic of the Cordillera in Southeastern British Columbia and Southwestern Alberta in The Proterozoic in Canada. Roy. Soc. Can. Spec. Pub. No. 2, 150-177.
- RICE, H.M.A. (1937): Cranbrook map area, British Columbia. Geol. Surv. Can. Mem. 207, 67 p.
- ROSS, C.P. (1959): Geology of Glacier National Park and the Flathead Region Northwestern Montana. U.S.G.S. Prof. Paper 296, 125 p.
- SAKAI, H. (1968): Isotopic properties of sulphur compounds in hydrothermal processes. Geochem. Journ. 2, 29-49.
- SKINNER, B.J., WHITE, D.E., ROSE, H.J. and MAYS, R.E. (1967): Sulphides associated with the Salton Sea geothermal brine. Econ. Geol. 62, 316-330.

- SMITH, A.G., and BARNES, W.C. (1966): Correlation of and facies changes in the carbonaceous, calcareous, and dolomitic formations of the Precambrian Belt-Purcell Supergroup. Geol. Soc. Amer. Bull. 77, 1399-1426.
- STEVENSON, R.W. (1968): Final report - 1967, Waterton Copper project, Waterton Area, Alberta. Kennco Explorations (Western) Limited report.
- UMPLEBY, J.B. and JONES, E.L., Jr. (1923): Geology and ore deposits of Shoshone County, Idaho. U.S.G.S. Bull. 732, 156 p.
- WALDRON, C.R. (supervisor) (1942): Bibliography of the geology and mineral resources of Montana. Mont. Bur. Mines and Geol. Mem. 21.

APPENDIX A.DESCRIPTION AND LOCATION OF SPECIMENS

RG - 1 Blind Canyon 4330N,2550E*

From upper chilled margin of diabase sill at base of Grinnell formation. Heavily altered. Contains large radiating zoned feldspar crystals, disseminated chalcopyrite with $\delta S^{34} = +20.7\%$.

RG - 2 Blind Canyon 4780N,2550E*

From diabase dyke near base of Grinnell formation. The intrusive is continuous from RG - 1. Contains a hematite-rich zone apparently caused by assimilation of Grinnell argillites.

RG - 3 Spionkop Creek 5000N,5000W*

From diabase dyke in lower Siyeh formation. Contains amygdules of sphalerite, carbonat, chalcedony.

RG - 4 Spionkop Creek 4775N,2265E*

From top mineralized quartzite bed in Grinnell formation on Spionkop Creek. Contains chalcocite pebbles, some disseminated chalcocite. $\delta S_{Cc}^{34} = +1.4\%$.

RG - 5 Spionkop Creek 5220N,2260E*

From bottom mineralized Grinnell quartzite bed on Spionkop Creek. Shows mud cracks, disseminated chalcocite, malachite.

RG - 6 Blind Canyon 4820N,2510E*

From diabase dyke in lower Grinnell formation. Contains

disseminated chalcocite.

RG - 7 Blind Canyon 4800N,2630E*

Diabase dyke in lower Grinnell formation. Disseminated pyrite. $\delta S_{py}^{34} = +12.5\%$.

RG - 8 Blind Canyon 4825N,2505E*

Diabase dyke in lower Grinnell formation. Disseminated covellite and hematite. $\delta S_{cov}^{34} = -3.6\%$.

RG - 9 Yarrow Creek 550N,3440E*

Diabase sill at base of Grinnell formation. Disseminated pyrite. Biotite crystals up to 5 mm.

RG - 10 Spionkop Creek 4475N,2120E*

Fourth mineralized Grinnell quartzite bed on Spionkop Creek. Casts of mud cracks; minor disseminated covellite, malachite. Malachite: $\delta O_{PDB}^{18} = -10.9\%$, $\delta C_{PDB}^{13} = -4.2\%$.

RG - 11 Yarrow Creek 700N,3520E*

Quartzite from pit on southeast side of main Yarrow Creek mineralized area. Diabase dyke beneath quartzite bed. Disseminated covellite and bornite. $\delta S_{bo}^{34} = -7.3\%$.

RG - 12 Yarrow Creek 985N,3490E*

Quartzite bed in upper Grinnell formation. Above RG - 11. Dyke below quartzite bed. Disseminated sphalerite, chalcopyrite, malachite. $\delta S_{sl}^{34} = +11.6\%$, $\delta S_{cp}^{34} = +9.8\%$.

RG - 13 Yarrow Creek 1045N,3340E*

Quartzite from upper Grinnell formation. Ripple marks,

minor disseminated covellite in argillite pebbles and in quartzite. $\delta S_{\text{cov}}^{34} = +5.7\text{‰}$. Malachite: $\delta O_{\text{PDB}}^{18} = -10.6\text{‰}$, $\delta C_{\text{PDB}}^{13} = -6.9\text{‰}$.

RG - 14 Yarrow Creek 1045N,3340E*

Same bed as sample RG - 13. Disseminated chalcopryrite, malachite. $\delta S_{\text{cp}}^{34} = +6.2\text{‰}$. Malachite: $\delta O_{\text{PDB}}^{18} = -10.5\text{‰}$, $\delta C_{\text{PDB}}^{13} = -4.4\text{‰}$.

RG - 15 Yarrow Creek 1015N,3330E*

Same bed as sample RG - 13. From pit blasted out. Fractures filled with bornite and covellite stringers 1 mm X 50 mm. Disseminated bornite and covellite. $\delta S_{\text{cov}}^{34} = +12.5\text{‰}$, $\delta S_{\text{bo}}^{34} = +8.3\text{‰}$.

RG - 16 Yarrow Creek 655N,3415E*

Appekunny quartzite from above a mineralized diabase sill. Disseminated chalcopryrite in and near argillite pebbles in quartzite.

RG - 17 Yarrow Creek 735N,3820E*

Appekunny quartzite from beneath main diabase sill. Disseminated chalcopryrite in argillite pebbles in quartzite. $\delta S_{\text{cp}}^{34} = +4.6\text{‰}$.

RG - 18 Yarrow Creek 730N,3830E*

Appekunny quartzite from beneath main diabase sill. Mud cracks. Disseminated chalcopryrite in and near argillite pebbles in quartzite. $\delta S_{\text{cp}}^{34} = +10.5\text{‰}$, $\delta S_{\text{cp}(\text{repeat})}^{34} = +10.2\text{‰}$.

RG - 19 Yarrow Creek 720N,3840E*

Appekunny quartzite from beneath main diabase sill. Disseminated chalcopryrite in and near argillite pebbles in quartzite. $\delta S_{cp}^{34} = +4.8\%$.

RG - 20 Yarrow Creek 1015N,3350E*

Grinnell quartzite from bed approximately 15 feet below sample RG - 15. Disseminated covellite and bornite, generally parallel to bedding in bottom half of bed.

$\delta S_{cov}^{34} = -4.6\%$, $\delta S_{bo}^{34} = -4.6\%$.

RG - 21 Yarrow Creek 1015N,3330E*

Grinnell argillite from same pit as sample RG - 15. Argillite cut by carbonate vein containing bornite and covellite.

RG - 22 Yarrow Creek 650N,3415E*

From diabase sill below sample RG - 16. Disseminated chalcopryrite. $\delta S_{cp}^{34} = +13.7\%$.

RG - 23 Yarrow Creek 1065N,3200E*

Quartzite from near top of Grinnell formation. Abundant disseminated bornite and covellite. $\delta S_{bo}^{34} = +0.6\%$, $\delta S_{cov}^{34} = +0.6\%$.

RG - 24 Yarrow Creek 950N,4155E*

From main diabase sill at base of Grinnell formation. Stellate arsenopyrite crystals present. Disseminated chalcopryrite. $\delta S_{asp}^{34} = +27.0\%$.

RG - 30 Yarrow Creek 660N,3350E*

Chalcocite from enriched margin of minor diabase sill in lower Grinnell formation. $\delta S_{cc}^{34} = +10.8\%$.

RG - 31 Yarrow Creek 1005N,3345E*

From diabase dyke approximately 20 feet below sample RG - 15. Fine stringers of carbonate with disseminated bornite and covellite along fractures.

RG - 32 Yarrow Creek 330N,2575E*

Siyeh quartzite from approximately 20 feet above Grinnell-Siyeh contact. Large argillite pebbles. Minor disseminated chalcopyrite and covellite in argillite pebbles and in quartzite.

RG - 33 Blind Canyon 4840N,2490E*

From diabase dyke. Zone of hematite and quartz rich material running through specimen, probably due to assimilation of Grinnell argillites.

RG - 34 Spionkop Creek 4930N,2110E*

Grinnell quartzite from approximately 35 feet below sample RG - 10. No visible copper minerals. Ripple marks.

RG - 35 Spionkop Creek 5200N,2290E*

Grinnell quartzite from approximately 30 feet above sample RG - 5. Taken 4 feet from unmineralized diabase dyke. No visible copper minerals.

RG - 36 Yarrow Creek 820N,3175E*

Upper Grinnell quartzite containing large hematite-rich pebble approximately 30 X 120 mm.

RG - 37 Spionkop Creek 5220N,2260E*

Same as sample RG - 5. Disseminated and veined covellite and malachite. Malachite: $\delta O_{PDB}^{18} = -10.3\%$, $\delta C_{PDB}^{13} = -3.4\%$.

RG - 38 Spionkop Creek 4995N,2260E*

From diabase sill. Disseminated chalcocite. Malachite along fractures. $\delta S_{cc}^{34} = -11.5\%$.

RG - 39 Spionkop Creek 5365N,2285E*

From diabase dyke at first drill site on access road. Near base of Grinnell formation. Disseminated chalcopyrite. $\delta S_{cp}^{34} = +6.2\%$.

RG - 40 Yarrow Creek 200S,3000E*

From main diabase sill at base of Grinnell formation. Large translucent feldspar crystals.

RG - 41 Yarrow Creek 650N,3415E*

Quartz crystals from main diabase sill at base of Grinnell formation. Chalcopyrite crystals among quartz crystals.

RG - 42 Spionkop Creek 5005N,2490E*

From diabase dyke crossing small saddle above first drill site on access road. No visible copper minerals.

RG - 43 Spionkop Creek 5005N,2490E*

Same as sample RG - 42. No visible copper minerals.

RG - 44 Yarrow Creek 950N,4050E*

Barite from main diabase sill at base of Grinnell formation. Approximately 100 feet west of sample RG - 24. Pyrite within barite. $\delta S_{ba}^{34} = +26.8\%$, $\delta S_{py}^{34} = +9.1\%$.

RG - 45 Yarrow Creek 1020N,3305E*

Barite from pit blasted out above sample RG - 15. Bornite and covellite within barite. $\delta S_{ba}^{34} = +23.0\%$, $\delta S_{bo,cov}^{34} = +3.8\%$.

RG - 46 Yarrow Creek 920N,4280E*

Barite and quartz crystals from approximately 5 feet above diabase dyke, approximately 100 feet east of sample RG - 24. Pyrite within barite. $\delta S_{ba}^{34} = +25.3\%$, $\delta S_{py}^{34} = -0.3\%$.

RG - 47 Yarrow Creek 900N,5000E*

Quartz crystals from upper Appekunny formation. Approximately 1000 feet east of sample RG - 24. Exact location and relation to intrusions unknown.

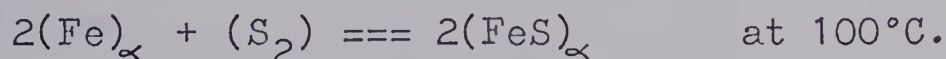
RG - 48 Yarrow Creek 500N,2670E*

Quartzite with pseudo-oolitic pyrite from approximately 20 feet above Grinnell-Siyeh contact. $\delta S_{py}^{34} = +10.9\%$.

*indicates distance in feet North and East of point marked as 000N,000E on Fig.9.

APPENDIX B.COMPUTATIONSMineral stabilities

Mineral stability fields were calculated using HOLLAND'S (1959,1965) data for ΔH and ΔS (Table 11) as is illustrated below for the sample reaction:



For this reaction:

$$K = (\text{FeS})^2 / f_{\text{S}_2} (\text{Fe})^2 = 1 / f_{\text{S}_2}$$

and:

$$\log K = -\log f_{\text{S}_2}.$$

From thermodynamics:

$$\Delta G_T = -2.303RT \log K = \Delta H - T\Delta S$$

or:

$$\log K = (-\Delta H + T\Delta S) / 2.303RT$$

but:

$$\log K = -\log f_{\text{S}_2},$$

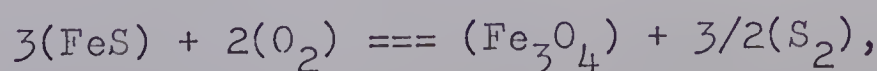
so:

$$\log f_{\text{S}_2} = (\Delta H - T\Delta S) / 2.303RT,$$

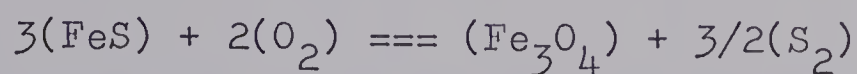
or in this case:

$$\begin{aligned} \log f_{\text{S}_2} &= (-74,320 + 373 \times 31.18) / 2.303 \times 1.987 \times 373 \\ &= -36.7. \end{aligned}$$

For cases such as:



the values of ΔH , ΔS are not available but the slope of the line separating the two mineral stability fields may be determined as follows:



$$K = (\text{Fe}_3\text{O}_4) f_{\text{S}_2}^{3/2} / (\text{FeS})^3 f_{\text{O}_2}^2.$$

Therefore:

$$-\log K = 3/2 \log f_{\text{S}_2} - 2 \log f_{\text{O}_2} = (\Delta H - T\Delta S) / 2.303RT$$

and:

$$3/2 \log f_{\text{S}_2} = 2 \log f_{\text{O}_2} + (\Delta H - T\Delta S) / 2.303RT$$

$$\log f_{\text{S}_2} = 4/3 \log f_{\text{O}_2} + 2/3(\Delta H - T\Delta S) / 2.303RT.$$

Thus we have a slope of $4/3$ for the boundary between the two mineral stability fields and a point on the line which can be determined by the first method outline above (i.e. the point where the phases Fe, FeS, and Fe_3O_4 are in equilibrium).

<u>REACTION</u>	<u>ΔH</u>	<u>ΔS</u>	<u>TEMPERATURE RANGE ($^{\circ}\text{K}$)</u>	<u>REF. *</u>
$2(\text{Fe})_{\alpha} + (\text{S}_2) === 2(\text{FeS})_{\alpha}$	- 74,320	- 31.18	298 - 412	1959
$2(\text{Fe})_{\beta} + (\text{S}_2) === 2(\text{FeS})_{\beta}$	- 71,820	- 25.12	412 - 1179	1959
$2(\text{FeS}) + (\text{S}_2) === 2(\text{FeS}_2)$	- 86,700	- 90.0	298 - 1100	1959
$3/2(\text{Fe})_{\alpha} + (\text{O}_2) === 1/2(\text{Fe}_3\text{O}_4)_{\alpha}$	-133,900	- 41.10	298 - 833	1959
$4(\text{Fe}_3\text{O}_4) + (\text{O}_2) === 6(\text{Fe}_2\text{O}_3)$	-119,200	- 67.2	300 - 1200	1959
$(\text{Fe}_2\text{O}_3) + (\text{S}_2) + 5/2(\text{O}_2) === 2(\text{FeSO}_4)$	-275,000	-147.1	300 - 1000	1959
$(\text{FeS}_2) + 2(\text{O}_2) === (\text{FeSO}_4) + 1/2(\text{S}_2)$	-162,600	- 57.8	300 - 1000	1959
$4(\text{Cu}) + (\text{S}_2) === 2(\text{Cu}_2\text{S})_{\alpha}$	- 71,310	- 54.6	298 - 376	1959
$4(\text{Cu}) + (\text{S}_2) === 2(\text{Cu}_2\text{S})_{\beta}$	- 71,280	- 90.96	376 - 623	1959
$4(\text{Cu}) + (\text{S}_2) === 2(\text{Cu}_2\text{S})_{\gamma}$	- 67,240	- 46.7	723 - 1383	1959
$1/2(\text{Cu}_9\text{S}_5) + (\text{S}_2) === 9/2(\text{CuS})$	- 42,960	- 48.5	298 - 376	1959
$1/2(\text{Cu}_9\text{S}_5) + (\text{S}_2) === 9/2(\text{CuS})$	- 44,800	- 53.4	376 - 623	1959
$1/2(\text{Cu}_9\text{S}_5) + (\text{S}_2) === 9/2(\text{CuS})$	- 45,200	- 54.0	623 - 900	1959
$(\text{Cu}_2\text{SO}_4) + 1/2(\text{S}_2) + 2(\text{O}_2) === 2(\text{CuSO}_2)$	-186,300	-122.5	300 - 1000	1959
$5(\text{CuFeS}_2) + (\text{S}_2) === (\text{Cu}_5\text{FeS}_4) + 4(\text{FeS}_2)$	- 50,728	- 56.95	525 - 725	1965

Table 11

<u>REACTION</u>	<u>ΔH</u>	<u>ΔS</u>	<u>TEMPERATURE RANGE (°K)</u>	<u>REF. *</u>
$2(\text{Pb}) + (\text{S}_2) === 2(\text{PbS})$	-145,420	- 68.3	298 - 600	1959
$2(\text{Pb}) + (\text{S}_2) === 2(\text{PbS})$	-150,320	- 76.5	600 - 1380	1959
$(\text{PbS}) + 2(\text{O}_2) === (\text{PbSO}_4)$	-197,000	- 84.6	300 - 1000	1959
$2(\text{Pb}) + (\text{O}_2) === 2(\text{PbO})$	-105,700	- 67.6	298 - 600	1959
$2(\text{Pb}) + (\text{O}_2) === 2(\text{PbO})$	-109,900	-100.2	600 - 1150	1959
$(\text{PbO}) + 1/2(\text{S}_2) + 3/2(\text{O}_2) === (\text{PbSO}_4)$	-182,600	- 81.7	300 - 1000	1959
$2(\text{Zn}) + (\text{S}_2) === 2(\text{ZnS})$	-127,300	- 73.4	298 - 693	1959
$2(\text{Zn}) + (\text{S}_2) === 2(\text{ZnS})$	-189,940	-149.8	693 - 1200	1959
$2(\text{Zn}) + (\text{O}_2) === 2(\text{ZnO})$	-168,200	- 88.3	298 - 693	1959
$2(\text{Zn}) + (\text{O}_2) === 2(\text{ZnO})$	-230,840	-164.8	693 - 1200	1959
$(\text{ZnS}) + 2(\text{O}_2) === (\text{ZnSO}_4)$	-185,700	- 81.2	300 - 1000	1959
$(\text{ZnO}) + 1/2(\text{S}_2) + 3/2(\text{O}_2) === (\text{ZnSO}_4)$	-166,200	- 80.5	300 - 1000	1959
$(\text{BaS}) + 2(\text{O}_2) === (\text{BaSO}_4)$	-244,200	- 88.4	300 - 1000	1959

Table 11 (continued)

<u>REACTION</u>	<u>ΔH</u>	<u>ΔS</u>	<u>TEMPERATURE RANGE ($^{\circ}$K)</u>	<u>REF. *</u>
$(S_2) + 2(O_2) === 2(SO_2)$	-173,240	- 34.62	298 - 2000	1965
$(S_2) + 3(O_2) === 2(SO_3)$	-218,440	- 77.34	318 - 1800	1965

Table 11 (continued)

*indicates date of reference (i.e. HOLLAND, 1959 or HOLLAND, 1965).

Solution geochemistry

As noted in CHAPTER V, a check was run by a computer program supplied by H. OHMOTO on the calculated ionic concentrations of the sulphur species present in the mineralizing solutions. The results are summarized in Tables 12, 13, 14, and 15 below.

An examination of these results reveals a generally good agreement with those results obtained in CHAPTER V. The major areas of uncertainty lie at low pH and low oxygen fugacity, where H_2S and sulphate are both present in significant quantities. This effect is of primary importance at 100°C and at 600°C and, since our solution sulphur geochemistry estimates are based on 400°C, should not jeopardize the validity of our conclusions.

Sulphur isotopes

The sulphur isotopic values were, as outlined in CHAPTER V, calculated by a method based upon correction factors determined by SASAKI, KAJIWARA, and OHMOTO. A sample calculation is shown on page A-17.

<u>pH</u>	<u>f_{O₂}</u>	<u>100°C</u>		<u>%HS^{-*}</u>	<u>$\delta S_{S^{34}}^{34}(\text{‰})^\#$</u>
		<u>%H₂S[*]</u>	<u>%sulphate[*]</u>		
2.1	-53 to -50.5	95	2		-10
	-50	87	12		-16
	-49.5	41	57		-39
	-49	6	94		-56
	-48.5 to -48		95		-59
4.1	-53 to -52.5	95			-10
	-52	93	6		-13
	-51.5	59	41		-30
	-51	13	86		-53
	-50.5 to -48		95		-59
6.1	-53	12	82	6	-50
	-52.5 to -48		95		-59
8.1	-53 to -48		95		-59

Table 12

*not recorded if <5%.

†indicates value of $\delta S_{S^{34}}^{34}$ if $\delta S_{\text{solution}}^{34} = 0\text{‰}$.

NOTE: %sulphate indicates %SO₄⁼ + %HSO₄⁻ + %KSO₄⁻.

<u>200°C</u>				
<u>pH</u>	<u>f_{O₂}</u>	<u>%H₂S*</u>	<u>%sulphate*</u>	<u>δS_S³⁴(‰)[‡]</u>
1.8	-37	46	52	-24
	-36.5	7	89	-36
	-36 to -32		95	-38.5
3.8	-37 to -32		95	-38.5
5.8	-37 to -32		95	-38.5
7.8	-37 to -32		95	-38.5

Table 13

<u>400°C</u>				
<u>pH</u>	<u>f_{O₂}</u>	<u>%H₂S*</u>	<u>%sulphate*</u>	<u>δS_S³⁴(‰)[‡]</u>
1.7	-25 to -24.5	95		-4.5
	-24	95	5	-5.2
	-23.5	67	32	-9.7
	-23	17	81	-17.8
	-22.5 to -20		95	-20.5
3.7	-25	89	10	-6.2
	-24.5	46	54	-13.2
	-24	8	92	-19.3
	-23.5 to -20		95	-20.5
5.7	-25 to -20		95	-20.5
7.7	-25 to -20		95	-20.5

Table 14

*not recorded if < 5%.

‡indicates value of δS_S³⁴ if δS_S³⁴_{solution} = 0‰.

NOTE: %sulphate indicates total sulphate.

<u>600°C</u>					
<u>pH</u>	<u>f_{O₂}</u>	<u>%_{H₂S}*</u>	<u>%_{sulphate}*</u>	<u>%_{HS⁻*}</u>	<u>δS³⁴_S(‰)[‡]</u>
1.6	-22 to -19	99			- 1.5
	-18.5	95	5		- 2.1
	-18	64	36		- 5.8
3.6	-22 to -20.5	95			- 1.5
	-20	92	8		- 2.5
	-19.5	53	44		- 7.1
	-19	10	90		-12.3
	-18.5 to -18		95		-13.5
5.6	-22	90	7		- 2.4
	-21.5	54	45		- 6.8
	-21	11	89		-12.2
	-20.5 to -18		95		-13.5
7.6	-22		72	28	- 9.8
	-21.5 to -18		95		-13.5

Table 15

*not recorded if <5%.

‡indicates value of δS³⁴_S if δS³⁴_{solution} = 0‰.

NOTE: %_{sulphate} indicates total sulphate species.

S^{34}/S^{32} FRACTIONATION STUDIES

Sample No: RG - 46 (barite)

Standard: YKS - GM1A

Date: March 3, 1970

Time: -start: 3:15
finish: 3:30

<u>X</u>	<u>X/S</u>	<u>S</u>
		749313
766349	1.02260	749410
766484	1.02265	749507
766619	1.02278	749542
766636	1.02276	749577
766652	1.02272	749622
		749667
766540		749516

$$\Delta = 766540 - 749516 = 1702.4$$

$$\alpha = 1702.4 \times 0.05 = 85.1$$

$$R_{xt}/R_{st} = (76654 + 85)/(74952 - 85) = 1.02500$$

$$1.02500 \times 0.99820 = 1.02316$$

$$(1.02316 - 1) \times 1000 \times 1.0907 = 25.26$$

$$\delta S^{34}(\text{‰}) = \underline{+25.3}$$

B29953